

---

# **Cosmology Meets Condensed Matter**

**Mark N. Brook**



The University of  
**Nottingham**

Thesis submitted to the University of Nottingham  
for the degree of Doctor of Philosophy. July 2010

---

*The Feynman Problem-Solving Algorithm:*

1. *Write down the problem*
2. *Think very hard*
3. *Write down the answer*

– **R. P. Feynman**  
att. to **M. Gell-Mann**

**Supervisor:** Prof. Peter Coles

**Examiners:** Prof. Ed Copeland  
Prof. Ray Rivers

# Abstract

This thesis is concerned with the interface of cosmology and condensed matter.

Although at either end of the scale spectrum, the two disciplines have more in common than one might think. Condensed matter theorists and high-energy field theorists study, usually independently, phenomena embedded in the structure of a quantum field theory. It would appear at first glance that these phenomena are disjoint, and this has often led to the two fields developing their own procedures and strategies, and adopting their own nomenclature.

We will look at some concepts that have helped bridge the gap between the two subjects, enabling progress in both, before incorporating condensed matter techniques to our own cosmological model. By considering ideas from cosmological high-energy field theory, we then critically examine other models of astrophysical condensed matter phenomena.

In Chapter 1, we introduce the current cosmological paradigm, and present a somewhat historical overview of the interplay between cosmology and condensed matter. Many concepts are introduced here that later chapters will follow up on, and we give some examples in which condensed matter physics has had a very real effect on informing cosmology. We also reflect on the most recent incarnations of the condensed matter / cosmology interplay, and the future of these developments.

Chapter 2 presents the Einstein-Klein-Gordon system of equations and their non-relativistic and nonlinear counterparts, the Schrödinger-Poisson, and nonlinear Schrödinger (Gross Pitaevskii)-Poisson systems. We give a more technical overview of the various applications of these systems of equations, as well as discussing the role and interpretation of condensates in the field of cosmology.

---

In Chapter 3 we discuss more qualitatively the fluid-mechanical methods used in a wave-mechanical approach to structure formation, and in formulations of condensed matter models. Taking a lead from the condensed matter side, we look at some of the details of the Gross-Pitaevskii equation, particularly with regard to quantum vortices, and then put this quantum-mechanical system into a cosmological environment by coupling it to the Poisson equation, in an effort to pin down some of the parameters that may be consistent with the existence of vortices in a cosmological Bose-Einstein condensate.

In Chapter 4 we turn to high-energy field theory and elucidate further some of the relationships with condensed matter physics that are present. We also critically examine a Bose-Einstein dark matter model in light of these considerations.

Chapter 5 rounds off with a discussion and suggestions for further work based upon models we have discussed, as well as some ideas for models that have not yet been mentioned.

An appendix discusses techniques for moving from the relativistic Einstein-Klein-Gordon equations to the Schrödinger-Poisson system.

# Acknowledgements

Gratitude is extended to those who have conspired to keep my life interesting. Including, but not limited, to:

David, Will, Edo, Jensen, Ryan, Sarah, Thea, Dan, Nic, Ben, Karen, Seb, Charlotte, Jon, Hari, Tony, Abigail, Ben, Dave, Matt, Bruce, Holger, Kiera, Martin, Bethan, Ed, Mike, Peter, Meghan, Kate, Kathleen, Omar, Paul, Nicky, Dan, Rob, Evelyn, Amanda, Beth, David, Lisa, Dolf, Emma, Steph, Dan, Mike, Ruth, Amanda, Ian, Malgorzata, Joe, Peter, Tom, Jesse, Amie, Jen, Shannon, Troy, Fred, Tiana, Charles, Justine, Joe, Richard, Andrew, Philip, Frazer, Anita, David, Ray, Sophie, BJ, Kyle, Carl, Chris, June, Simon, Sean, Gemma, Iris, David, Mike, Christine, Rowena, Janine, Emma, Gustavo, Emmaline, Dale, Jon, Katrina, David, Peter, Aman, Jonathan, Kate, Chris, Kev, Boris, Magda, Mark, Dave, Carly, Lizzy, Belinka, Elisa, Judith, Daniele, Jesús, Dan, Maryam, Marco, Natasha, Giordano, Riccardo, Marion, Lynne, Jennie, Danny, Phillip, Harvey, Anne, Tim, Duncan, Mitsuo, Graeme, Marianne, Bec, Karima, Marco, Kate, Julie, Ben, Martyn, Clare, Michelle, Nara, Nat, Phil, Fiona, Caitlin, Alberto, Ned, Karen, Alessandra, Rachael, Alkistis, Becca, Tom, Claire, Gary, Martin, Arianna, Yara, Olivia, Philip.

# Contents

<b>Abstract</b>	<b>ii</b>
<b>Acknowledgements</b>	<b>iv</b>
<b>List of Figures and Tables</b>	<b>viii</b>
<b>1 Cosmology and Condensed Matter</b>	<b>1</b>
1.1 Cosmology . . . . .	1
1.1.1 The Birth of General Relativity . . . . .	1
1.1.2 Inflation and Dark Energy . . . . .	13
1.1.3 The Traditional Approach to Structure Formation . . . . .	27
1.1.4 Dark Matter . . . . .	30
1.2 Cosmology Meets Condensed Matter . . . . .	38
1.2.1 The ‘Higgs-Anderson’ mechanism . . . . .	39
1.2.2 Kibble-Zurek mechanism - Condensed Matter again informs Cosmology . . . . .	41
1.3 The Future of Multi-Disciplinary Research . . . . .	45
1.4 Discussion . . . . .	48
<b>2 Technical Background</b>	<b>49</b>
2.1 Beyond Cold Dark Matter . . . . .	50
2.2 A Wave-Mechanical Approach to Structure Formation . . . . .	52
2.3 Quantum Mechanical Dark Matter . . . . .	55
2.3.1 Dark Matter as a Bose-Einstein Condensate . . . . .	56
2.4 Scalar Field Dark Matter . . . . .	59
2.4.1 Scalar Fields and Bose-Einstein Condensation . . . . .	63
2.5 Exotic Objects . . . . .	66
2.5.1 Boson Stars . . . . .	66
2.5.2 Oscillatons . . . . .	68
2.6 Penrose and the Quantum State Reduction Problem . . . . .	69

2.7	Discussion . . . . .	71
<b>3</b>	<b>The nonlinear Schrödinger Equation in Condensed Matter and Cosmology</b>	<b>73</b>
3.1	The Bose-Einstein Condensate . . . . .	74
3.2	The Gross-Pitaevskii Equation . . . . .	77
3.2.1	The Madelung Transformation . . . . .	82
3.2.2	Vortices . . . . .	83
3.2.3	Approximations to the Density Profile . . . . .	86
3.3	The Wave-Mechanical Approach to Structure Formation . . . . .	88
3.4	Gravitational Stability of Vortices in Bose-Einstein Condensate Dark Matter . . . . .	90
3.4.1	Vortices in Gravitationally Coupled Bose-Einstein Condensates	92
3.4.2	Vortex Stability in Gravitationally Coupled Bose-Einstein Condensates . . . . .	93
3.4.3	Bounds on Parameters . . . . .	95
3.4.4	Results . . . . .	99
3.5	Discussion . . . . .	100
<b>4</b>	<b>Relations to Field Theory</b>	<b>105</b>
4.1	Comparison of Related Models . . . . .	106
4.1.1	The Abelian-Higgs Model . . . . .	106
4.1.2	The Goldstone Model . . . . .	110
4.1.3	The Landau-Ginzburg Model . . . . .	111
4.1.4	The Gross-Pitaevskii Equation . . . . .	113
4.2	The Relationship between Bose-Einstein Condensation and Spontaneous Symmetry Breaking, and the Role of Temperature . . . . .	115
4.3	The Axion . . . . .	120
4.4	The Domain Wall Problem in a Model of Bose-Einstein Condensate Dark Matter . . . . .	123
4.4.1	The Model . . . . .	124
4.4.2	Existence of Domain Walls in the Silverman-Mallett Model . . . . .	125
4.4.3	Cosmological Constraints on the Existence of Domain Walls . . . . .	125
4.4.4	Mass and Symmetry-Breaking Parameters in the Silverman-Mallett Model . . . . .	127
4.4.5	Final Remarks . . . . .	129
4.5	Discussion . . . . .	130

<b>5</b>	<b>Conclusions and Further Work</b>	<b>133</b>
<b>A</b>	<b>From Einstein-Klein-Gordon to Schrödinger-Poisson</b>	<b>138</b>
	<b>Bibliography</b>	<b>142</b>

# List of Figures

1.1	Hubble’s original data [23], compared with that of more recent surveys (see Kirshner [24] for image and data references). Note the difference in scale. . . . .	7
1.2	Comparison of $\Lambda$ CDM models. From Choudhury and Padmanabhan [99]. Observational data points are obtained from the ‘Gold’ sample of Riess et al. [100] from the High-z Supernova Search. . . . .	24
1.3	Equation of state. From the Supernova Cosmology Project [89]. . . . .	25
1.4	Temperature anisotropies from WMAP 5 year data [101]. . . . .	26
1.5	Power spectrum from WMAP 5 year data [102]. . . . .	27
3.1	Numeric solution to eqn. (3.59) (blue), the Padè approximation, eqn. - (3.62) (red), and the scaled approximation used in this analysis, eqn. - (3.61) (green). . . . .	87
3.2	Velocity Profiles for $v_G$ (green, dot dash) and $v_\omega$ (blue, dash). Density profile plotted schematically for comparison (red, solid). . . . .	95
3.3	Allowed region in $(V_0, m)$ parameter space, for a healing length of $a_0 = 1 \times 10^{16}$ m ( $\sim 1$ parsec). . . . .	100
3.4	Allowed regions in $(V_0, m)$ parameter space, with $n = 10$ . Healing lengths as labelled. . . . .	101

# List of Tables

1.1	WMAP 5 Year Parameters. . . . .	26
3.1	Vortex Energy per Unit Length. . . . .	103

# Chapter 1

## Cosmology and Condensed Matter

### 1.1 Cosmology

#### 1.1.1 The Birth of General Relativity

The Einstein centenary in 2005 was a chance to celebrate the significant achievements made in cosmology in particular, and physics in general, during the hundred years since Einstein's *annus mirabilis*. This Latin phrase has also been linked to Newton's own miracle year in 1666, three hundred and thirty nine years previously, and one might begin to wonder when another might be due.

The history of progress in cosmology is interesting in its own right. A revolution in science is rarely as drastic or cataclysmic as the image invoked. The history of progress, as reported, does seem to come in fits and starts, but it is by more of an evolutionary process that the standard paradigms are formed. Often, many incorrect suggestions or interpretations are made, with a theory becoming established within the scientific community only by virtue of being the most resilient, rather than being recognised as correct overnight. The theories that are replaced can rarely be thought of as incorrect, rather, the new theory is a more general form of the old, with the old being recovered in some limiting regime.

Here, the relationship between mathematics and physics enters, and can generate a lot of philosophical discussion. Physical theories can be expressed in mathematical

language, and the limiting regime described above can be formulated as a mathematical limit process. Why the abstract concepts of mathematics can be translated into physical concepts is essentially still a mystery. The Hungarian physicist, Eugene P. Wigner, expressed it thus [1]:

*“The miracle of the appropriateness of the language of mathematics for the formulation of the laws of physics is a wonderful gift which we neither understand nor deserve.”*

It is usually due to more and more refined experimental measurement techniques, or through a desire for increased accuracy, that deviations from theoretical predictions are uncovered.

Many examples from the field of cosmology present themselves. Planetary models can be traced back at least as far as Aristotle’s *De Caelo* in the third century B.C. [2]. The ancient Greeks sought a mathematical beauty and simplicity in their models of the Universe, and so the motions of the planets and all celestial bodies were assigned to perfect spheres orbiting around the Earth. In this system it was difficult to accurately explain the motion of bodies in the sky. Rather than give up on the notions of mathematical beauty and geocentricity, Eudoxus [3], Aristotle, Ptolemy [4] and Apollonius of Perga [5] designed a system of epicycles, in which planets moved on smaller perfect circles around a point that would be traced out by the standard spherical orbit. This concept helped to explain the retrograde motions of celestial bodies, and the apparent change of distance between the Earth and the planets. As astronomers and navigators pressed for higher accuracy in predicting the motions of celestial bodies, it was found that the epicycle model did not match observations. Eventually, the geocentric models were replaced by Heliocentric ones, such as proposed by Copernicus [6]. Copernicus was driven by what would become known as the Copernican principle, which states that the Earth is not in a specially favoured position. Copernicus’ systems were still not quite correct, and still required the use of epicycles, and there is some debate as to whether Copernicus’ system was more or less complicated than the previous Ptolemaic one. See Neugebauer [7] for example, for a Ptolemaic-sided view. Copernicus would never encounter the controversy that would envelop Galileo when he made observations of Jupiter’s moons; the first decisive evidence that the Earth was not at the centre

of the Universe. Galileo's findings are documented in his famously diplomatic *De revolutionibus orbium coelestium, Libri VI* (On the Revolutions of the Heavenly Spheres, Six Books) in 1543.

The need for epicycles was done away with less than a hundred years later, when the perfect orbital circles were replaced by Kepler's ellipses [8]. Here, we can see an example of the old theory emerging as a mathematical limit of the new one, as in terms of Fourier analysis, an elliptical path can be built up mathematically as a series of 'epicycles' on a circular orbit.

Kepler's laws of planetary motion were later encapsulated in Newton's laws of motion and gravitation [9]. Newton's laws were sufficiently accurate to be used right up to the twentieth century, and indeed are still adequate for problems in celestial mechanics, such as space flight. Later, as technology advanced to enable more accurate astronomical observations, there were a few predictions for which Newton's law of gravitation were inaccurate: the prediction of the advance of the perihelion of the planets, particularly Mercury, and the angle through which light is deflected by the sun.

The beauty of the interplay of mathematics and physics is that laws can be manipulated according to a set of abstract mathematical rules, to produce sometimes equally abstract concepts which, given the right interpretation, can be once again expressed as physical entities that can be probed in experiment. The question would seem to be, "how did these rules come about?" In the *Almagest*, Ptolemy himself seems to accept the limitations of any progress made [4], suggesting that there is no way to know which theory is true, since any model is a mathematical construct.

One of the most notable examples of discovery as a consequence of theoretical prediction is the discovery of Neptune. The eighth planet was discovered by analysing irregularities in the orbit of Uranus, and predicting that they be caused by the dynamics of another, as yet undetected body, with properties that would have the required influence. On the back of the success of this prediction, another undetected planet was posited to exert the required influence on Mercury to explain the advance of its perihelion. This prediction, unfortunately, turned out to be erroneous. More abstract examples of mathematics prediction can be found in the field of particle physics. Paul Dirac, who expressed that "the laws of nature should be expressed in beautiful equa-

tions” [10], predicted the positron essentially as a consequence of the second root of the Dirac equation; in some sense the negative energy quantum states turned up as ‘merely’ an artefact of the mathematics [11]. Although Dirac’s prediction was verified by the detection of a positron by Carl Anderson in 1932, whose achievement gained him a Nobel prize, Dirac’s initial concept of a ‘sea’ of negative energy particles was flawed because a vacuum state would require an infinite density of positrons, as well as the overall negative charge of the Universe that this would imply. The idea was eventually superseded by Quantum Field Theory. As it turns out, it seems likely that Anderson was unaware of Dirac’s prediction at the time, his results only receiving the correct interpretation once the theory was brought to his attention. Anderson would later suggest that his discovery of the positron was “wholly accidental” [12].

The General Theory of Relativity laid the foundation for people to start wondering about the evolution and structure of the Universe, based purely on the matter and energy content that we are able to observe. This has been complemented only very recently by the high precision observational experiments designed to probe this content. It is an inherently mathematical theory, as Einstein favoured mathematical elegance in physical theories, and as such it has had its own share of interpretational issues, and mathematical ‘artifacts’.

Einstein combined space and time into one single, dynamical entity, which could be described purely in terms of derivatives of a *metric*,  $g_{\mu\nu}$ . The metric is a tensor that tells us how to calculate the distance between two events in a spacetime. The curvature of spacetime is also related to the energy or matter content of the Universe; matter tells spacetime how to curve, curvature tells matter how to move.

Einstein’s field equations can be written as

$$R_{\mu\nu} - \frac{1}{2}g_{\mu\nu}R = \frac{8\pi G}{c^4}T_{\mu\nu} \quad (1.1)$$

The Ricci tensor,  $R_{\mu\nu}$ , is given by

$$R_{\sigma\mu\nu}^{\rho} = \partial_{\mu}\Gamma_{\nu\sigma}^{\rho} - \partial_{\nu}\Gamma_{\mu\sigma}^{\rho} + \Gamma_{\mu\lambda}^{\rho}\Gamma_{\nu\sigma}^{\lambda} - \Gamma_{\nu\lambda}^{\rho}\Gamma_{\mu\sigma}^{\lambda}, \quad (1.2)$$

with the Christoffel symbols,

$$\Gamma_{\nu\rho}^{\mu} = \frac{1}{2}g^{\mu\alpha}(g_{\alpha\rho,\nu} + g_{\alpha\nu,\rho} - g_{\rho\nu,\alpha}), \quad (1.3)$$

where we use the notation

$$\partial_\mu \equiv \frac{\partial}{\partial x^\mu}, \quad \text{and} \quad g_{\alpha\rho,\nu} \equiv \frac{\partial g_{\alpha\rho}}{\partial x^\nu}. \quad (1.4)$$

From time to time, we may also use an overdot to represent differentiation with respect to time, and a dash to represent differentiation with respect to a spatial coordinate.

We see that the left-hand-side of Einstein's equations are made up of terms purely involving curvature, or the derivative of the metric. The right-hand-side consists of the energy-momentum tensor, the matter-energy content of the Universe. For an empty Universe, we could simply set this to zero.

Once Einstein's equations had been formulated in 1915, Einstein himself suggested that he expected that they were too complex to ever be solved exactly. Karl Schwarzschild would prove him wrong the same year, with the discovery of the metric that bears his name [13, 14]. The Schwarzschild metric describes the spacetime around any spherically symmetric, non-rotating, non-charged object, and hence is a good candidate for a first attempt at modelling objects such as stars or galaxies. It was noted at the time that the mathematics described a more exotic object, a *Black Hole*. Such objects were dismissed as mathematical curiosities, until the singularity theorems of Hawking and Penrose showed singularities to be a generic feature of many cosmological scenarios [15, 16]. The Schwarzschild metric was used to model the sun in a new prediction of the angle through which light would be deflected, and in a famous expedition in 1919, Arthur Eddington, a British scientist, found that Einstein's theory was in much better agreement than the Newtonian estimate. The new theory also accurately predicted the perihelion advance of Mercury, and solved the problem of "action at a distance" inherent in Newton's theory. Mathematically, Newton's theory of gravity appears in Einstein's field equations in the weak field limit, or equivalently in the limit of small mass densities. We will come across this limit again, and it is demonstrated in Appendix A.

Einstein was not comfortable with his own equations, which seemed to be suggesting that the Universe should be collapsing under its own gravity, and so he added a term that he called the "kosmologische Gleichung", which translates as the "Cosmological term" [17], or *Cosmological Constant*, to keep the Universe static, in line with the current

scientific consensus. Einstein's field equations with this extra term added are

$$R_{\mu\nu} - \frac{1}{2}g_{\mu\nu}R + g_{\mu\nu}\Lambda = \frac{8\pi G}{c^4}T_{\mu\nu}. \quad (1.5)$$

Often, this term is absorbed into the right-hand-side of this equation, making it part of the energy content of the Universe, as we will soon come to.

Actually, the Einstein universe is only static by construction, but is unstable. This can even be seen in Newtonian mechanics, via Poisson's equation for gravity

$$\nabla^2\phi = 4\pi G\rho. \quad (1.6)$$

If there is a constant density of matter in the Universe,  $\rho = \rho_0 \neq 0$ , then the gravitational potential must be spatially varying, and so the homogeneous density distribution must be globally contracting or expanding.

The next few years in the emergence of a standard Cosmological model are typically convoluted. In 1922 [18] and 1924 [19], Friedmann, considering Einstein's equations, published what would become known as the Friedmann equations, and the Friedmann-Robertson-Lemaitre-Walker (FRLW) metric. The results were largely unnoticed at the time and, in 1927, Lemaitre independently came to the same conclusions [20]. In considering a dynamical Universe, Lemaitre predicted that expansion would lead to a linear relation between the redshift and distance of nebulae around us in the Universe. In an expanding Universe, nebulae would appear to be moving away from us, and the recession speed would manifest itself as a redshift in the light produced by those nebulae.

Edwin Hubble, in 1926, had only just shown that these nebulae were indeed other galaxies, and not part of our own galactic system [21]. Lemaitre also conjectured that if the Universe is expanding now, then moving into the past, it would contract, until it reached a point of infinite density.

This theory did not receive its familiar *Big Bang* name until Fred Hoyle described it as such during one of his popular radio broadcasts in 1949. It is not quite clear whether he coined this term to be derogatory, which would seem to be the case, as he was a proponent of the *steady state* theory and was not known for his affable nature, or, as he later claimed, to provide a more striking image to better elucidate the concept for his home listeners. See, for example, Crosswell [22].

In 1929, Hubble discovered that such a redshift-distance law did exist [23], and this caused Lemaitre's work to be reassessed by Eddington, who had led the research on the previous eclipse experiments. Hubble came up with a ratio of recession velocity to distance, the *Hubble constant*, of about  $500 \text{ km s}^{-1} \text{ Mpc}^{-1}$ , out by a factor of ten on today's best calculation and, looking at the data points Hubble had to work with, it is remarkable that he came this close, see Fig. 1.1. This evidence for an expanding Universe caused Einstein to drop the Cosmological Constant from his equations and regret that he had not originally followed where the mathematics led him; to foresee a dynamical Universe.

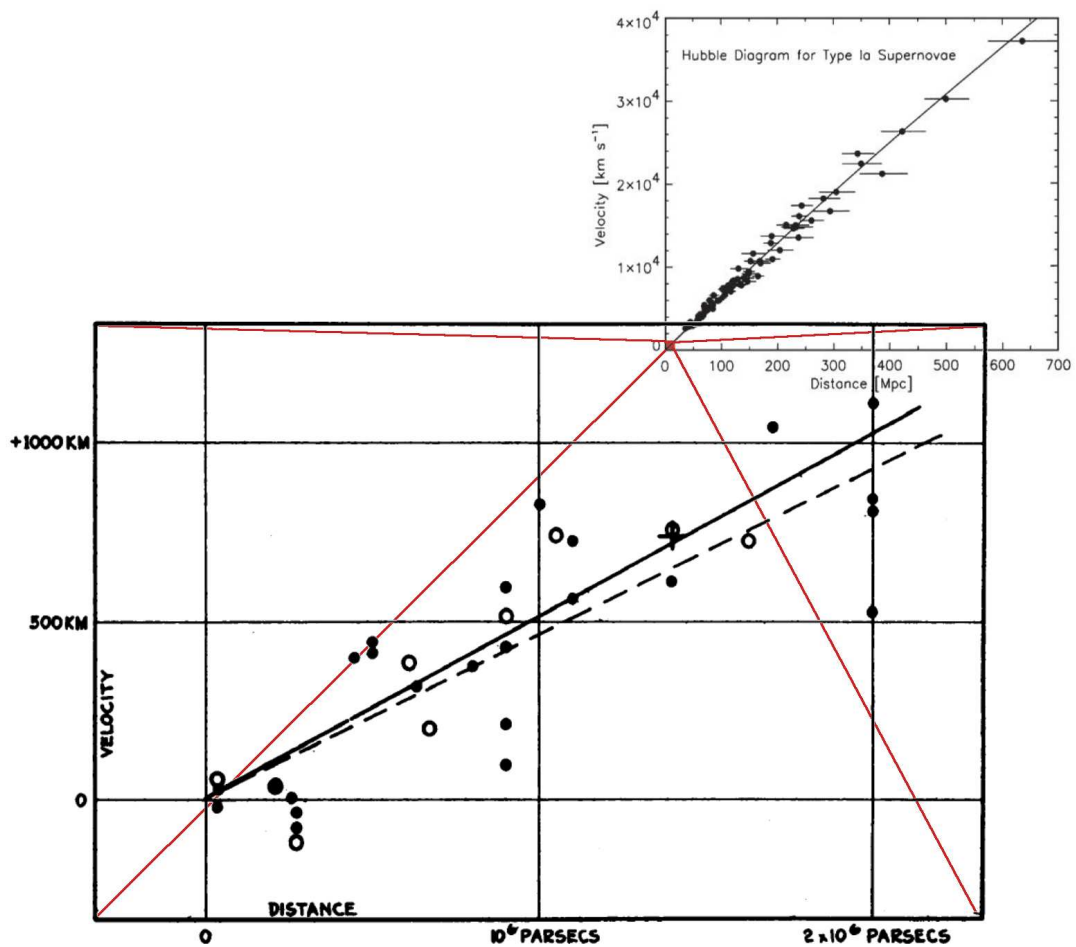


**Figure 1.1:** Hubble's original data [23], compared with that of more recent surveys (see Kirshner [24] for image and data references). Note the difference in scale.

In formulating the FLRW metric, and subsequent Friedmann equations, Friedmann and Lemaitre had employed a modern version of the Copernican Principle, the Cosmological Principle. This assumed that the Universe on large scales is homogeneous and

isotropic. That is, the same everywhere and with no preferred direction. Friedmann and Lemaitre had previously assumed that their metric was the only one consistent with the Cosmological principle, and in 1935, Robertson [25] and Walker [26] independently proved this rigorously.

The FRLW metric can be written in dimensionless, co-moving spherical coordinates as

$$ds^2 = c^2 dt^2 - a^2(t) \left( \frac{dr^2}{1 - kr^2} + r^2 (d\theta^2 + \sin^2\theta d\phi^2) \right). \quad (1.7)$$

We use a Lorentzian metric with convention  $(+, -, -, -)$ , although personal experience suggests that this convention is becoming increasingly less common. We set  $c = 1$  from now on, unless otherwise stated. The scale factor,  $a(t)$  describes the expansion or contraction of the Universe, while the curvature enters as  $k$ , scaled to be  $+1$ ,  $0$ , or  $-1$  for Universe exhibiting positive, zero, or negative constant curvature.

Generally, the energy-momentum content of the Universe is considered to take the form of a perfect fluid. This can be written

$$T_{\mu\nu} = (\rho + p)u_\mu u_\nu - pg_{\mu\nu}, \quad (1.8)$$

where  $\rho$  is the energy density,  $p$  is the pressure, and  $u_\mu$  is the four-velocity of the fluid. In co-moving coordinates, the four-velocity will take the form  $u_\mu = (1, 0, 0, 0)$ . Local conservation of energy,  $\nabla_\mu T_\nu^\mu = 0$ , with the covariant derivative

$$\nabla_\mu T_\nu^\mu \equiv \partial_\mu T_\nu^\mu + \Gamma_{\alpha\mu}^\mu T_\nu^\alpha - \Gamma_{\nu\mu}^\alpha T_\alpha^\mu \quad (1.9)$$

leads to an equation known as the *fluid equation*, or the *energy conservation equation*

$$\dot{\rho} + 3\frac{\dot{a}}{a}(\rho + p) = 0. \quad (1.10)$$

Substituting the energy-momentum tensor and the FLRW metric into the Einstein equations gives the *Friedmann equation* (the i-i component)

$$\left(\frac{\dot{a}}{a}\right)^2 = H^2 = \frac{8\pi G}{3}\rho - \frac{k}{a^2}, \quad (1.11)$$

and the *acceleration* or *Raychaudhuri equation* (0-0 component)

$$\frac{\ddot{a}}{a} = -\frac{4\pi G}{3}(\rho + 3p). \quad (1.12)$$

We note that the Friedmann equation and energy conservation equation imply the Raychaudhuri equation, or alternatively, the Raychaudhuri equation and the energy conservation equation can be combined to obtain the Friedmann equation. That is, the equations are not independent. We have also defined here the *Hubble parameter*,  $H_0 = \dot{a}/a$ ; the rate of expansion of the Universe that first emerged in Hubble's law as the constant of proportionality between the speed of a galaxies recession, and its distance from us. From the Friedmann equation, we can define a critical density in the Universe,  $\rho_{\text{crit}}$ , that would be required to make the Universe flat ( $k = 0$ ),

$$\rho_{\text{crit}} = \frac{3H_0^2}{8\pi G}. \quad (1.13)$$

This allows a convenient way of considering the different types of matter that appear in the Universe. We write

$$\Omega_i = \frac{\rho_i}{\rho_{\text{crit}}}, \quad (1.14)$$

where the subscript  $i$  can represent matter, radiation or a term encompassing any other type of matter-energy component that we might envisage. For a *flat* Universe, where the global geometry is Euclidean, we necessarily have  $\sum_i \Omega_i = 1$ . There have recently been indications that the simplifying assumptions of homogeneity and isotropy in the Universe may be too specific. It has been suggested that the much discussed 'axis of evil' [27, 28] may highlight a specific direction in the Universe. There has also been a large amount of study on the Bianchi models (see, for example, Matzner and Tolman [29]), which discuss isotropy, with the FLRW universe being a special case of certain types of Bianchi classification.

### First Indications of Dark Matter

Once the nebulae had received their correct interpretation as galaxies in their own right, rather than objects within our own galaxy, it wasn't long before there appeared to be something wrong with the observations that were being made.

Using 'just' Newtonian mechanics, Fritz Zwicky was the first to notice that something was amiss [30]. In applying the virial theorem to the Coma cluster, he noticed that a large proportion of its mass appeared to be 'missing', that is, unseen. The virial

theorem says that

$$\text{Total K.E of a stable system} \sim \frac{1}{2} \text{Gravitational binding energy} \quad (1.15)$$

By measuring the movement of a system, one can infer its mass. Comparing the average mass of the galaxies in the Coma cluster, with the mass expected from the cluster's luminosity, the visible part of the system, he found that the amount of visible mass was  $\sim 100$  times smaller than the mass that appeared to be there. This observation was largely dismissed at the time.

We have given an overview of how the *Hot Big Bang* model came to be established; the 'hot' part of the name describing the extremely high temperatures and energies present in the earlier stages. We are of course missing one famous, and critical piece of evidence that we now come to.

### The CMB

The Hot Big Bang model has many successes. Perhaps, most notably, it predicts the decoupling of photons and matter after *recombination*, to produce a black-body spectrum of radiation in the Universe, which would become known as the *Cosmic Microwave Background* (CMB). Theoretical suggestions that could be interpreted as early forerunners of CMB physics were predicted as early as 1941 by McKellar [31], and Dicke [32]. The first serious estimate of a microwave background temperature of cosmic origin were made by Gamow, Alpher and Hermann in 1948 [33, 34, 35], but these were not recognised widely in the community. A few authors worked on the idea, perhaps most notably Doroshkevich and Novikov [36] who suggested that the CMB should be detectable. Dicke, Peebles, and Wilkinson at Princeton set up an experiment to go about detecting the background radiation.

At this point, the history of CMB experimentation takes a serendipitous turn. Penzias and Wilson were two experimental physicists from Bell Labs, developing extremely sensitive microwave receivers for radio astronomy. Working on the removal of residuals and systematics, they found a microwave signal with an approximate temperature of 3K. This signal was found to be independent of the direction that their Horn Antenna was pointed in, and of constant magnitude. Understandably flummoxed by this system-

atic error that they could not get rid of, they eventually concluded that the source was extra-galactic. Penzias then came across a preprint of a paper by Peebles, describing the possibility of a relic radiation from the Big Bang. The two groups got in contact and came to the conclusion that Penzias and Wilson had indeed discovered the relic radiation. They arranged to publish their findings simultaneously in the *Astrophysical Journal* [37]. The Dicke collaboration continued with their own experiment, which confirmed the findings of Penzias and Wilson [38, 39].

In a somewhat controversial move, in 1978 the Nobel prize committee awarded Penzias and Wilson the physics prize for their discovery. Questions were raised about the award because, although the two physicists were obviously highly skilled in their field, they were apparently unaware of the theoretical progress that had been made on the concept of a relic radiation from the Big Bang, and made the discovery essentially by accident.

Another success of the Hot Big Bang model is its accurate prediction of the light element abundances, or *primordial nucleosynthesis* [40], correctly predicting the fractions of Hydrogen, Helium and Lithium that are observed today. These two pieces of evidence are perhaps the Big Bang model's biggest achievements.

### Problems with the Hot Big Bang Model

There are, however, a number of problems associated with the Big Bang model. These are commonly known as the *flatness* problem, the problem of *unwanted relics*, and the *homogeneity and isotropy* problem, which stems from the *horizon* problem.

The *flatness problem* appears as a fine tuning problem. We have seen from Einstein's equations how the matter and energy content of the Universe defines for us the global curvature. It turns out that if the Universe is not flat, then it evolves away from flatness very quickly. From observations, the Universe appears very flat today [41], so earlier in the history of the Universe, it must have been even closer to flatness.

It should be noted that the flatness problem is only really a problem if the Universe does not have precisely zero curvature. Current measurements seem to be focusing in on the exactly flat case, however, any deviation would mean that the Universe is not flat. If the Universe was flat to start with, then the problem becomes moot, as the

Universe will remain flat, otherwise a topology change would be required to take place at some stage in the Universe's history. As flatness ( $k = 0$ ) is a particular case of the of the topologies that the Universe could have chosen,  $k = -1, 0, 1$ , then the question could be changed to "why flat?", but it would not be a problem inherent in the Big Bang model.

The *horizon problem* is a problem of causality in the early Universe. The particle horizon at last scattering represents an angle of only about one degree on the sky at the present day. That is, regions of space that subtended an angle of about one degree on the sky have never been in causal contact. Yet the temperature that we measure in each of these regions agrees to about one part in ten thousand. This is an unprecedented level of agreement for regions of space that have never been in contact with each other. This in turn leads to the problems of *homogeneity and isotropy*. Again, the CMB tells us that the temperature fluctuations at decoupling were very smooth. From this we can infer that the density perturbations in the early Universe were also particularly smooth. This level of smoothness in the early Universe requires a high level of fine tuning in the Big Bang scenario. One could imagine that a 'generic state' of density perturbations produced by the Big Bang would be far from smooth.

There are also problems with *unwanted relics* in the early Universe for the Big Bang model. It is expected that the fundamental forces that we see today emerged from the breaking of symmetries representing unified forces at higher temperatures, early in the Universe. The electroweak force, for example, can be represented by the gauge group  $SU(2) \times U(1)$ . This is spontaneously broken at lower temperatures to the  $U(1)$  group of electromagnetism. With the Higgs mechanism, this spontaneous symmetry breaking produces the force carrying *gauge bosons* of the electromagnetic and weak interactions:  $W^\pm$ ,  $Z^0$  and  $\gamma$ . We will discuss these concepts in more detail later. The formulation of the electroweak theory by Glashow, Weinberg and Salam correctly predicted the masses of the gauge bosons, before they were subsequently discovered in 1983 at the UA1 and UA2 experiments carried out with the Super Proton Synchrotron at CERN. Carlo Rubbia and Simon van der Meer led these experiments, and were subsequently awarded the Nobel prize in 1984. Glashow, Weinberg and Salam were awarded the Nobel prize for their theoretical work in 1979.

Many theorists anticipate that the other fundamental forces will unify at higher temperatures into a *Grand Unified Theory* (GUT). The problem with this in terms of Big Bang cosmology is that the breaking of these higher symmetries typically produces topological defects such as magnetic monopoles. These monopoles would be expected to dominate the energy density of the Universe. However, not one has been observed at this time. Other relics that are possibly more relevant with regard to the interest in supersymmetry and string theory are the gravitino and the spin-zero particles corresponding to the moduli in string theories. The effects of the gravitino on nucleosynthesis have been considered [42], as well as the implications for cosmology from moduli [43, 44].

The origin of the *matter-antimatter asymmetry* is also a problem for the Big Bang scenario. The Big Bang scenario suggests that matter and anti-matter should be produced in equal amounts at the time of formation, and hence one would expect to observe nothing today, as all matter and antimatter would have annihilated. This is clearly not the case. There must be some mechanism to produce a matter-antimatter asymmetry in the early Universe.

## 1.1.2 Inflation and Dark Energy

### Resolving the Problems: Enter Inflation

A period of exponential expansion in the early Universe, would solve the problems associated with the Hot Big Bang model. Just such a model was proposed independently by Starobinsky [45, 46] and Guth [47], and later revised by Linde [48, 49] and Albrecht and Steinhardt [50], to become the standard *slow roll inflation* model.

Inflation is a period of super-luminal expansion, and can be defined in terms of the scale factor as occurring when  $\ddot{a} > 0$ . We recall that the Raychaudhuri equation, eqn. (1.12) is

$$\frac{\ddot{a}}{a} = -\frac{4\pi G}{3}(\rho + 3p),$$

and we can see that a period of inflation leads to the condition

$$p < -\frac{1}{3}\rho. \tag{1.16}$$

We recognise this as meaning that the *strong energy condition* is violated. For a fluid with general equation of state

$$p = \omega\rho, \quad (1.17)$$

we get a period of inflation if

$$-1 \leq \omega \leq -\frac{1}{3}. \quad (1.18)$$

This leads to the scale factor behaving as

$$\begin{aligned} a \propto t^{\frac{2}{3(1+\omega)}} & \quad \omega \neq -1 \\ e^{Ht} & \quad \omega = -1. \end{aligned} \quad (1.19)$$

Hence, if  $-1 < \omega \leq -\frac{1}{3}$ , we have power law inflation, and if  $\omega = -1$  (the Cosmological Constant case), then we have exponential inflation.

We can use this idea to solve the flatness problem. We have already seen that a flat geometry requires  $\sum_i \Omega_i = 1$ . Using eqns. (1.10), (1.12) and 1.12, along with the equation of state  $P = \omega\rho$ , we can write

$$\dot{\Omega} = (1 + 3\omega)H\Omega(\Omega - 1). \quad (1.20)$$

If  $\omega > -1/3$ , then  $\Omega = 1$  (the flat case) can be shown to be an unstable fixed point. If, however,  $\omega < -1/3$ , then  $\Omega = 1$  instead becomes an attractor, so at the end of inflation,  $\Omega \rightarrow 1$ , regardless of its value previously.

Inflation can also ‘flatten’ density perturbations. Eqn. (1.20) can also be considered on a local scale. If  $\Omega > 1$ , then there is an overdensity, while  $\Omega < 1$  corresponds to an underdensity. If  $\omega > -1/3$  then perturbations grow, while if  $\omega < -1/3$ , perturbations decay. In this way, inflation drives the Universe towards a smooth distribution, and the Universe effectively loses memory of the state it was in before inflation. This goes some way to solving the homogeneity and isotropy problems.

There is also a resolution of the horizon problem. The particle horizon can be written as

$$d_H(t) = a(t) \int_0^t \frac{dt'}{a(t')}, \quad (1.21)$$

or, changing variables, as

$$d_H(t) = a(t) \int_0^a \frac{da'}{a'^2 H(a')}. \quad (1.22)$$

We can see from eqn. (1.19) that

$$H \propto a^{-\frac{3}{2}(\omega+1)}, \quad (1.23)$$

so

$$d_H \propto a^{\frac{3}{2}(\omega+1)}. \quad (1.24)$$

Below the critical value of  $\omega = -1/3$ , we see that the horizon distance decreases with increasing time. During a period of inflation, the co-moving Hubble radius decreases, and so the particle horizon tends to infinity. If inflation continues for long enough, the entire observable Universe can emerge from a single causally connected region.

Inflation will also dilute the number of unwanted relics, so that the predicted number and energy densities are not in conflict with what is observed today.

To obtain a period of exponential inflation, we require a form of energy that violates the strong energy condition, and gives rise to negative pressure. A scalar field can be imbued with the properties necessary to fulfil these conditions.

### Scalar fields in Cosmology

Scalar fields have been used recently to describe the unknown forms of matter and energy we believe to be prevalent in the Universe. Invoking as yet unseen fields imbued with the properties we require, in order to explain observations, could be considered to be a statement of our ignorance concerning the nature of the substances that appears to dominate our Universe, but there are also very good reasons for suggesting that they should play an integral role in our understanding of the matter content of the Universe.

The primary motivation comes from particle physics. In the Standard Model, the particle content is made up of quarks and leptons, spin-half particles, and the gauge bosons which mediate the interactions between them: the photon for the electromagnetic force, the  $W^\pm$  and  $Z^0$  bosons for the weak nuclear force, and the gluon for the strong force, all of which are spin-one particles. The graviton mediates the gravitational interaction, and is a spin-two boson, but is not part of the Standard Model as the Standard Model has not yet been successfully extended to include gravitational interactions. The mass of a particle also tells us something about the interaction strength associated with it. The photon and the graviton are both massless, and hence travel at the speed of light

and have a range of interaction that is infinite. The gluon is theoretically massless, but its range is limited by colour confinement. The  $W$  has a mass of 80 eV, while the  $Z$  has a mass of 91 eV, and their range is limited. The question is, how do particles acquire this mass? The prevailing theory at the moment is the Higgs mechanism, which gives the mass of the particles through a phenomena known as *symmetry breaking*. This idea is explained in much more detail later in this thesis. This theory completes the Standard Model by positing a spin-zero particle known as the Higgs boson. Spin-zero particles can be associated with scalar fields. The pion field, for example, can be associated with a scalar field, and so can the other mesons and the bosons. However, the pion field is not a true scalar, but rather a pseudo-scalar, as it breaks parity invariance. It is also not a fundamental scalar particle, as it can be broken down into quarks. So far, no fundamental scalar particles have been detected; the Higgs would be the first.

Supersymmetry is an extension to the Standard Model that posits a symmetry between bosons and fermions. It was originally introduced in order to solve the hierarchy problem. That is, why the gravitational force is so much weaker than the other forces. If supersymmetry is correct, it would also provide a natural way of acquiring fundamental scalar fields in particle physics, and hence cosmology. Every spin-half field would be associated with a spin-zero or spin-one field, in what is called a chiral, or gauge, multiplet. This explanation also requires us to understand why the symmetry between fermions and bosons is broken. That is, why we have not seen any of the superpartners. We expect each superpartner to have an identical mass to its partner, but know that this is not the case, as we would have already seen them. At some energy scale, supersymmetry is broken. This could be viewed as merely shifting the hierarchy problem. We may start to see signs of the superpartners, as well as the Higgs, at the LHC. The lightest of these, and hence the most likely to be seen, is the neutralino. This is formed from mass eigenstates of the superpartners of the gauge bosons, and has also been suggested as a promising dark matter candidate [51].

In what might be considered more speculative theories, a field known as the *dilaton* is present in string theories, and mediates the string coupling between strings or branes in higher dimensions. The dilaton has also been considered as the scalar field responsible for inducing inflation [52, 53]. Kaluza-Klein [54] theories use a scalar field to

attempt to unify the gravitational and electromagnetic interactions in a higher dimensional space. Whether this higher dimensional space takes on a real physical meaning, or is just a mathematical tool awaiting a more ‘acceptable’ interpretation, is an open question. In Tensor-Vector-Scalar theories [55], which usually seek to explain the discrepancies in the matter-energy content of the Universe as deviations from Newton’s law or General Relativity, scalar fields are often used to model the gravitational interaction in a similar way to Kaluza-Klein theories.

Scalar fields also abound in condensed matter, and we will see how the phenomena of symmetry breaking can be interpreted as introducing a photon mass term, explaining the cutoff in the interaction length present in superconductors, in what is known as the *Meissner effect*. The scalar fields in this case are not fundamental, instead representing some macroscopic order parameter that has an interpretation in terms of, for example, the density of particles or charge carriers in a material. The question of interpretation is important, and there have been suggestions that the Higgs field, or other fundamental scalar fields, may also turn out to be similarly phenomenological [56, 57], possibly awaiting a microscopic description in terms of quantum gravity.

We can see very easily why scalar fields are a candidate for driving a period of exponential expansion. A scalar field has a kinetic and potential term associated with it, and so we can write down a Lagrangian for a non-spatially varying scalar field,  $\phi \equiv \phi(t)$ ,

$$\mathcal{L} = g^{\mu\nu} \partial_\mu \phi \partial_\nu \phi - V(\phi), \quad (1.25)$$

and vary it with respect to the metric to obtain the energy-momentum tensor

$$T_{\mu\nu} = \partial_\mu \phi \partial_\nu \phi + g_{\mu\nu} \left( -\frac{1}{2} g^{\alpha\beta} \partial_\alpha \phi \partial_\beta \phi + V(\phi) \right). \quad (1.26)$$

With the perfect fluid form of the energy-momentum tensor, eqn. (1.8), we find that

$$p_\phi = \frac{\dot{\phi}^2}{2} - V(\phi), \quad (1.27)$$

$$\rho_\phi = \frac{\dot{\phi}^2}{2} + V(\phi), \quad (1.28)$$

with the Euler-Lagrange equations giving

$$\ddot{\phi} + 3H\dot{\phi} + \frac{dV(\phi)}{d\phi} = 0. \quad (1.29)$$

If  $\dot{\phi}^2 \ll V(\phi)$ , and  $\ddot{\phi} \ll 1$ , then we find that the scalar field mimics a fluid with equation of state

$$P_\phi \simeq -\rho_\phi, \quad (1.30)$$

i.e.  $\omega \simeq -1$ , just what we require for exponential inflation, with the evolution given by the *slow roll* equations,

$$3H\dot{\phi} = -\frac{dV(\phi)}{d\phi}, \quad (1.31)$$

$$H^2 = \frac{8\pi G}{3}V(\phi), \quad (1.32)$$

from eqns. (1.13) and (1.29). This also provides a natural mechanism with which to end inflation. The slow roll conditions are violated when the field begins to fast roll along its potential, eventually reaching the minimum and oscillating around it. *Reheating* occurs due to this oscillation, and the energy of the inflaton field is transferred to radiation.

### Density Perturbations from Inflation

Once Guth's idea had time to develop, it was quickly realised that inflation may provide a mechanism for producing the density perturbations required to kick-start structure formation. This was realised essentially simultaneously by a number of people participating in the Very Early Universe Conference in Cambridge in 1982 [58]. A number of papers that provided an explanation of the density perturbations were produced in quick succession [59, 60, 61, 62].

The inflationary paradigm has attracted some criticism as it is not really able to explain the origin of the inflaton field, which is added in a rather ad hoc fashion, but it has endured precisely because it does so well in explaining the observations taken by the various precision instruments that have been recently commissioned. A number of potential pitfalls have also arisen in the inflationary scenario, usually in relation to the fine tuning of initial conditions [63, 64]. One of the most serious problems could be considered to be that, in order for inflation to start, the Universe must already be homogeneous on superhorizon scales [65], leading again to the fine tuning of initial conditions present in the problem of homogeneity and isotropy. We will not dwell on

such problems here, except to note that they exist. For progress in their resolution see, for example, Lieu and Kibble [66].

A particular success of the inflationary paradigm comes from the prediction of density fluctuations, leading to an explanation of the large scale structure that we see today.

The explanation of primordial density perturbations is perhaps one of the most successful attempts, along with Hawking radiation, to combine General Relativity and Quantum Field Theory.

Classically, we expect the inflaton field,  $\phi$ , to be homogeneous and isotropic. Quantum mechanically however, there will be a perturbation around the vacuum,  $\delta\phi$ . We can decompose this fluctuation into a Fourier expansion of wave modes

$$\delta\phi(\mathbf{x}, t) = \frac{1}{(2\pi)^3} \int \delta\hat{\phi}(\mathbf{k}, t) \exp(i\mathbf{k} \cdot \mathbf{x}) d^3\mathbf{k}. \quad (1.33)$$

An auto-covariance function can be written as

$$\langle \delta\hat{\phi}(\mathbf{k}_1, t), \delta\hat{\phi}(\mathbf{k}_2, t) \rangle = (2\pi)^3 P_{\delta\phi}(|\mathbf{k}|, t) \delta^{(3)}(\mathbf{k}_1 - \mathbf{k}_2), \quad (1.34)$$

defining for us a *power spectrum* of fluctuations in the inflaton field. There are then some complicated steps to relate the fluctuations in the inflaton field to perturbations in the matter density, which we will leave out as they are not especially illuminating from the point of view of this introduction and the rest of the thesis, but we can explain qualitatively.

We have already seen how the matter-energy content of the Universe, which can include scalar fields, is coupled to the spacetime metric via Einstein's equations. Hence, any fluctuation in the inflaton field will also be manifest as fluctuations in the metric describing the geometry of spacetime. We can think of this as different regions of the Universe experiencing slightly less, or slightly more, inflation. Metric perturbations will also be stretched to cosmological scales, and cause baryons and photons to cluster together in the gravitational potential wells created. When inflation ends, increasingly large wavelengths will gradually become shorter than the causal horizon length, setting up *acoustic oscillations* in the photon-baryon fluid. So, any perturbation in the inflaton field  $\delta\phi(\mathbf{x}, t)$ , will lead to perturbations in the density field  $\delta\rho_m(\mathbf{x}, t)$ . At the end of inflation, the inflaton field may also decay into conventional matter, producing inherited perturbations  $\delta\rho_i(\mathbf{x}, t)$  in the densities of each particle species,  $i$ .

Defining the density contrast

$$\delta_m(\mathbf{x}, t) = \frac{\delta\rho_m(\mathbf{x}, t)}{\bar{\rho}_m}, \quad (1.35)$$

where  $\bar{\rho}_m$  is the homogeneous mean density value, we can decompose the density perturbations into a Fourier series

$$\delta_m(\mathbf{x}, t) = \frac{1}{(2\pi)^3} \int \hat{\delta}_m(\mathbf{k}, t) \exp(i\mathbf{k} \cdot \mathbf{x}) d^3\mathbf{k}, \quad (1.36)$$

and define a power spectrum from the correlation function,

$$\langle \hat{\delta}_m(\mathbf{k}_1, t) \hat{\delta}_m(\mathbf{k}_2, t) \rangle = (2\pi)^3 P_m(|\mathbf{k}|, t) \delta^{(3)}(\mathbf{k}_1 - \mathbf{k}_2). \quad (1.37)$$

It is then possible to relate the two power spectra by a transfer function, encapsulating the physics we described above.

$$P_m(|\mathbf{k}|, t) \sim \mathcal{T}(|\mathbf{k}|, t) P_{\delta\phi}(|\mathbf{k}|, t). \quad (1.38)$$

The density of a photon fluid is related to the temperature by  $\rho_r \sim T^4$ , and so the density perturbations can be related to the temperature on the sky,

$$\delta_m(\mathbf{x}, t) = \frac{\delta\rho_m(\mathbf{x}, t)}{\bar{\rho}_m} \sim \frac{\delta T}{T}. \quad (1.39)$$

It is precisely these temperature differences that satellites such as COBE and WMAP measure, and hence calculate the correlation functions. The acoustic oscillations manifest themselves as Doppler peaks in the CMB power spectrum. That these measurements agree so well with the fluctuations predicted by the inflationary paradigm gives significant credence to the model.

The power spectrum then, is the two-point correlation function of the Fourier transform of the density contrast. If the vacuum fluctuation for each Fourier component of the inflaton  $\delta\hat{\phi}_{\mathbf{k}}(t)$  are uncorrelated and evolve independently of each other, then they can be represented by a Gaussian distribution function, so that the real-space one-point probability distribution of matter fluctuations is given by

$$p_m(\delta_m) = \frac{1}{(2\pi\sigma_m^2)^{\frac{1}{2}}} \exp\left(-\frac{\delta_m^2}{2\sigma_m^2}\right), \quad (1.40)$$

where the variance,  $\sigma_m^2 = \sigma_m^2(t)$ , is defined by  $\sigma_m^2 = \langle \delta_m^2 \rangle$ , and is related to the power spectrum via

$$\sigma_m^2 = \frac{1}{2\pi^2} \int_0^\infty P_m(k, t) k^2 dk. \quad (1.41)$$

For a Gaussian distribution, the two-point correlation function provides a complete statistical coverage of the density perturbations.

Further information about particular models of inflation is bound up in the *non-Gaussianity*, and the *spectral running*. Non-Gaussianity will reveal itself in the higher order correlation functions such as the bispectrum [67, 68, 69, 70]. It is usually assumed that the power spectrum defined by the two-point correlation function will take the form of a power law

$$P_m(|\mathbf{k}|, t) \sim k^{n_s-1}, \quad (1.42)$$

where  $n_s$  is known as the *spectral index*, or *running*. For  $n_s = 1$  we have the scale invariant *Harrison-Zeldovich* spectrum. Standard inflation models also assume that the inflaton vacuum fluctuation has negligible interaction with itself and other fields, leading to a prediction of a Gaussian adiabatic density perturbation, and a spectral index close to 1. This is in agreement with what is observed. Experiments with higher precision, such as the Planck satellite, will hopefully be sensitive enough to detect deviations, and hence be able to place bounds on various inflationary models.

### Experiments, and a Surprising Result

After Penzias and Wilson's CMB detection, a number of experiments were designed with the hope of measuring the CMB more accurately, and detecting anisotropies, which would help to constrain models of the early Universe, such as inflation. A Soviet satellite, RELIKT-1, was launched in 1983 and produced upper limits on the anisotropies in the CMB [71]. The *Cosmic Background Explorer* (COBE) experiment was launched in 1989, and the Far Infrared Absolute Spectrophotometer (FIRAS) instrument on board measured with unprecedented accuracy the black-body form of the CMB, providing unambiguous evidence for a Big Bang scenario [72, 73, 74]. The Differential Microwave Radiometer (DMR) instrument found for the first time evidence of anisotropies in the CMB spectrum [75], although the resolution of the satellite was not enough to extract much meaningful information about them. Results from the RELIKT-1 satellite were also reexamined around this time, and claimed a detection of a black-body curve and anisotropies [76]. George Smoot and John Mather of the COBE team were awarded the Nobel prize in 2006 for the discovery.

Three balloon-based experiments TOCO/MAT (or QMAP), the Millimetre Anisotropy eXperiment IMaging Array (MAXIMA) and the Balloon Observations Of Millimetric Extragalactic Radiation and Geophysics (BOOMERanG) experiment were launched around 1998. TOCO published the first accurate detection of the CMB acoustic oscillation peaks in 1999 [77, 78], which were quickly confirmed by the MAXIMA [79] and BOOMERanG experiments [80, 81]. In the year these experiments were launched, an unexpected detection would come to make their results even more relevant. Galaxy rotation curves, mass-to-light ratios, CMB anisotropies and light element abundances all suggested that the majority of matter in the Universe is non-baryonic. Inflation suggested that spatial sections of the Universe should be flat. We have seen that this requires  $\sum_i \Omega_i = 1$ . In lieu of any other evidence for other matter sources, and in spite of no direct physical evidence, most theorists were of the opinion that the Universe should be flat, and consisted only of matter,  $i = m$ , so that  $\Omega_m = 1$ . Others took the view that the evidence was pointing to the  $k = -1$  case, and some inflationists modified their models to allow for an open Universe [82, 83]. Regardless of the topology, all the available evidence from observations and measurements of galaxy cluster dynamics, galaxy clustering, large-scale galaxy motions and gravitational lensing suggested a baryonic to dark matter ratio of about 30:70, see Ellis and Coles [84] for a review. This suggested that the majority of matter in the Universe should be dark. That is, almost inert with respect to three of the physical forces. Not responding to the electromagnetic force, for example, would render it invisible. Its only interaction would be gravitational, so its influence would be seen only as an effect on surrounding baryonic matter. There were some early suggestions that a *dark energy* component might account for the  $\sim 70\%$  discrepancy between the measured mass density and the critical energy density predicted by inflation [85, 86, 87, 88], but generally it was expected that if the discrepancy was to be made up, it would be made up by dark matter. This picture describing the matter components of the Universe would be overhauled by an influx of observational evidence due to advances in experimental techniques. High precision measurements of supernova brightness and redshift by the Supernovae Cosmology project [89, 90], and the High- $z$  Supernova Search [91], indicated that the Universe was not only expanding, but accelerating in that expansion. Other evidence later emerged to suggest that the onset of this expansion was only fairly recent [92, 93].

This most recent period of accelerated expansion of the Universe can be thought of as another period of inflation, albeit a less dramatic one. For a period of accelerated expansion, we again need a contribution to the energy-matter component of the Universe that will give rise to negative pressure. From the acceleration equations we again need  $\ddot{a} > 0$  for accelerated expansion, which requires an equation of state for the dark energy fluid of

$$P = \omega\rho, \quad (1.43)$$

with

$$-1 \leq \omega \leq -\frac{1}{3}. \quad (1.44)$$

Data provided by the Supernova search teams allows one to plot luminosity distance against redshift and compare the values against theoretical curves. This is shown in Fig. 1.2, and from Fig. 1.3, we can see that a value of  $\omega = -1$  seems to be preferred. The luminosity distance - redshift relation can also provide information about possible evolution of  $\omega$ . Some scalar field models of dark energy consider an  $\omega$  parameter that is greater than  $-1$ , or can evolve in time, sometimes tracking the radiation density to provide a natural solution to the cosmological constant problem. These are known as *quintessence models*. See Copeland, Sami and Tsujikawa [94] for a review.

So, the cosmological constant,  $\Lambda$ , has reappeared. Rather than keeping the Universe static, by providing support against gravitational collapse, as originally envisaged by Einstein, it now produces the driving force behind the accelerated expansion.

Two other survey experiments were conducted around this time, which would determine more accurately the cosmological parameters. The 2dF Galaxy Redshift Survey (2dFGRS) produced an accurate measurement of the density parameter of matter, as well as detecting the baryon acoustic oscillations, leading to an estimate of the ratio of dark matter to normal matter [95, 96]. The Sloan Digital Sky Survey (SDSS) complemented this by putting constraints on the parameters describing the matter and energy contents of the Universe [97, 98].

But perhaps the most significant experiment was a satellite based one, the Wilkinson Microwave Anisotropy Probe (WMAP). This was launched in 2001, and released its first dataset in 2003. Combined with the datasets provided by all the previous experiments, it mapped out with unprecedented accuracy the peaks of the baryon acoustic

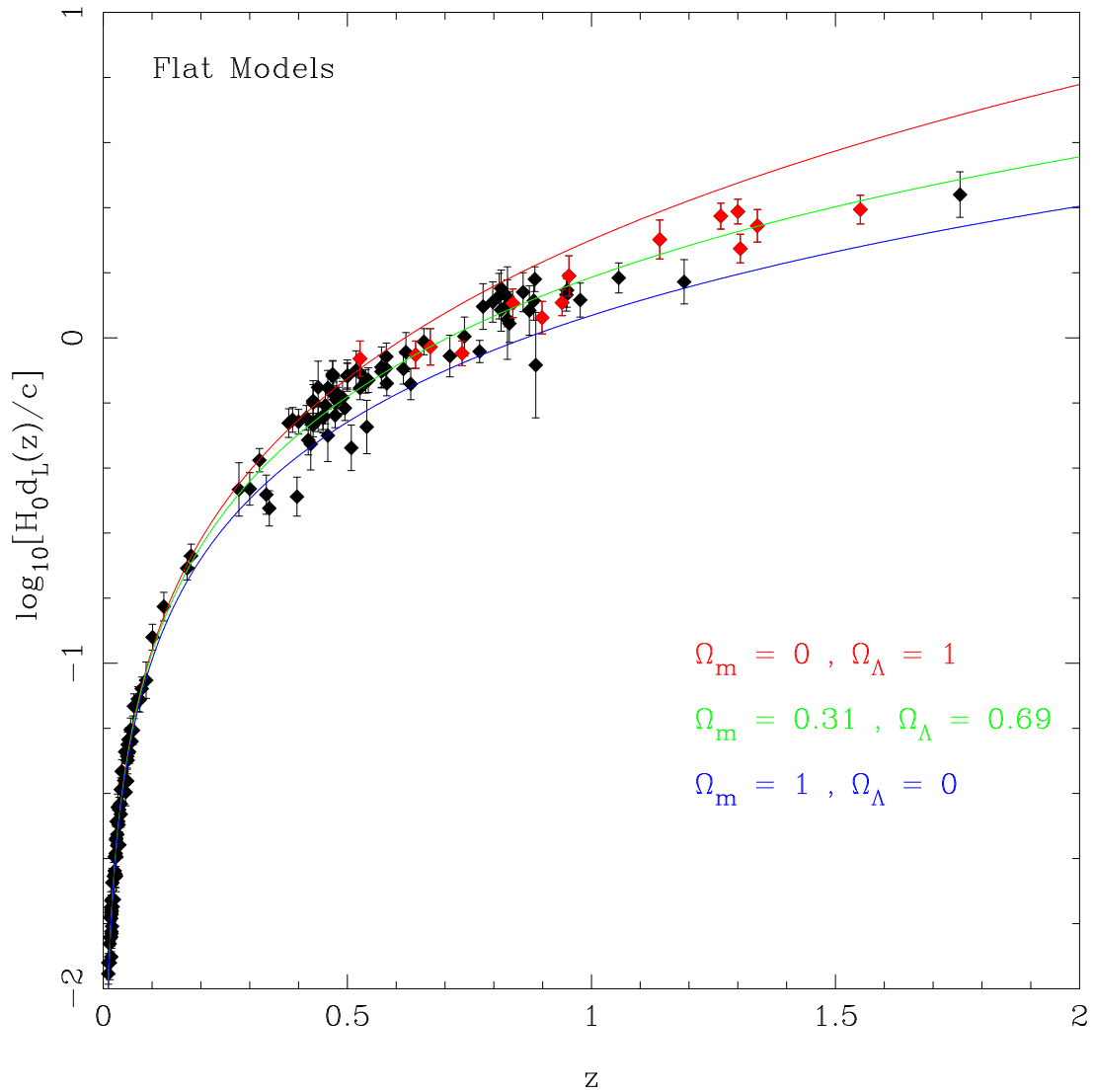


**Figure 1.2:** Comparison of  $\Lambda$  CDM models. From Choudhury and Padmanabhan [99]. Observational data points are obtained from the ‘Gold’ sample of Riess et al. [100] from the High- $z$  Supernova Search.

oscillations, and so provided accurate measurements of the curvature of space, the percentage of dark matter and the cosmological constant.

Figs. 1.4 and 1.5 show the temperature anisotropies and power spectrum from the WMAP five year data release.

It is worth briefly commenting on how this data allows a calculation of the cosmological parameters. To calculate the curvature, we look at the size of the hot and cold spots caused by density fluctuations in the early Universe. We can calculate the actual size that we would expect perturbations, and hence the temperature fluctuations, to have. If we compare this to the apparent size that we actually see, we measure a combination

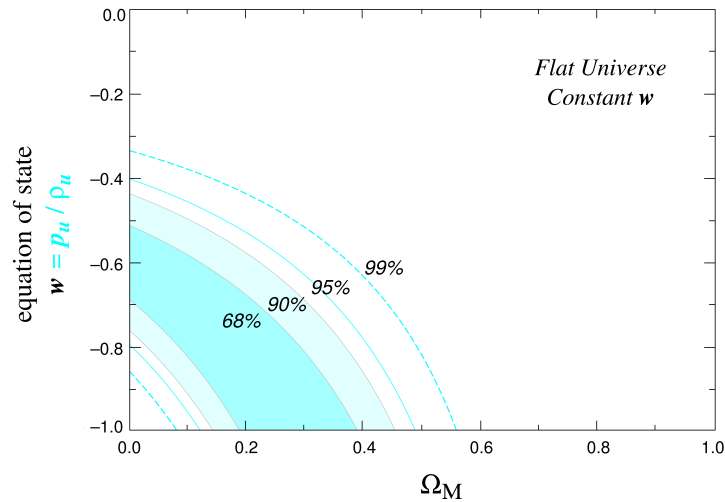


**Figure 1.3:** Equation of state. From the Supernova Cosmology Project [89].

of the distance to the last scattering surface, and the curvature of the path that a photon has taken to reach us. An independent measurement of the Hubble constant tells us the time at which the Universe became transparent to radiation, and hence the distance to the last scattering surface, so defining the curvature uniquely. The size of the spots manifests itself in the location of the peaks. So a negatively curved geometry will push the peaks to the right, while a positively curved one will push them to the left.

The ratio of dark to baryonic matter manifests itself in the height of the peaks. When the acoustic oscillations are set up, the baryonic matter responds to the gravitational pull of the dark matter. Compressions in the primordial sound waves, which correspond to the odd peaks in the power spectrum, will be enhanced by this attraction. The even peaks are produced by the ‘rarefaction’ phase of the oscillation, so comparing the relative heights of the even and odd peaks gives information about the ratio of dark to baryonic matter. The presence of baryonic matter also decreases the sound speed, leading to a lower frequency oscillation. This increases the spacing between peaks.

A cosmological constant would act to reduce gravitational potential wells produced by large scale density perturbations, leading to enhanced power on large angular scales.

The five year data release from WMAP gives some incredibly tight bounds on the parameters describing the Universe. Some of those relevant to our discussion so far are listed in Table 1.1.

The latest satellite mission Planck, will map the temperature power spectrum with

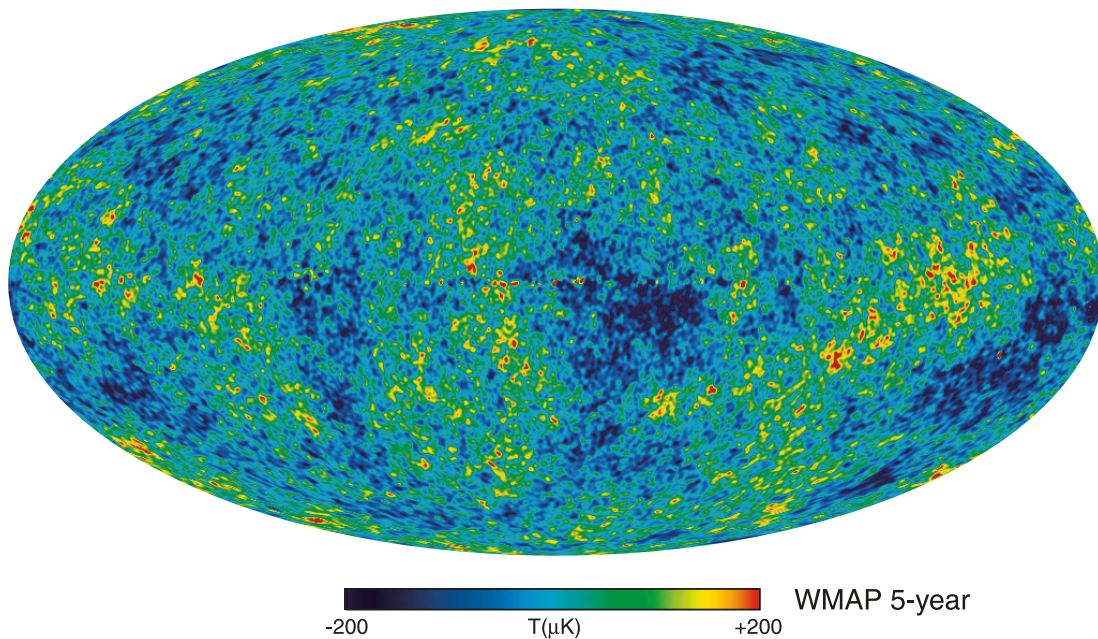


**Figure 1.4:** Temperature anisotropies from WMAP 5 year data [101].

Parameter	Value
Age of Universe	$13.69 \pm 0.13$ Gyr
$\Omega_B$	$0.0441 \pm 0.0030$
$\Omega_{DM}$	$0.214 \pm 0.027$
$\Omega_\Lambda$	$0.742 \pm 0.030$
$\Omega_{Tot}$	$1.099^{+0.11}_{-0.085}$
Equation of State, $\omega$	$-1.06^{+0.41}_{-0.42}$

**Table 1.1:** WMAP 5 Year Parameters.

unprecedented accuracy and resolution, providing the tightest limits yet on the parameters described above. It will also measure parameters describing the non-Gaussianity and spectral running, as well as hopefully producing an unambiguous detection of the CMB *polarisation*.

We now have a Universe that is well described by the FLRW metric, with a cosmological constant. This is known as the  $\Lambda$ CDM model and is currently our best model for the Universe we see around us. We will not be so concerned with dark energy in this thesis, but we will describe models of dark matter, and so we will discuss progress in that area in a bit more detail. Before we do, we will mention some of the techniques used in investigating structure formation.

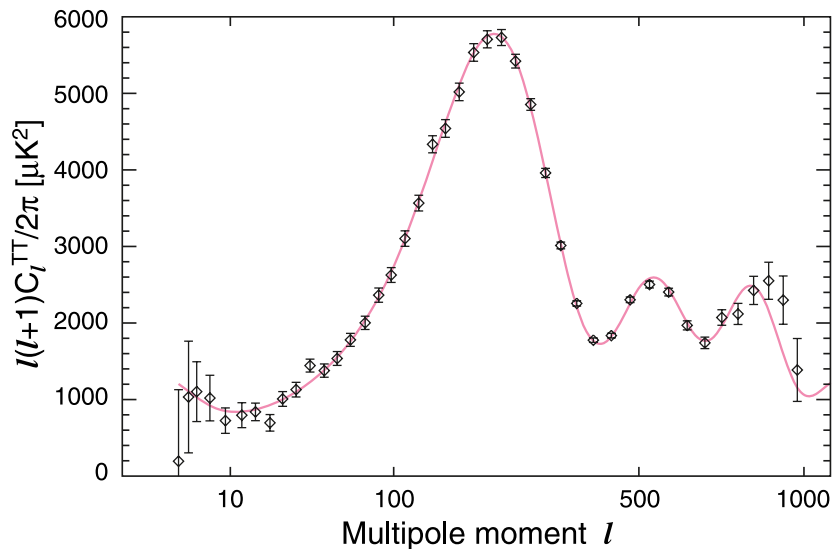


**Figure 1.5:** Power spectrum from WMAP 5 year data [102].

### 1.1.3 The Traditional Approach to Structure Formation

We have seen how perturbations in the inflaton field can seed the density perturbations that lead to large scale structure formation.

In this section we give a brief overview of the techniques used in structure formation scenarios. We will not detail the mathematical steps, but rather state how to get to what we will consider the ‘end result’: the coupled continuity, integrated Euler, and Poisson equations. We will also discuss some of the limitations of these approaches, discussing their possible resolution in terms of a wave-mechanical approach using the Schrödinger-Poisson system in Sections 2.2 and 3.3.

Large-scale structure formation in the early Universe is driven predominantly by gravity. Hydrodynamical and radiative effects can be effectively ignored when considering the density perturbations induced by inflation. Inflationary models also motivate a dark matter candidate. For baryonic matter, radiation pressure prevents the growth of density perturbations until recombination is complete, and small scale density perturbations are largely suppressed by *Silk damping*. Hence, baryonic models struggle to produce sufficiently large density perturbations to generate galaxies and clusters. Non-baryonic matter would not couple electromagnetically, so dark matter density perturbations can start growing long before recombination ends.

At late times in structure formation scenarios, the equations of fluid dynamics, cou-

pled to the Poisson equation are sufficient to give an accurate description. The two predominant fluid dynamic approaches are the *Eulerian* and *Lagrangian* approaches.

In the Eulerian approach, macroscopic fluid quantities such as density and velocity are considered. The evolution of a large number of particles is most conveniently described in terms of a *phase-space distribution function*. If the flow of particles is laminar, as opposed to turbulent, then this distribution function is constant along particle trajectories in phase space; *Liouville's theorem*. These conditions lead to an equation for a collisionless fluid; the *Vlasov equation*, or *collisionless Boltzmann equation*. The *Euler* and *continuity* equations can be obtained directly from the Vlasov equation, by taking *velocity moments* of the distribution function [103]. By specifying an equation of state for the substance being studied, and coupling these two equations to the Poisson equation, we obtain a set of equations that gives an excellent approximation for studying large-scale structure formation in the early Universe.

To make the derivation of these equations simpler, often a laminar approach is used, where fluid stream lines do not cross. This is equivalent to the approximation of vanishing velocity dispersion. To simplify things further, as these coupled equations are often difficult to solve in the general case, the linear regime is often studied. This regime is valid if the density fluctuations are smaller than the mean density, on the large scales associated with structure formation. The other condition required is that the amplitude of each Fourier mode

$$\hat{\delta}_m = \int \delta_m(\mathbf{x}, t) \exp(-i\mathbf{k} \cdot \mathbf{x}) d^3\mathbf{x}, \quad (1.45)$$

should be small, i.e.  $|\hat{\delta}_m| \ll 1$ . When these conditions are valid, the evolution of growing and decaying modes can be readily tracked. It can be shown that in the linear regime, each Fourier mode will evolve independently. Hence, Gaussian perturbations will remain Gaussian in the linear regime.

In hierarchical clustering scenarios, one of the problems with the linear regime is that significant amounts of power can survive the radiation era, and fluctuations start to become nonlinear on small scales, or large  $k$ , with larger and larger scales becoming nonlinear as time goes on.

We remember from eqn. (1.40) that for a Gaussian random field, the real-space one-

point probability distribution of matter density fluctuations is given by

$$p_m(\delta_m) = \frac{1}{(2\pi\sigma_m^2)^{\frac{1}{2}}} \exp\left(-\frac{\delta_m^2}{2\sigma_m^2}\right)$$

Once the variance on a given scale approaches unity, the probability distribution of matter density fluctuations above starts to assign significant probability to the existence of spatial regions with  $\delta_m < -1$ , i.e. negative matter densities. This is clearly unrealistic. In reality, non-linear evolution causes Fourier modes to couple to each other, resulting in the distribution evolving away from Gaussianity, and becoming well approximated by a log-normal distribution [104, 105].

In the *Lagrangian approach* the trajectories of individual fluid elements are followed, where the trajectory of a fluid element is written as  $\mathbf{x} = \mathbf{x}(\mathbf{q}, t)$ , with the Lagrangian coordinate  $\mathbf{q}$ . This approach is used ubiquitously in numerical simulations such as the *Millennium Run*, or other simulations using *Smoothed Particle Hydrodynamics* (SPH). A set of relations exists to move between the Lagrangian and Eulerian prescriptions.

Again, we will not explicitly go through the equations, except to say that they are again only valid in the laminar, or single stream, regime, and can be very difficult to solve analytically. A linearised approach can again be taken, resulting in the *Zeldovich approximation* [106, 107]. The Zeldovich approximation is capable of handling density perturbations  $\delta_m \sim 1$ , and hence can be used to evolve the system beyond the linear regime. N-body simulations can follow the nonlinear regime, or the Vlasov equation, directly.

As the gravitational attraction moves fluid elements closer, mathematical singularities develop where the mapping from  $\mathbf{q}$  to  $\mathbf{x}$  is not unique. This corresponds to different fluid elements with different Lagrangian coordinates arriving at the same Eulerian position. This is known as *multi-streaming*, or *shell crossing*, resulting in the formation of density singularities known as *caustics*.

If we continue to apply the Zeldovich approximation after multi-streaming has occurred, fluid elements simply carry on on their initial trajectories, dissolving any structure that might have formed. In reality, we would expect the large gravitational interactions in these multi-streaming regions to act to bind structure together. The *adhesion model*, where fluid elements ‘stick’ to each other when shell crossing occurs, goes

some way to resolving these problems with the Zeldovich approximation, but fails as it does not follow the nonlinear motion of fluid elements within high density regions.

We have given a brief, but fairly extensive qualitative introduction to methods of modelling structure formation. We have done this partly because it is a fundamental part of any introduction to Cosmology, and partly because it forms a background for a novel approach to structure formation that utilises the Schrödinger-Poisson system. We will elaborate further on this approach in Sections 2.2 and 3.3. This *wave-mechanical approach* can be seen to circumnavigate many of the problems with the traditional approaches that we have mentioned above.

### 1.1.4 Dark Matter

So, we have seen how the energy-matter component of the Universe appears to be made up of  $\sim 5\%$  baryonic matter,  $\sim 21\%$  dark matter, and  $\sim 74\%$  dark energy. We now concentrate on dark matter's role in the evolution of the Universe, some possible candidates, and some of the problems that arise in trying to implement various models.

We have already mentioned that Zwicky was the first to notice that something may be amiss in measurements of a galaxy's mass. Later evidence came in the 1970s, largely from observations of galaxy rotation curves [108, 109, 110, 111, 112]. These measurements showed that the orbital velocities of galaxies appeared to be reaching a plateau, rather than decaying away as one moved further out from the galaxy's centre. This implies a form for the distribution of matter in a galaxy that the visible part was clearly not following. Evidence from these rotation curves suggested that the visible part of the galaxy was set in a halo of unseen matter.

Evidence from the observation of H1 rotation curves [113] and other galactic dynamics, such as the kinematics of satellite galaxies (see e.g. Zaritsky et al. [114]) for example, led to the formation of the *Cold Dark Matter* (CDM) model [115, 116, 117, 118]. This model described a Universe in which the constituents were baryonic and dark matter only.

The rotation curves of galaxies and their associated density profiles are possibly the most powerful tools for probing dark matter distributions. Analysing a large num-

ber of galaxies, Persic et al. [120] developed a model of a ‘universal rotation curve’, whose form, they claimed, could be fit to any type of galaxy. Models such as these have been complemented by recent breakthroughs in the simulation of dark matter and the evolution of structure formation, due partly to the increase in available computer power. As we have seen in Table 1.1, the ratio of baryonic matter to dark matter is approximately 1:5. When simulating structure formation, it is usually assumed that the evolution is driven by the gravitational interaction of the dark matter. This assumption simplifies the problem somewhat, as one does not have to deal with the complicated gas physics, which is very difficult to implement. Since the emergence of the  $\Lambda$ CDM, or *concordance model* of Cosmology, simulations have again made tremendous strides in modelling structure formation in the Universe. The Millennium simulation by the VIRGO consortium was one such simulation that made considerable achievements by, for example, explaining some of the observations of black hole candidates in quasars made by the Sloan Digital Sky Survey (SDSS). Other progress has been made in explaining the structure of dark matter halos [134].

There are however a number of problems that arise in numerical simulations of the concordance model that do not appear to fit observations. The two main problems are the appearance of *cuspy halo cores*, and the *overabundance of substructure*. To understand these problems, we need to understand a little bit about the simulations themselves.

One of the most important simulations was done by Navarro, Frenk and White [121]. This established an analytic form for the dark matter distribution in virialised structures. The *NFW profile* provides the best fit to simulated data, and has a *universal* form, meaning that it can be scaled to fit the characteristics the majority of galaxies and galaxy clusters. The NFW profile can be written

$$\rho = \frac{\rho_s}{(r/r_s)(1 + r/r_s)^2}, \quad (1.46)$$

where  $r_s$  and  $\rho_s$  are some characteristic scale and density. This profile applies to stable, bound systems, where the virial theorem holds. A distance scale within which this is the case is known as the *virial radius*,  $r_{\text{vir}}$ . This is often difficult to determine, in observations as well as simulations, and so it is often approximated as the radius within which the average density of the dark matter is greater, by a specified factor, than the

critical density,  $\rho_{\text{crit}}$ , given by eqn. (1.13). A factor of 200 has generally become the standard in simulations, if only to enable comparisons between studies. This radius is written as  $r_{200}$ , and also allows for the detection of subhalos within halos. See papers by the recent Aquarius project [122] for example. Two further parameters are often defined; the *characteristic density*,  $\delta_c = \rho_s/\rho_{\text{crit}}$ , and the *concentration parameter*,  $c = r_{\text{vir}}/r_s$ , where  $r_{\text{vir}}$  is the virial radius. The NFW profile then, can be rewritten as

$$\rho(r) = \frac{\delta_c \rho_{\text{crit}}}{(r/r_s)(1 + r/r_s)^2}. \quad (1.47)$$

It can be shown [121], that with the defined factor of 200, the characteristic density can be related to the concentration parameter by

$$\delta_c = \frac{200}{3} \frac{c^3}{(\ln(1 + c) - c/(1 + c))}. \quad (1.48)$$

In this case, for a given halo mass, eqn. (1.47) has one free parameter, which can be expressed either as the characteristic density, or the concentration parameter. With these free parameters, the NFW profile is currently the model that provides the best fit to any simulated data for a dark matter halo. The validity of these results are still widely debated within the community [123, 124, 125, 126, 127, 128, 129], and eqn. (1.47) also appears to be in disagreement with observations, though this again has generated a lot of discussion [130, 131, 132].

An in depth study of the density profile of the Milky Way was done by Battaglia et al. [133], and suggests that the dark matter halo is consistent with an NFW profile of mass  $0.8_{-0.5}^{+0.2} \times 10^{12} M_{\odot}$ , and a concentration parameter of  $c = 18$ . Observationally, it can be difficult to obtain a value for the virial radius, but, as described in the Battaglia paper, the NFW profile can be described by the concentration parameter  $c$ , and by the virial mass, *or* the circular velocity at the virial radius. For this reason, they take the mass within 120 kpc, as this is the furthest distance at which there was a reliable tracer. This can be considered an effective virial radius, and is approximately the extent of the dark matter halo. The radius of the stellar disk is of order 20 kpc.

One of the problems is that the NFW profile becomes singular at small radii. The N-body and hydrodynamic simulations of dark matter halos, from which the NFW profile is derived, tend to show large spikes in the dark matter density profile when approaching the centre of the halo [135, 136]. This problem typically starts to manifest

itself within a radius  $\sim r_{\text{vir}}/100$ . These singular cores are not seen in observations [137, 138, 139], in either clusters of galaxies observed by gravitational lensing [140], ordinary spiral galaxies [141, 142], or some low brightness systems [130]. Dwarf galaxies, for example, have nearly uniform density cores, in contrast to the expected cuspy density profile [143, 144]. Within simulations this may be a problem with the resolution within the core regions, or it is possible that theoretical predictions of cuspy profiles may not be as accurate as is often suggested [145, 126, 146]. The *Einasto profile* may better represent the dark matter halo of a simulated galaxy [147], but this is in some doubt because of the limited resolution of N-body simulations. The Einasto profile is given by

$$\rho(r) \propto \exp(-Ar^\alpha), \quad (1.49)$$

where  $A$  and  $\alpha$  are constants. It can be seen that the Einasto profile does not become singular in the core region.

The amount of observed galactic substructure, associated with galaxy and cluster formation, is not as abundant as predicted by either theory or simulation. In the process of a hierarchical structure formation scenario, where larger objects are formed by the merger of smaller objects over time, the merging process is not 100% efficient in destroying the accreted satellites, resulting in the structures such as the Large and Small Magellanic Clouds that orbit our own galaxy. These structures are of order  $10^{10} M_\odot$ . From observations of the Milky Way and Andromeda, the current cosmological models predict that galaxies such as these should have  $\sim 50$  dark matter satellites of mass  $> 3 \times 10^8 M_\odot$  within a 570 kpc radius, while present detections number only about a dozen or so. The simulated data is worse, predicting  $\sim 300$  satellites in a 1.5 Mpc radius, while we see only  $\sim 40$  [148, 149]. This is the problem of the overabundance of substructure. Interestingly, just as the models of the density profiles of dark matter are scale free, the amount of substructures associated to a halo is also scale free. In numerical simulations, the properties of a galaxy and its associated satellites are the same as a galaxy cluster, and *its* associated satellites [149]. Observationally, again, this is not the case, and there are far fewer satellites observed than in simulations. This may be a problem of detection and observation. Indeed, new satellites are still being discovered [148], and it is possible that some of the satellites will be completely dark. It should be possible to detect small galaxy halos from the lensing effects that they would have on

their host galaxy. Evidence of such effects is currently inconclusive [150]. These small galaxy halos should also make disc galaxies thicker than observed [151, 152, 153]. Again, it is possible that this problem may be resolved with higher resolution of the simulations. Observations too may be prone to selection effects. There are also some more speculative suggestions that the deficit of substructure may be explained if dark matter particles are allowed to decay into other particles [154].

Simulations are also still fairly limited when it comes to describing the interactions of baryonic matter. Some hydrodynamic simulations produce galaxy discs that are too small and have too little angular momentum compared to observations [136], while many high surface brightness galaxies exhibit rotating bars, which are normally only stable if the core density is lower than predicted [155]. The distribution of dark matter in the Universe is also a puzzle, and a problem for simulations. Some ellipticals appear to be completely void of dark matter [156]. This may be the result of mergers or other interactions, as evidenced by the so called *Bullet cluster* [157] and *Train Wreck* [158], but it would still be very difficult to explain the loss of all dark matter from an old, and hence dynamically settled, elliptical galaxy. One explanation suggests that the dark matter may be there, but its dynamics may be confusing the observational signatures [159]. There also appears to be evidence of galaxies lacking any visible matter component [160]. Dubbed *dark galaxies*, it is difficult to be sure of their existence or number density, for obvious reasons. There also appears to be a low ratio of visible matter to dark matter in *Low Surface Brightness* (LSB) galaxies. Examples such as these are difficult to simulate without correctly addressing the interaction of baryonic matter. Weinberg and Katz [161] stressed that the inclusion of the baryon component in N-body simulations may be crucial, as the effects of baryons may smooth the central dark matter cusps. Sellwood however, developed simulations that appeared to contradict this [162].

There have also been suggestions that dark matter may not be the solution to the apparent mismatch between the dynamics predicted by Newtonian mechanics, and the lack of visible matter. Some theorists advocate versions of *Modified Newtonian Dynamics* (MOND) [163], where the laws of gravitation are modified on some scale larger than we have experimental access to. Relativistic versions of these theories such as *Ten-*

*tor Vector Scalar* theory (TeVeS) [55, 164] and *Scalar Tensor Vector Gravity* (STVG) [165] have also been developed. These theories are often able to do a good job of describing galactic dynamics without invoking dark matter, see MOND's explanation of dark matter ellipticals [166] for example, but they often invoke instead an unexplained scalar field, or include adjustable free parameters. Some might argue that this is no worse than the scalar fields invoked by inflation. When the Bullet cluster and the Train Wreck were discovered, it seemed that they might kill off these types of theories [57], as the centre of mass of the visible matter and that of the dark matter, as observed by gravitational lensing, did not coincide. The object VIRGOHI21, which appears to be a dark galaxy, also does not appear to follow the dynamics predicted by MOND [168]. The recent discovery of a dark matter ring in the galaxy cluster CL0024+17 adds further evidence to the dark matter proposition [169]. It may be possible to test theories of modified gravity when gravitational wave detectors such as LIGO and GEO600 are able to conclusively detect gravitational waves. In theories of modified gravity, photons and neutrinos produced in a cataclysmic event, such as a supernova, should lag behind the arrival of gravitational waves by an appreciable amount [170]. This would produce an unambiguous result in favour of MOND-type theories.

A number of dark matter candidates have been proposed, and experimental searches now seem to be on the brink of coming to fruition. Some of the early suggestions included monopoles and massive neutrinos [171]. These are currently unlikely candidates as they would require a neutrino mass that is unreasonably large, or a large number of monopoles, of which we have not seen even one. If dark matter was comprised of neutrinos with the mass that we currently expect  $\sim 0.1$  eV, then it would be relativistic. *Hot Dark Matter* (HDM) is generally ruled out as a dark matter candidate, as the relativistic speeds mean that structure formation is inhibited.

The axion was first hypothesised as a solution to the strong CP problem in QCD, and we will discuss further the relation to field theory in Section 4.3. When the dark matter content of the Universe became apparent, the possible mass range and interaction strength of the axion made it a good candidate for a dark matter particle. See, for example, Turner [172]. After some promising initial experimental results, the non-detection of dark matter axions by the Polarizzazione del Vuoto con LASer experiment (PVLAS)

[173] and the Axion Dark Matter Experiment (ADMX) [174] seem to rule the axion out as a candidate.

*Massive Compact Halo Objects* (MACHOs) have also been proposed as a solution to the dark matter problem that removes the need to resort to new, exotic forms of matter. MACHOs would be composed of normal baryonic matter, but would not emit light of their own, and so be quite hard to detect other than with gravitational lensing and other gravitational effects, such as rotation curves. Examples of MACHO's could be planets, or low luminosity stars such as brown dwarves, or even black holes. Searches to this effect, by the MACHO [175] and EROS2 [176] collaboration for example, have not detected significant amounts of mass to be tied up in such astronomical bodies, with an upper limit of  $\sim 20\%$  of the dark matter fraction. The most promising candidates are currently considered to be *Weakly Interacting Massive Particles* (WIMPs). As the name suggests, they interact only with the weak nuclear force, and gravitationally. In Section 1.1.2 we suggested how one such particle, the *neutralino*, may emerge naturally from *supersymmetric theories* (SUSY) and may be the only stable particle left over from the decay of heavier SUSY particles.

Like 'dark energy' and 'dark matter', the name WIMP reflects the properties we currently believe that the particle should have, rather than any experimental verification of such a particle. However, there have recently been a number of experimental results that may be shedding light on dark matter's parameters.

One experimental method is direct detection. These experiments work by detecting the recoil of nuclei after a collision with a dark matter particle. As dark matter particles are expected to be weakly interacting, these experiments require a large collection area, a target particle with a large interaction cross-section, or preferably both. Examples of these experiments are the Cryogenic Dark Matter Search (CDMS) detector and the Directional Recoil Identification From Tracks (DRIFT) experiment. The direct detection experiments DAMA/NaI and the later DAMA/Libra aimed to detect dark matter by exploiting the Earth's rotation around the sun. If the galaxy is embedded in a dark matter halo, then Earth's orbit should produce a bi-annual modulation in the flux of dark matter flowing through the planet, reminiscent of the Michelson-Morley 'aether' experiments. Both of these experiments claimed a signal detection, although these re-

sults remain somewhat tentative as a number of other experiments reported a null result [177].

Other experimental searches concentrate on the detection of cosmic rays. WIMPs may annihilate with each other to produce high energy cosmic rays or electron-positron pairs, which may themselves annihilate to produce cosmic rays. If WIMPs interact gravitationally, then we might expect more cosmic rays to come from the centres of large mass objects, such as galaxies, where the densities, and hence interaction rates, will be higher.

One unexpected result to come from the WMAP data was the detection of an excess of microwave radiation coming from the Milky Way core [178]. The Compton Gamma Ray Observatory (CGRO) and INTERNATIONAL Gamma-Ray Astrophysics Laboratory (INTEGRAL) experiments have also found a flux of photons at 511 keV [179], the energy one would expect if positrons and electrons were annihilating, coming from the same region.

It has been suggested that high energy dark matter particles may result from the annihilation of neutralinos, a SUSY candidate for dark matter, with the ‘WMAP haze’ resulting from annihilation in the inner galaxy [180]. Neutralinos could possibly create new light bosons [181], or dark matter particles in excited states [182], with the WMAP signal again produced when these annihilate or decay [183, 184].

Gamma ray detectors, such as the Energetic Gamma Ray Experiment Telescope (EGRET) on board the Compton Gamma Ray Observatory (CGRO), have seen more gamma rays than expected in the energy range 1 - 10 GeV, while the High Energy Antimatter Telescope (HEAT) and the Alpha Magnetic Spectrometer (AMS-01) mounted on the International Space Station, both detected excess positrons in the range 10 - 100 GeV, a result that was later confirmed by the satellite experiment Payload for Antimatter Exploration and Light-nuclei Astrophysics (PAMELA).

An important limiting factor for the energies of cosmic rays is the Greisen-Zatsepin-Kuzmin (GZK) cutoff [185, 186]. High energy cosmic rays from distant sources should interact with the photons of the CMB, and so lose energy over long distances. This puts a limit on the energies of cosmic rays that are detectable on Earth. A number of experiments, for example the High Resolution Fly’s Eye cosmic ray detection (HiRes),

and Akeno Giant Air Shower Array (AGASA) have detected cosmic rays that are above the GZK limit. It is suggested that a dark matter candidate could annihilate or decay to produce these energetic cosmic rays [187].

These detections are in their early stages, and it is hoped that the Pierre Auger Cosmic Ray Observatory and the Fermi Gamma-ray Space Telescope (formerly GLAST) will provide more detail on these observations.

## 1.2 Cosmology Meets Condensed Matter

Cosmology is in the somewhat unenviable position of being an observational discipline. We are forced to make observations of the only Universe we have, in its current state, and infer what we can.

Condensed matter physics is generally concerned with explaining the macroscopic properties of materials, by understanding the behaviour of the material at the microscopic level. It seeks to describe phenomena such as phase transitions, condensates, superconductors and semiconductors. Of course, Einstein himself made several important and fundamental contributions to the field of condensed matter. Extending Bose's idea [188] of indistinguishable photons to matter particles [189] gave rise to the prediction of Bose-Einstein condensation, while the prediction of stimulated emission from atomic transitions [190] is generally regarded as the advent of laser physics.

In order to facilitate experimental tests of theoretical predictions, physicists have often appealed to analogue models in an attempt to better understand the physics of cosmological phenomena. An example of such a proposal is the liquid drop models of gravity. While investigating the effect of self-gravitation on large bodies, Plateau [191] developed a model where the surface tension of a liquid drop took the role of the gravitational force. A later example is a proposal by Bohr and Wheeler [192] that uses the surface tension of a charged liquid drop to describe the nuclear forces in a model of nuclear fission.

Analogue models have developed significantly in recent years, in terms of both the experimental techniques that are available to test them, and the level of mathematical

rigour between the two sides of the analogy.

The first Bose-Einstein gas was produced experimentally only relatively recently by Cornell, Wieman, and Ketterle in 1995, giving an idea of the level of technological advancement required for such experimental techniques, and earning the Nobel prize in 2001. Analogue models have (therefore) concentrated on superconductors and superfluids, which were discovered much earlier, in 1911 and 1938 respectively [193]. Experimental analogue models have been proposed to test early Universe processes such as topological defect production and interaction, and the production of primordial magnetic fields. Analogies between the mathematical structure of the two systems have also been proposed.

First we give a brief historical overview of the development of condensed matter theory, particularly in relation to an idea that it inspired in high energy particle physics.

### 1.2.1 The ‘Higgs-Anderson’ mechanism

In 1937, Landau had the first major success in trying to formulate a general theory for second-order phase transitions (see, for example, Landau and Lifshitz [194]). He recognised that phase transitions could be characterised by an order parameter, such as the density of a fluid or the magnetisation of a ferromagnet. In the case of a superfluid, the macroscopic density of particles can be represented as the square of a wavefunction, and Landau identified this wavefunction as the relevant order parameter.

In 1950, developing Landau’s earlier work, Landau and Ginzburg [195] formulated a macroscopic theory of superconductivity; the phase transition from normal conductivity to superconductivity also being second-order. This theory described how properties associated with the superconductor, such as density or the flow of current, behave. Once again, the relevant order parameter was identified as the averaged macroscopic wavefunction of the superconducting electrons, with the density of superconducting carriers being given by its square. The wavefunction in this case is a complex field, interacting with the electromagnetic force.

The BCS theory of superconductivity, developed by Bardeen, Cooper and Schrieffer in 1957 [196, 197], gave a microscopic description of the phenomena of superconduc-

tivity, and for the development of this theory the trio were awarded the Nobel prize in 1972. The gap between the microscopic and macroscopic regimes was filled by Gorkov in 1959 [198], who showed that the Landau-Ginzburg theory could be derived from the BCS theory.

Landau's contribution to condensed matter was recognised by the Nobel prize committee in 1962, while Ginzburg had to wait until 2003 to share the prize with Abrikosov and Leggett for 'pioneering contributions to the theory of superconductors and superfluids'.

The Landau-Ginzburg theory contains a nice example of symmetry breaking and, in applying it to superconductors, can explain the exclusion of magnetic field, the *Meissner effect*, by giving the photon an effective mass. This idea was considered by a number of people around the same time. Notable amongst these, from our point of view, is the condensed matter physicist P. W. Anderson, who shared the 1977 Nobel prize with Mott and Van Vleck for their 'fundamental theoretical investigations of the electronic structure of magnetic and disordered systems'. Anderson discovered the mechanism for mass generation via symmetry breaking in condensed matter systems [199], as noted above, and suggested that it may have cosmological implications. The other major players in suggesting this idea for the generation of mass are Englert and Brout [200], Guralnik, Hagen and Kibble [201] and, of course, Higgs [202, 203].

The relationships between cosmology and condensed matter have been elucidated much further in recent years, and because of technical developments in both subjects, there have been a number of attempts to model early Universe processes in the laboratory. To emphasise and encourage cross-disciplinary research in this area, the European Science Foundation set up a five year Research Networking Programme, COSLAB [204] (Cosmology in the Laboratory), chaired by Prof. Grigory Volovik and Prof. Tom Kibble.

## 1.2.2 Kibble-Zurek mechanism - Condensed Matter again informs Cosmology

We have seen one example of Kibble's work in the cosmology / condensed matter interface. We look at another example that is more immediately observable in experimental setups.

The Kibble mechanism [205] describes the production of topological defects in the early Universe. As the Universe cooled, it may have gone through a second-order phase transition at some critical temperature, breaking symmetry groups as described previously, and producing particles. The breaking of certain symmetries can produce *topological defects*, where the order parameter changes discontinuously across some boundary separating two regions of degenerate vacua.

As a system moves through a second-order phase transition, the temperature drops until it reaches a critical temperature  $T_{\text{crit}}$ . It is at this temperature that degenerate minima of the potential first appear. The field can however move between the different vacua if the thermal fluctuations are greater than the height of the potential barrier. This is no longer possible once the temperature drops below the *Ginzburg temperature*, at which point any topological defects are 'frozen in'.

Kibble was the first to estimate the density of topological defects formed by spontaneous symmetry breaking after a cosmological phase transition. His argument was based upon considerations of causality at the Ginzburg temperature. Correlations cannot establish themselves over distances greater than the causal horizon, so the causal correlation length should satisfy the causality constraint

$$\xi < d_{\text{H}}, \quad (1.50)$$

where  $d_{\text{H}}$  is the distance to the causal horizon. The correlation length can also be related to the Ginzburg temperature. One defect would take up a region  $\sim 1/\xi_d^{1/3}$ , and Kibble identified the length scale  $\xi_d$ , with the correlation length  $\xi$ . This is obviously a sensible suggestion to make, and gives rise to a density of one defect per Hubble volume at the time of formation.

A potential problem with this argument arises when one considers the Universe in terms of a thermal system. The equilibrium correlation length  $\xi_{\text{eq}}$ , that is, the correla-

tion length of the system if the system could reach thermal equilibrium, changes very rapidly in the vicinity of a second-order phase transition. The difference between the causal and equilibrium correlation length is essentially the time it takes a system to react. Two regions may be in causal contact, but will not immediately be in thermal equilibrium. At what time, or temperature, should we equate  $\xi_d$  with  $\xi$ ?

Zurek [206, 207, 208] considered the defect density within the framework of second-order phase transitions, and the equilibrium correlation length. As the system passes through the second-order phase transition,  $\xi$  is able to keep up with the equilibrium correlation length  $\xi_{\text{eq}}$ , until  $d\xi_{\text{eq}}/dt$  becomes larger than the speed at which correlations can propagate in the system, and the system falls out of equilibrium. On the other side of the transition,  $\xi$  eventually becomes equal to the decreasing  $\xi_{\text{eq}}$ , and it is at this time we should identify  $\xi_d$  with  $\xi$ , so that  $\xi \equiv \xi_d \equiv \xi_Z$ . This time is often now called the *Zurek time*,  $t_Z$ , and gives a prediction of the defect density  $\sim k/\xi_Z^2$ , where  $k$  is a constant of order 1 [209].

This concept is interesting because analogous scenarios occur in condensed matter physics. When various substances, such as  $^3\text{He}$ ,  $^4\text{He}$  or nematic liquid crystals, are subject to a temperature quench, taking them rapidly through a phase transition, then topological defects such as vortices can appear within the substance. Initial numerical simulations [210] seemed to agree with the Zurek scenario, although the constant  $k$  mentioned above, seemed to be less than order one.

The first experiments were done in nematic liquid crystals [211, 212]. The Zurek scenario is not strictly applicable, as the nematic phase transition is first-order. The defect density did however, appear to agree approximately with the estimates.

A number of other experiments were then performed in  $^3\text{He}$  [213, 214] and in  $^4\text{He}$  [215, 216, 217] to investigate the Kibble-Zurek scenario. Interpreting the results is somewhat inconclusive, but this is due to the complexity of the experimental detail, rather than incorrect physical concepts. However, the laboratory tests confirmed the formation of defects at the end of a symmetry-breaking transition, and did not agree with the defect density predicted by Kibble.

A number of other experiments have been performed in order to exploit the analogies present in cosmological and condensed matter scenarios.

Recent *braneworld* scenarios inspired by string theory have suggested a mechanism for inflation caused by the interaction and annihilation of higher dimensional branes. These models often predict that topological defects, such as cosmic strings, will be left behind as relics of this collision, as well as the associated particle production [218]. Superfluid Helium-3 has two phases, A and B, and can be arranged in such a way that the sample contains vertical regions of A phase, then B, then A, with the boundary between each phase being a topological defect. These simulated branes then move together and annihilate, producing line-like topological defects, and a variety of excitations that one can associate with particles [219]. This type of experiment goes some way to giving credence to brane inspired models of the Universe.

It has also been suggested that the interaction of excitations in the two phases of  $^3\text{He}$  could be analogous to baryogenesis during the electroweak transition [220, 221].

Primordial magnetic fields in the Universe may also be generated from cosmological phase transitions, with concepts that could also potentially be tested in the laboratory [222].

### **A Mathematical Analogy**

Volovik, the other chair of the COSLAB programme, has worked on many ideas that relate condensed matter to cosmology [224], and proposes a mathematical analogy based upon the group structure of the standard model, the model of the fundamental interactions in the Universe, and the different phases of  $^3\text{He}$ . Helium-3 is proposed as analogous to the quantum background, out of which photons, gravitons and gluons emerge as collective excitations. The idea is largely related to the concept of symmetry and symmetry breaking, and comparing the symmetry groups one can use to represent the interactions.

A physical system generally has a number of symmetries associated with it; classical symmetries such as translational and rotational invariance, and less tangible quantum symmetries such as the isospin symmetry associated with the charge of a particle.

According to Noether's theorem [223], transformations that leave the structure of a system unchanged correspond to conservation laws. A time translation, for example,

leads to the conservation of energy. These transformations are known as the symmetries of a system, and these symmetries form a group. Three of the fundamental interactions in particle physics can be shown to be associated with a particular type of symmetry, known as a *local*, or *gauge* symmetry.

For example, the free Lagrangian of quantum electrodynamics, the highly successful field theory of the electromagnetic force, is invariant under a *global* (U(1)) *transformation*. That is, the wavefunction of the electromagnetic field can be changed by any factor that is independent of the position in spacetime, and the Lagrangian, and hence the physics, will remain the same. If, however, we try to make this factor depend on spacetime coordinates, a *local transformation*, the Lagrangian is not invariant. In order to induce gauge invariance, we must introduce a gauge field, the electromagnetic potential, invariant under its own transformation. By doing this we find that we introduce a term in the Lagrangian that gives rise to the photon-electron interaction. In a similar way, the weak interaction can be associated with the group SU(2).

The theory of the electroweak interaction, which we have already mentioned, can be represented by the group  $SU(2) \times U(1)$ . As the early Universe cooled, it passed through the electroweak phase transition, at about 200 GeV. The electroweak symmetry  $U(1) \times SU(2)$  was violated, and broke down to the independent electromagnetic U(1) and weak SU(2) forces, in the process giving a mass to the  $W^\pm$  and  $Z^0$  gauge bosons via the Higgs mechanism.

In a similar way, the theory of the strong force, named *quantum chromodynamics*, is encapsulated in the SU(3) group. The group corresponding to the full Standard Model Lagrangian is then given by

$$SU(3)_{\text{strong}} \times SU(2)_{\text{weak}} \times U(1)_{\text{EM}}. \quad (1.51)$$

It is expected that at some higher temperature, earlier in the history of the Universe, the symmetries of fundamental interactions will be restored to some higher symmetry group, as happened with the electroweak interaction. At this point the forces will become unified into a Grand Unified Theory (GUT).

To see how this might be related to the structure of Helium-3, we can look at the fluid's group structure. The translational and rotational symmetries of Helium-3 can

be represented as the product of three global symmetries

$$\mathrm{SO}(3)_{\mathrm{orbrot}} \times \mathrm{SO}(3)_{\mathrm{spinrot}} \times \mathrm{U}(1)_{\mathrm{trans\ inv}}. \quad (1.52)$$

We see that the unbroken sectors can be considered almost equivalent, as there is an isomorphism between  $\mathrm{SO}(3)$ , and  $\mathrm{SU}(2)$  modulo  $\mathbb{Z}_2$ ,

$$\mathrm{SO}(3) \cong \frac{\mathrm{SU}(2)}{\mathbb{Z}_2}. \quad (1.53)$$

This can be described qualitatively because  $\mathrm{SO}(3)$  has a periodicity of  $2\pi$ , while  $\mathrm{SU}(2)$  has a periodicity of  $4\pi$ . The parameter space of  $\mathrm{SU}(2)$  can be taken to correspond to a sphere, while the space of  $\mathrm{SU}(3)$  only requires a half sphere to completely describe. For more details, see Jones [225].

When Helium-3 passes through its superfluid A phase transition, at some critical temperature, this symmetry group is broken to  $\mathrm{U}(1) \times \mathrm{U}(1)$ , breaking again at a lower temperature to the B phase, represented by  $\mathrm{SO}(3)$ . Volovik is fairly clear in suggesting that the analogy is not complete, but does give two important aspects in which the standard model group, and in particular the electroweak sector, is equivalent to the group structure of  ${}^3\mathrm{He}$ . First, the symmetry groups are very similar, and secondly, the interactions of the low energy fermions with the  ${}^3\mathrm{He}$  – A order parameter closely resembles the interactions of the fermions with the gauge fields present in the electroweak model [226]. We will not discuss the details of this here, but clearly there is potential for further investigation, and more work to be done.

### 1.3 The Future of Multi-Disciplinary Research

Future interactions between the field of cosmology and condensed matter may come from a direction that is somewhat unexpected, and goes some way to making the relationship more mathematically formal. The holographic principle stems from an idea first suggested independently by Crane [227], 't Hooft [228] and Susskind [229]. It was formalised by Maldacena in 1997 [230] as is known as the *Anti-de Sitter / Conformal Field Theory correspondence* (AdS/CFT). This correspondence postulates that a conformal field theory in  $d$  dimensions, is dual to a string-based gravitational theory in  $d + 1$  dimensions. Maldacena's idea in particular, relates type IIB string theory in an

$AdS_5 \times S_5$  background, to a four dimensional supersymmetric conformal field theory. For this correspondence to hold, the requirements are that the symmetries of the two theories match, and that the operators in the CFT are in 1:1 correspondence with the fields in the string theory. The details of this conjecture are entirely beyond the scope of this thesis, but we can note some of the main points, and hopes for the progress of the subject in the future.

Usually, calculations in a gravitational theory or quantum field theory can only be done at low energies. This would correspond to small curvatures for the string theory, or small coupling for the field theory, where perturbative calculations can be done. By exploiting the duality postulated by Maldacena, calculations done at low energy on one side correspond to the high energy regime on the other, allowing insights into, so far, unexplorable regions.

At the present time, the physics on either side of the duality could be considered far from ‘realistic’ physics. Our Universe appears to be 3 + 1 dimensional, and is certainly not AdS, while the quantum theories we have to describe the standard model, such as QED and QCD, are neither conformal nor supersymmetric. To be able to approach a dual theory describing QCD, for example, progress towards a non-AdS / non-conformal gauge theory duality is necessary. Some headway has already been made. The holographic conjecture may be exploited to help understand the strongly coupled regime of superconductivity, the physics of which is often considered to be 2 + 1 dimensional [231]. See Section 17.6 of Waldram [232] for some comments. This would be dual to a 3 + 1 gravitational theory, making the two sides of the duality closer to what we experience, at least dimensionally. For progress on formulating a ds/CFT correspondence see Ness and Siopsis [233, 234], and comments in Podolski [235].

A series of papers has made some considerable progress regarding symmetry breaking and phase transitions within this duality [236, 237, 238], as well as CFTs that embody the mechanisms of superconductivity [239, 240, 241, 242, 243, 244]. A number of papers regarding some of the non-trivial technicalities in realising these ideas have also appeared [245, 246, 247].

Of particular interest is the relation of some real-world phenomena to solutions in general relativity. The Rayleigh-Plateau instability [191] describes the breakup of a flow of

liquid into droplets, as is seen in a dripping tap. The relation to electromagnetic pinch in plasma physics [248] has already been noted [249]. This phenomenon would appear to have a counterpart in the Gregory-Laflamme instability in black strings [250, 251]. Most recently has come the realisation that stable spinning lobed configurations of fluid, governed by the balance of surface tension and centrifugal forces as demonstrated experimentally by Hill and Eaves [252], should have counterparts in new black hole configurations [253].

There are also promising developments on the experimental side. The prediction of Hawking radiation is a result of one of the most successful attempts to combine General Relativity and Quantum Field Theory [254, 255]. This prediction is, however, unlikely to be observable within the foreseeable future, but one can again turn to analogous systems that can be built in a laboratory. Crucial to the concept of Hawking radiation is an event horizon, a region from inside of which wave modes cannot propagate. Quantum fluctuations in the vacuum result in the production of virtual particle-antiparticle pairs, which usually annihilate again after a short time. If this occurs at the boundary of a horizon, one particle can fall beyond the event horizon, leaving the other to escape as radiation. Black holes can then be treated as thermodynamic objects, and are subject to analogous thermodynamic laws [256, 257].

Unruh suggested an analogue to a black hole horizon that could be probed experimentally [258]. Instead of the speed of light being the causal propagator, he suggested using the speed of sound. Fluids that change from subsonic to supersonic flow at some point along their path would then have a ‘sonic horizon’, across which sound waves could travel in one direction but not the other. The production of radiation wave modes would now come from phonons; quantised modes of sound waves in the fluid ‘vacuum’.

The problem with such setups is that the Hawking radiation effect would usually be masked by a random thermal signal generated by the movement of atoms in the fluid. This problem is significantly reduced in Bose-Einstein condensates, where the dynamics of the matter is dominated by quantum mechanical effects, resulting in a much higher radiation signal to thermal noise ratio. Recent advances in the production and manipulation of Bose-Einstein condensates, for example the use of atom chip technol-

ogy pioneered at the University of Nottingham, combined with theoretical [259] and numerical [260] developments in the detection of the Hawking signal, means that such analogue Hawking radiation experiments are now feasible.

While this would not be a direct detection of Hawking radiation, it would give strong support that the theory behind the prediction is correct.

## 1.4 Discussion

In this chapter we have presented an extensive overview of modern cosmology, highlighting some of the problems that need to be overcome. Specifically, we discussed problems in the modelling of dark matter and structure formation that may be overcome by appealing to systems of equations that are typically used in condensed matter systems.

We then looked at two examples of where condensed matter physics has had an impact on cosmology, particularly with regard to symmetry breaking and phase transitions, where the relativistic versions of the equations just mentioned are important. These ideas will be presented in more detail later on in this thesis. We also saw that mathematical, as well as physical analogies can be made.

Finally, we anticipated some areas in which cosmology and condensed matter may further interact in the future. We saw how some of the mathematical analogies have been made more rigorous, although perhaps not quite describing the Universe as we see it. We also described some recent developments on the experimental side, which will hopefully lend support to promising attempts to unite General Relativity and Quantum Field Theory.

# Chapter 2

## Technical Background

In this chapter, we attempt a systematic review of literature relevant to a more technical discussion, specifically with regard to the systems of equations we will be using. We look at uses of the the linear and nonlinear Schrödinger-Poisson system and their relativistic extensions, the linear and nonlinear Klein-Gordon-Einstein equations, particularly within a cosmological context. Use of the nonlinear Schrödinger equation also prompts the consideration of a cosmological Bose-Einstein condensate.

The standard  $\Lambda$ CDM model has some problems associated with it, which we described in Section 1.1.4, and many authors use the properties of the above systems to try and alleviate these issues. We will try to give an overview of these different approaches.

Using the Schrödinger equation to model matter allows one to take advantage of the quantum-mechanical nature of the particles one is describing. This leads to a particularly innovative solution to the problems of cuspy halo density cores and the overproduction of substructure predicted by standard CDM models.

Adding a nonlinear term like  $\phi^3$  to the Schrödinger equation is equivalent to adding a  $\phi^4$  interaction term to the corresponding Lagrangian, and, as the name suggests, this has the effect of allowing particles to interact with each other. This technique is used ubiquitously in quantum field theory to describe interactions. An interaction coefficient allows the strength of the interaction to be regulated. When applied to Cold Dark Matter, this can alter the large scale behaviour, giving a viable alternative to the  $\Lambda$ CDM model.

The nonlinear Schrödinger equation is used in condensed matter theory, where it describes Bose-Einstein condensates. In this field it is often known as the Gross-Pitaevskii equation, and we will use the two terms interchangeably. The Gross-Pitaevskii equation is the equation of motion obtained from varying the Landau-Ginzburg Lagrangian. Consideration of the nonlinear Schrödinger equation has led some authors to suggest that the dark matter component of the Universe may reside in a Bose-Einstein condensate.

Other approaches use the wavefunction of the above systems to describe dark matter in terms of a scalar field, which can again provide a phenomenological description of a condensate. The scalar field interpretation can also lead to some interesting solitonic solutions, which some authors suggest may appear as exotic objects in the Universe. These objects include *boson stars* and *oscillatons*, and we will comment on these briefly. The Schrödinger-Poisson system has also been used to investigate the phenomenon of *quantum state reduction*. This is a very interesting concept, and provides some background for the implications of a dark matter model that we will investigate in Section 3.4. The Schrödinger-Poisson equation has also been analysed in relation to some other problems in quantum mechanics [261].

The Schrödinger equation is a wave equation, and as such, can also be used in an entirely classical context, with  $\hbar$  becoming an adjustable parameter, rather than a constant. This approach has also been used in with regard to structure formation and, after some brief comments motivating a self-interacting dark matter candidate, it is here that we will start.

## 2.1 Beyond Cold Dark Matter

As noted in Section 1.1.4, there may be problems with the CDM model on smaller scales. If these are real effects, and at times the evidence seems ambiguous, then one idea often posited is to allow dark matter particles to self-interact. Several authors have suggested such models, which we will review in this chapter. An overview of some of them has also been given by Ostriker [262]. We introduce the concept by describing one such model, known as *Self-Interacting Dark Matter* (SIDM).

Motivated by the problems of cuspy density profiles in galaxies, Spergel and Steinhardt [263] propose that this and other problems of the CDM picture may be alleviated if dark matter particles are allowed to self-interact with a large scattering cross-section, but with negligible annihilation or dissipation. They make some qualitative arguments based upon the mean free path of a dark matter particle in a galaxy or galaxy cluster, as follows. If the mean free path of a dark matter particle is greater than 1 Mpc, then the particle does not experience any interactions as it moves through the halo, and the usual triaxial halo predicted by simulations, forms with cuspy density profiles and large amounts of substructure via gravitational collapse. On the other end of the scale, if the particles mean free path is less than 1 kpc, then dark matter behaves as a collisional gas and ‘shocks’, heating up the surrounding gas to produce core densities with a shallower profile. Collision between dark matter particles also lead to isotropic velocity distributions, leading to spherical halos, which can only be flattened by significant rotation. Spergel and Steinhardt cite some well accepted observational evidence, showing that dark matter halos seem to form with little angular momentum and so, if the dark matter is not dissipative, halos should be nearly spherical. X-ray observations of clusters reveal that most halos are moderately ellipsoidal. For this reason, they suggest that a dark matter particle should have a mean free path somewhere in the intermediate region, thus flattening density cusps, but not conflicting with observations. As the mean free path can be related to the mass and scattering cross-section, they put a range on the mass of their dark matter particle as 1 MeV - 10 GeV. The SIDM model is followed up by simulations in further papers [264, 142], whose results confirm the qualitative arguments made previously for the mass ranges, as well as showing that substructure is also somewhat reduced, and that SIDM produces more spherical inner regions of halos than the standard CDM model, which is favoured by observations. They note, however that the triaxiality of these inner regions may be masked by the effects of baryons.

## 2.2 A Wave Mechanical Approach to Structure Formation

In Section 1.1.3, we saw some of the approaches that are typically used in modelling large-scale structure, and some of the problems associated with them. A *wave-mechanical* approach, using the Schrödinger-Poisson system in a classical context, can alleviate some of these problems. This section concentrates on the literature associated with this approach, while Section 3.3 will describe the mathematics in more detail.

A wave-mechanical approach to simulations of structure formation, utilising the Schrödinger-Poisson system was first proposed by Widrow and Kaiser [265], subsequently developed by Coles, Spencer and Short [266, 267, 268, 269, 270], and applied recently to systems involving more than one fluid by Johnston, Lasenby and Hobson [271]. This allows regions of dark matter fluid that may be experiencing different dynamics to be modelled more easily.

Widrow and Kaiser [265] motivate their approach by suggesting that a coherent scalar field, such as the axion, could be a potential dark matter candidate; axions being extremely light ( $m \sim 10^{-5}$  eV), but nonrelativistic. We have already discussed the role of scalar fields in Cosmology in Section 1.1.2, and we will come to discuss the particular case of the axion in more detail in Section 4.3. Generally in N-body simulations, the scales of interest are much greater than the de Broglie wavelength of the particles being considered. For a particle with a very low mass, such as the axion, the de Broglie wavelength would be of order 10 m - an unreasonably small scale when discussing structure formation. Using realistic numbers of particles quickly becomes computationally expensive, with the simulation run-time typically going as  $N^2$  or  $N \ln N$  [272], where  $N$  is the number of particles. For an effective N-body simulation, it is necessary to ensure a statistical coverage of the velocity and position distribution functions. Typically, simulations use particles that are much more massive, and much less numerous than one might expect to see in the Universe, in order to fulfil this requirement. Widrow and Kaiser propose a simulation where the wavefunction of the system, rather than individual particles, is evolved instead. To evolve a gravitationally-coupled wavefunction, the coupled Einstein-Klein-Gordon equations are used. The Klein-Gordon equation was

originally introduced to describe a single, relativistic, quantum-mechanical boson. In order to describe large particle numbers, the appropriate thing to do should be to interpret the Klein-Gordon equation as describing the evolution of field operators, with appropriate commutation rules. However, in the limit of large particle numbers, it is possible to consider the Klein-Gordon equation as a classical wave equation, with the square of the wavefunction interpreted as the particle density. We will describe this large particle limit further in Section 3.2. In the weak field limit, the Einstein-Klein-Gordon system reduces to the Schrödinger-Poisson system, as outlined in Appendix A, and in the limit of large numbers, the Schrödinger equation can also be interpreted as a classical wave equation. The particle density, and hence the evolution of the system can then be tracked by following the evolution of the wavefunction. In this case, the ‘classical de Broglie’ wavelength ( $\lambda = v/m$ , we explain further the meaning of the parameter  $v$  in Section 3.3) of the system is a free parameter that can be tuned to the size of the simulation that one requires. As the de Broglie wavelength is related to the mass of the particles making up the system, this means that simulations set up in this manner may sometimes be using overly large numbers of ultralight particles. This is not prohibitive in terms of computer time, as it is the evolution of the wavefunction of the system that is being followed, rather than individual particles. Employing a more sophisticated approach to representations of the wavefunction, such as the coherent state formalism of Husimi [273] means that the particle distribution function in the wave-mechanical approach reduces to the full Vlasov (or collisionless Boltzmann) equation, so long as the de Broglie wavelength is smaller than the scales of interest, and larger than the grid spacing of the simulation. This setup of the system is also able to handle multi-streaming, which we noted as one of the problems of traditional approaches to structure formation in Section 1.1.3. Widrow and Kaiser evolve the Schrödinger-Poisson system using various numerical techniques, and compare this method to a standard N-body technique consisting of a self-gravitating, one-dimensional system, and a particle mesh technique describing a self gravitating system in a two-dimensional Einstein de-Sitter universe, dominated by a nonrelativistic classical field. Results are shown to be comparable, with the Schrödinger wave-mechanical approach being slightly faster, computationally.

It has long been known that the evolution equations of fluid dynamics can be put into

the form of a Schrödinger equation, via a *Madelung transformation* [274], and this is a trick that is employed regularly in condensed matter physics. Conversely, applying this transformation to the Schrödinger equation yields the continuity equation, and the *integrated Euler*, or *Bernoulli* equation, with an additional term. This additional term is known as the *quantum pressure*, although dimensionally it is a chemical potential. The quantum pressure term is the only term in this system of equations where  $\hbar$  makes an appearance. The extra ‘pressure’ can be thought of as a manifestation of the uncertainty principle, whereby the particle’s position becomes ‘de-localised’. In some sense, this provides a minimum volume for each particle, and acts as a kind of interaction, or a form of pressure support. We will describe these concepts more mathematically in Section 3.3.

Coles [267, 269] pointed out that the Schrödinger-Poisson system of Widrow and Kaiser was equally amenable to a Madelung transformation, leading to the classical Eulerian equations of motion traditionally used to model structure formation, along with the extra pressure term. Being a fully classical system, however,  $\hbar$  is replaced by an adjustable parameter that acts as a regularising term in the Bernoulli equation, preventing the formation of density singularities and multi-streaming regions where shell-crossing occurs. Less abstractly, this corresponds to the suppression of cusps in the density profiles of dark matter halos; one of the problems with the standard CDM models that we have mentioned previously. This classical wave-mechanical approach to structure formation was greatly elucidated by Short and Coles [268, 266], and extended to include the effects of gas pressure, using the nonlinear Schrödinger equation, by Coles and Spencer [270]. In particular, Coles and Spencer also found that a description in terms of the nonlinear Schrödinger equation lead to a density profile described by a polytropic fluid. Coles [269, 267] also provided an explanation of why the distribution of density fluctuations from an initial Gaussian distribution, as predicted by inflation, should be so close to the log-normal form that is observed.

## 2.3 Quantum Mechanical Dark Matter

Hu, Barkana, and Gruzinov [275] proposed a solution to the problems of the CDM model that is both complimentary, and in contrast to the ideas of the preceding section. The Schrödinger-Poisson is again considered, but here the quantum mechanical nature of the system is kept explicit. Their dark matter model consists of non-interacting particles, whose number densities are high enough that the dark matter behaves as a classical field. The evolution equations for this field turn out to have the form of the Schrödinger-Poisson system, and they note that if a particle description is considered, then the field will be proportional to the wavefunction of each particle. A standard Jeans analysis is performed, and the resulting Jeans length, where classically the gravitational forces of a gas cloud balance the thermal pressure outwards, is reinterpreted in the quantum framework as the de Broglie wavelength of the dark matter particles in the halo. Stability below the Jeans wavelength is then guaranteed by the uncertainty principle - an increase in momentum opposes any attempt to confine the particle further. Scaling the Jeans/de Broglie length to be such that dark matter density cusps and substructure are heavily suppressed, they show that the mass of the dark matter particle corresponding to this length is ‘ultralight’, of order  $10^{-22}$  eV. We can compare the concepts of this model with those presented in the papers of Widrow, Kaiser and Coles mentioned above. These previous papers made use of a Schrödinger approach in a purely classical manner, treating  $\hbar$  as a parameter to be adjusted to fit the length scales required. In Widrow and Kaiser’s simulations this sometimes meant dealing with an ultralight particle with a high number density, but this was considered to be an artefact of the numerical process. Hu et al. instead keep  $\hbar$ , so that low scale power is suppressed by the uncertainty principle, and adjust the Jeans length to the scales of interest, thus interpreting the low mass prediction as a real particle. The final part of this paper is dedicated to some exploratory one-dimensional numerical simulations, demonstrating that a low mass particle can indeed go some way to solving the problems associated with structure formation. Hu et al. mention in passing that these ultralight scalar dark matter particles should reside initially in a Bose-Einstein condensate, similar to axion dark matter models.

Bose-Einstein condensation appears in both condensed matter physics, and also in

high-energy field theories describing particles such as axions, ghosts and the Higgs. We will discuss the formalities of ‘standard’ Bose-Einstein condensation in Section 3.1, and its relation to symmetry breaking and field theory in Section 4.2. The models reviewed in this chapter generally consider the condensation of nonrelativistic bosons, and it is sufficient from the point of view of these models to consider a condensate as formed when the thermal de Broglie wavelength is of order the interparticle spacing.

### 2.3.1 Dark Matter as a Bose-Einstein Condensate

Dark matter as a quantum-mechanical phenomenon, described by the nonlinear Schrödinger equation, the mean field equation for a Bose-Einstein condensate, prompts the question of whether dark matter itself may reside in such a condensate.

Motivated by a description of CDM, and the phenomenological descriptions of dark matter using the Schrödinger-Poisson system that we have mentioned previously, two papers of importance to later work in this thesis suggest a description of dark matter in terms of a Bose-Einstein condensate.

Böhmer and Harko [276] employ a mean field description of a quantum system of  $N$  interacting particles, as described in Section 3.2 and hence arrive at the Gross-Pitaevskii, or nonlinear Schrödinger equation, as one would expect. The quantum condensate wavefunction is replaced by the expectation value of the field operator, with its square modulus describing the density of the condensate. The nonlinear Schrödinger equation is coupled to an external potential that, in the context of galactic dynamics, is taken to be the gravitational potential, defined by the Poisson equation. They demonstrate the Madelung transformation, and drop the kinetic term from the resulting equations. This is known as the *Thomas-Fermi* approximation, which is again described in Section 3.2. In a system with a large number of atoms and repulsive interactions, the regime where the ratio of kinetic to potential energy is small is a good approximation to the full system. Its major advantage is that it makes analytic solutions more tractable. This approximation leads to the Lane-Emden equation, which has been analysed in great detail by Chandrasekhar [277] to describe the dynamics of stars. In this case, Böhmer and Harko find a description in terms of a polytropic fluid of index  $n = 1$ , as also found by Coles and Spencer [270]. The use of the Thomas-Fermi approximation rules out

the inclusion of phenomena such as vortices, as in this regime the wavefunction only varies slowly on the scales of interest. Slowly rotating polytropes were also studied in detail by Chandrasekhar, and this analysis is also presented in this paper. The radius of the dark matter halo can be related to the mass of the particle and the particle scattering length, so by considering ‘sensible’ values for the radius of a galaxy and scattering length of the particle, they make an estimate of the dark matter particle mass of  $1 - 10^{-3}$  eV. Once the density profile is described, it is fairly easy to obtain Newtonian rotation curves. They fit several curves according to their prescription, with fitting parameters of the radius, total mass and density of the halo taken from experimentally measured values. The model fits the rotation curve fairly well, with  $\chi^2$  fits of order 1.

This model also discusses the interesting possibility of employing gravitational lensing to make the distinction between a Bose-Einstein condensate dark matter halo and other models of dark matter. To make this comparison, they take the standard Weyl metric, and use the Tolman-Oppenheimer-Volkoff equations as the general relativistic equations for a static dark matter distribution. To completely define these equations, one must also give the equation of state of the dark matter fluid. They specify the equation of state for an  $n = 1$  polytrope, as previously described. A ratio between the light deflection produced by this and other models can then be calculated in order to discriminate between models.

Bose-Einstein condensates coupled to different potentials, including a gravitational one, were considered in Jones and Bernstein [278], leading to structures very similar to that of Böhmer and Harko.

Silverman and Mallett [279] discuss a similar paradigm. Again motivated by the possibility that dark matter with a quantum-mechanical nature may solve some of the problems associated with the CDM model, they use an Abelian-Higgs-like symmetry-breaking approach to endow a real scalar field with mass, relating the particle’s Compton wavelength and the cosmological constant of the spacetime to parameters in the underlying Lagrangian. If at some point in the cosmic history the condensation temperature of these bosons is greater than the CMB, then they make the transition to a Bose-Einstein condensate. For nonrelativistic bosons this is dependent on the particle’s mass and number density. To alleviate the problem of cuspy cores in galaxies,

they identify a length scale associated with the equilibrium between quantum pressure and gravitational attraction to be of the order of the size of a galactic core. This length scale can be expressed in terms of the particle's Compton wavelength, so Silverman and Mallett estimate a particle mass of order  $10^{-23}$  eV.

To describe evolution of the condensate, they employ a slightly modified Gross-Pitaevskii equation, which they are able to solve exactly. Unfortunately, this form of the Gross-Pitaevskii equation is not derived, and it is difficult to see where it has come from. Newtonian mechanics again provides the rotation curves from the resulting mass distribution, which are scaled to observations of the rotation velocity and size of various galaxies.

The interesting speculation in this paper concerns the formation of superfluid vortices. From considerations of Bose-Einstein condensates in condensed matter systems it is known that above a critical rotation velocity, quantum vortices will form. If a galactic halo consists of a Bose-Einstein condensate with the parameters described by Silverman and Mallett, then it would seem to be difficult to prevent quantum vortices from forming. Observational evidence of these vortices would obviously be a heavy indicator that dark matter does indeed reside in a Bose-Einstein condensate. Silverman and Mallett suggest that a detection of such vortices may come from frame-dragging effects, manifested in gravitational lensing or variation in polarisation of light from distant background sources. We will return to the concepts raised in this paper in Section 3.4, and also point out some of the shortcomings of this approach in Chapter 4.

A paper by Yu and Morgan [280] follows on from that of Silverman and Mallett, by considering the motions of a network of vortices in a galactic background as described above. The network of vortices consists of ultra-light scalar bosons generated by a cosmological phase transition. To describe the evolution of such a network, Morgan and Yu's procedure is to calculate the motion of one vortex due to a background phase gradient induced by the surrounding vortices. This is done by first considering Nielsen-Olesen vortices, or *cosmic strings* in the Abelian-Higgs model, and adding a term motivated from physical considerations due to a background phase gradient. The concept of vortex scattering in the Abelian-Higgs model using background phase gradients was largely considered in Thatcher and Morgan [281]. Yu and Morgan consider

this to be the relativistic version of a Gross-Pitaevskii equation describing vortices in a stirred Bose-Einstein condensate. We will discuss in more detail in Chapter 4 how the Abelian-Higgs model can be considered to be the relativistic version of the Landau-Ginzburg, so that superconducting flux tubes become the analogues of these high energy vortices. They then derive a weak field version of the Abelian-Higgs, and from their previous field theory motivation, include a term based on the background phase gradient. Using numerical techniques, a dark matter Bose-Einstein condensate galaxy is given an initial Kelperian velocity profile. Once the galaxy exceeds some critical speed, quantum vortices form, and interact both with the background phase gradient produced by the rotation of the galaxy, and that of the neighbouring vortices. The configuration is shown to evolve towards that of a flat velocity profile, similar to what is observed.

The papers we have mentioned so far in this section broadly cover the concepts we will be exploring in the rest of this thesis. There are, however, an number of other papers that could be considered relevant.

## 2.4 Scalar Field Dark Matter

In Section 1.1.2 we discussed how scalar fields can be used to describe the matter-energy content of the Universe. Scalar fields, endowed with different potentials, can represent the general properties of a large variety of forms of matter. As the properties of dark matter are largely unknown, this can make scalar fields an ideal candidate for modelling dark matter.

A vast amount of literature is devoted to attempts to model dark matter as a scalar field. We will not give a pedagogical discussion of all of these models, as the ideas are not central to this thesis, but we will try to give an outline of some of the main concepts. We will concentrate on scalar field models that suggest a resolution to the problems associated with the Cold Dark Matter paradigm. Almost all of these models use the nonlinear Einstein-Klein-Gordon equations, or its nonrelativistic and noninteracting counterpart, to describe the structure and evolution of the scalar field(s) proposed, and this is partly our motivation for presenting them here.

Scalar field models of the dark matter halo can bear more than a passing resemblance to bound solitonic solutions that are admitted by the Einstein-Klein-Gordon equations. These solutions are known variously as *geons*, *boson stars* or *oscillatons*. Many authors have commented on the connection between these bound solutions and the galactic halo. Solitonic solutions were largely described in the literature before scalar field dark matter solutions were considered, with scalar field dark matter proponents only making the connection later. This can make a linear discussion of this topic difficult. We will run through the scalar field dark matter models first, commenting later on the nature of the bound solutions.

A large amount of scalar field dark matter candidates were proposed when it was first suggested that the axion might make suitable dark matter candidate. See, for example, reference 1 in Hwang [282].

One of the first suggestions for scalar field dark matter was given by Press, Ryden and Spergel [283], who use the nonlinear Einstein-Klein-Gordon Lagrangian to describe particles with an exceptionally large Compton wavelength. Density cusps in galactic halos are then suppressed for the same reason described in Section 2.3; the Heisenberg uncertainty principle.

Sin [284] uses the nonlinear Schrödinger equation coupled to the Poisson equation to describe an ultralight boson (hence with large Compton wavelength) and obtains mass profiles for a galaxy that resemble the excited states of Newtonian solitonic solutions known as boson stars, although these bounds states are never referenced directly. The mass profiles are adjustable by choosing different excited states of the boson star. The rotation curves from these mass profiles resemble those obtained observationally. This paper is the first in this vein to mention that galactic halos could be considered to be ‘giant systems of a condensed Bose gas’. A follow-up paper varies the percentage of baryonic mass in their simulations to see how it effects the rotation curves. Lee and Koh [285] consider a relativistic extension of Sin’s model by suggesting that excited boson stars described by the nonlinear Klein-Gordon equation are an adequate relativistic approximation to Sin’s solutions. The rotation curves obtained from such an energy distribution are again approximately what is observed. The total mass of the halo and the excited mode of the boson star are again adjustable parameters.

Schunck [286] considers the massless Einstein-Klein-Gordon equations, as well as pointing to previous literature suggesting that the higher mode solutions of boson stars considered previously are generally known to be unstable. As this scalar field is massless, the boson star solution is ‘transparent’. However, the energy density still couples to normal matter gravitationally, and so they take a Newtonian limit in order to obtain rotation curves that again approximately plateau with increasing radius. Again, two adjustable parameters allow for better fitting.

Peebles and Vilenkin [287, 288, 289] attempt to use scalar fields to incorporate inflation and dark matter into one model. Both fields have a quartic potential and initially the dark matter field behaves like radiation. If, however, the quartic potential is suppressed later on, so that the potential is dominated by the quadratic term, then the scalar field behaves like an ideal non-relativistic gas. A similar idea was posited in Goodman [290]. Assuming that the field is nonrelativistic at later times, these papers make some quantitative predictions based upon the Jeans scales of the resulting fluid. The resulting fluid equations give the required suppression of substructure and core density cusps. Allowing the potential to be rather less than quartic ( $\sim y^{3.7}$ ), allows an even better fit to the observed astronomical data.

Matos, Guzman and Ureña-López study the evolution of real scalar field solutions to the Einstein-Klein-Gordon equations. In their early papers [291, 292], they are motivated by the fundamental scalar fields in cosmology that high energy models of the early Universe would seem to predict, such as the dilaton, and suggest that scalar fields may provide an explanation of the dark matter problem too. They study a real scalar field with an exponential scalar potential, and using a method previously developed by Matos in the context of Kaluza-Klein theory, called the ‘harmonic maps ansatz’ [293, 294, 295], which is beyond the scope of this thesis, the Einstein-Klein-Gordon equations are reduced to a ‘Poisson-like structure’. The velocities of test particles following circular trajectories around such configurations give rotation curves that approximately match those observed in dark matter halos. Two fitting parameters must be arbitrarily chosen to scale the curves appropriately.

Further papers [296, 297] try to model the evolution of dark matter and dark energy as two different real scalar fields, in a similar vein to the Peebles and Vilenkin pa-

pers mentioned above. The dark matter and dark energy are given potentials that go as  $V(\Phi) \sim \cosh(\Phi)$  and  $V(\Psi) \sim \sinh^\beta(\Psi)$  respectively, giving the scalar field quintessence-like properties. The scalar field energy density is found to track the radiation energy density in a similar way to a model of Sahni [298]. Relating the observed values of the matter and radiation density to the coefficients of the scalar field potential, Matos et al. predict that the dark matter particle in this scenario would have to be ultra-light,  $m \sim 10^{-23}$  eV. They suggest that the Jeans length for this model is related to the mass of the dark matter particle, and because of this, the problems of dark matter halo cusps and the dearth of small scale structure are avoided.

Other papers by the same authors [299, 300] consider a similar paradigm. In this case, two scalar fields are introduced; one to model the central massive galactic object, and one to model the overall dark matter halo that extends far from the galactic centre. The authors make the link that the galactic centre solution could be considered to be an oscillaton solution. An oscillaton is a soliton solution to the Einstein-Klein-Gordon equations, which we will discuss along with other more ‘exotic’ objects in a later section. Oscillaton solutions have been discussed, away from the considerations of their role in a dark matter galactic environment, by one of the authors [301], and will be mentioned later. Again, this model involves an ultralight boson, two parameters that require fitting from observations, and rotation velocities that approximately agree with what is seen.

Another series of papers by Arbey, Lesgourgues and Salati, [302, 303, 304, 305] discusses work that is very similar to the above papers by Matos, Guzman and Ureña-López. The main difference between these two strands of work is that Arbey, Lesgourgues and Salati consider a complex scalar field, while the previous group discuss a real field.

Fuchs and Mielke [306] consider the nonlinear Klein-Gordon equation, this time with a  $\phi^6$  interaction. They find approximate fits to the central density profiles of low surface brightness galaxies. There are again two adjustable parameters to fit.

Further papers by Matos et al. [307, 308] consider the weak field limit for a real scalar field described by the Einstein-Klein-Gordon equations with  $\cosh \phi$  or  $\phi^2$  potentials. They show that these models can produce density profiles for dark matter halos that

are close to what is observed. These later papers also make the connection that the scalar field can be considered to be a Bose-Einstein condensate.

Papers by Lee [309, 310, 311] reiterate what has gone before, as well as suggesting that two scalar field dark matter galaxies may be able to pass through each other, like solitons. They suggest that the Bullet cluster and Train Wreck remnants may be evidence that this has happened.

Interestingly, this brings us to a connection between scalar field dark matter models and experimental physics.

Giovanazzi, O'Dell, Kurizki and Akulin [312, 313] developed an experimental technique, whereby illuminating a cloud of trapped atoms in laser light will induce a long-range inverse square force between every atom in the system. In this way, it is possible to simulate gravitationally bound structures in the laboratory with Bose-Einstein condensates. This procedure is also summarised in a nice *Nature* article by Anglin [314]. Choi [315] follows this up by numerically evolving this system for the collision of two 'gravitationally' bound solitonic objects; the analogue of a colliding boson star system. This paper describes the solitonic nature of 'self-gravitating' Bose-Einstein condensates undergoing head-on collision. This is another example of numerical or experimental techniques helping to make inroads into domains of cosmological physics that would otherwise be observationally inaccessible.

### 2.4.1 Scalar Fields and Bose-Einstein Condensation

Scalar field dark matter models allow for the possibility of Bose-Einstein condensation, because of their bosonic nature. Discussion of the condensation of a spin-zero boson in a cosmological context has been around since at least 1978 [316]. Bose-Einstein condensation in field theory will be discussed further in Chapter 4. The relativistic equations for evolving a scalar field reduce to the nonlinear Schrödinger-Poisson system in the weak field limit. This system is of the same form as the Gross-Pitaevskii equation describing a Bose-Einstein condensate, with a gravitational coupling term. If we interpret the scalar field as the order parameter of a condensate, then it is possible to interpret the model as a cosmologically relevant Bose-Einstein condensate

[298, 308, 317, 318]. This is one way of considering the boson stars and oscillatons that we will discuss in the next section.

Some authors have tried to describe dark energy and dark matter using the same scalar field [319, 320]. We briefly describe some papers where the condensed fraction of the scalar field is identified as dark matter.

Ferrer and Grifols [321] describe an effect where scalar particles are coupled to matter fermions via a usual Yukawa-type potential. When this coupled system is embedded in a background made of the same scalars, they find that the range of the potential interaction goes from finite to infinite when the scalar background undergoes Bose-Einstein condensation. In a followup paper [322], the condensate is identified with the dark matter component of the Universe, and they describe the possibility of anomalies in the peak structure of the CMB that may arise from the interaction between dark and normal matter. Investigating the parameter space of  $m_\phi$ , the mass of the scalar particle, and  $g_{\text{eff}}$ , the interaction strength, they find that it is possible that the scalar particles still exist within a Bose-Einstein condensate, but to be consistent with the CMB peak locations, nucleosynthesis and large-scale structure formation, the interaction strengths would have to be so weak as to go unnoticed today. They show that other parts of the  $m_\phi - g_{\text{eff}}$  parameter space could produce cosmologies that are obviously erroneous. This effect is also applied to the equilibrium of degenerate stars, such as white dwarves [323]. Scalar field dark matter permeates the galaxy, and some will become gravitationally trapped by, for example, a white dwarf star. This provides the setup of the coupled fermionic particles embedded in a scalar particle background. Ferrer and Grifols conclude that the new star configurations should populate different regions of the mass-radius plane compared to the standard white dwarves described by the pioneering Chandrasekhar models [277], and hence provide observational consequences.

Morikawa [324], along with Morita and Nishiyama [325] introduce a model where a boson fluid, described by a scalar field, is identified as the dark matter component of the Universe, with an equation of state of dust,  $p = 0$ . This scalar field is identified as the classical mean field used to describe a Bose-Einstein condensate. This, they claim, provides an explanation for the origin of the scalar field that drives the late-time expansion of the Universe (dark energy). As the Universe cools below some

critical temperature, the dark matter boson fluid condenses, taking its equation of state to the form  $p = -A\rho^\alpha$ . The case of  $\rho = -p$  is identified as the simplest case, and investigated. They also suggest that the energy density of the Bose gas is diluted with the expansion of the Universe. The condensed phase, however, is not. Hence, the condensate will dominate over the normal fluid component and the expansion of the Universe will switch from decelerated to accelerated expansion. On local scales, once the energy density of the condensate reaches some critical value, fluctuations in the density quickly collapse to form boson stars, which may fragment because of the negative pressure of the fluid. So, dark matter condenses to form dark energy, which can collapse to form localised sources of dark matter. In this way, many seeds for structure formation are formed. This idea is restated in Fukuyama and Morikawa [326], and reviewed in added detail in Fukuyama et al.[327]. By considering the temperature of the boson gas when it was coupled to the radiation component of the Universe, they set limits on the condensation temperature, and hence the boson mass. They set a limit of  $m_\phi < 2$  eV, and suggest that ultralight masses are more likely. What would appear to be the major drawback in this model is that in order to obtain a dark energy with the required equation of state, the authors attribute negative pressure to an attractive interaction potential in the Gross-Pitaevskii equation. Attractive interactions generally lead to negative values of the particle scattering length, and an imaginary sound speed [328], making this form of matter even more exotic than usual. They extend this model to inflation in Fukuyama and Morikawa [329].

Similar models have been discussed previously. Madsen, for example, discussed the possibility of a 17 keV neutrino condensing, so that galaxy formation might proceed as a hybrid hot and cold dark matter model, with the same particle responsible for both components. The evidence for a 17 keV neutrino unfortunately turned out to be erroneous [330]. Dymnikova and Khlopov [331] and Bassett et al. [332] both also consider models where dark energy emerges as the condensate of a dark matter particle when the Universe cools past some critical temperature.

## 2.5 Exotic Objects

In the previous section, we came across some solitonic solutions to the Einstein-Klein-Gordon equations that were adopted by authors investigating scalar field dark matter models. As we mentioned previously, such solutions were described much earlier, outside of a dark matter context.

The first such description can be traced back to Wheeler [333] who described solutions of the Einstein-Maxwell equations. He considered the mass associated with an electromagnetic disturbance, and concluded that the gravitational attraction of such a disturbance is capable of holding the disturbance together for a long time in comparison with the characteristic periods of the entity. This might be recognised as soliton-like behaviour. Wheeler called such disturbances *geons*, a contraction of *gravitational magnetic entity*.

Kaup would then go on to describe *Klein-Gordon Geons* [334]. In seeking a counter example to the conjecture that gravitational collapse is inevitable, he suggested eigenstates of the coupled Einstein-Klein-Gordon equations; solitonic objects whose quantum nature would hold them up against collapse to a singularity.

### 2.5.1 Boson Stars

Boson stars are self-gravitating solutions to the Einstein-Klein-Gordon equations for a complex scalar field, first investigated by Feinblum and McKinley [335] and Ruffini and Bonazzola [336, 337]. The latter authors described them as being analogous to the Hartree-Fock description of the atom. Boson star solutions can be constructed by seeking solutions to the equations of motion derived from the Einstein-Klein-Gordon action, with the spherical symmetric metric

$$ds^2 = e^{\nu(r,t)} dt^2 - e^{\lambda(r,t)} dr^2 - r^2(d\theta^2 + \sin^2\theta d\phi^2). \quad (2.1)$$

Following Jetzer's thorough review article [338], we can find equilibrium solutions by working in the gauge  $A_\mu = (A_0, 0, 0, 0)$  and setting  $\phi(r, t) = \phi_0 e^{i\omega t}$ . Calculating the components of the energy momentum tensor at this point can be fairly involved, but

eventually we find a scalar wave equation

$$\phi_0'' + \left[ 2/r + \frac{1}{2} (v_0' - \lambda_0') \right] \phi_0' + e^{\lambda_0} [(\omega + eA_0)^2 e^{-\nu_0} - m^2] \phi_0 = 0. \quad (2.2)$$

We see that any solution is now time independent. To obtain bound solutions, the boundary conditions  $\phi_0 = \text{const}$ ,  $\phi_0' = 0$  and  $\phi_\infty = \phi_\infty' = 0$  are imposed. The field  $\phi_0$  may also have nodes, corresponding to excited states of the system. In considering boson stars as a description of a galactic halo, it has been found [302, 304, 305] that higher node solutions produce rotation curves that correspond better to those observed. These higher nodes are unfortunately unstable, and decay quickly to the 0-node solution [339, 340], possibly via the emission of particles [341]. It should be noted that equilibrium solutions exist as there is a Noether current associated to the gauge field, which corresponds to a conservation of particle number [338]. This is an important comparison for the oscillaton solutions we will consider next.

Many authors then looked at adding an interaction term to the Klein-Gordon equation. Mielke and Schunck in particular [342], found that adding a repulsive  $\phi^6$  self-interaction term allows the corresponding Klein-Gordon equation to be simplified to a Lane-Emden equation, familiar from the astrophysics of gaseous spheres, as we have also mentioned in the discussion of Bose-Einstein condensate dark matter papers by Coles and Spencer [270] and Böhmer and Harko [276]. Colpi et al. [343] also looked at boson stars with an interaction term and found that the soliton solutions formed tended to be extended in space, as one might expect for a distribution of particles with a repulsive interaction added.

Boson star configurations experienced a slight resurgence in popularity in the early 1990s, driven by the possibility that scalar fields may have an important role to play in fundamental physics. Ferrer and Gleiser [344] investigated the gravitational radiation from excited states of a boson star, while other authors started to concern themselves with the formation of such objects in a cosmological environment, and their implications for observations [345, 346, 347, 348].

Madsen and Liddle [345] suggest that for boson stars to have a astrophysically meaningful mass (solar mass  $\sim 2 \times 10^{30}$  kg) the boson mass needs to be of order  $10^{10}$  eV. This can be altered somewhat with the addition of a self-coupling term. We will see

later that this term can be written in the Lagrange density as

$$\mathcal{L}_{\text{sc}} = \frac{\lambda}{2} (\phi^\dagger \phi)^2. \quad (2.3)$$

Madsen and Liddle showed that even for very small values of  $\lambda$ , this coupling may be crucially important. They show that the self-coupling term is important for

$$\lambda > 1000 \frac{m^2}{m_{\text{pl}}^2}. \quad (2.4)$$

For a boson with a mass similar to that of the neutron, this only requires that  $\lambda > 10^{-35}$ . They suggest then, that unless there is a huge suppression of  $\lambda$ , then the case  $\lambda = 0$  is unlikely to be astrophysically relevant.

Seidel and Suen [349] gave a description of a post-Newtonian solution for the boson star configuration, while Guzman and Ureña-López [339, 340] look at the formation of solitonic objects in the weak field limit, using a Schrödinger-Poisson system of equations.

Torres et al. [350] appear to be the first authors to make the connection that a scalar soliton solution might be a good description of the core of some galaxies, while Guzman and Ureña-López [351] make the connection that these scalar field systems could be considered to be gravitationally bound solutions of a Bose-Einstein condensate. The behaviour of non-spherical collapse of scalar field dark matter and the late time behaviour is studied in Bernal and Guzman [352]. Rotating boson stars have also been shown to have an effective metric that describes a torus of mass [353].

### 2.5.2 Oscillatons

If solitonic solutions to the Einstein-Klein-Gordon equations are sought for real, rather than complex scalar fields, it is not possible to find time-independent solutions. For real scalar fields, there is no longer a conserved Noether current corresponding, for instance, to the conservation of particle number [338]. Instead, regular boundary conditions are satisfied by time dependent solutions; collapsing or expanding configurations, or periodic solutions. In this case, both the metric  $g_{\mu\nu}$ , and the scalar field  $\phi$ , oscillate in time, similar to the ‘breather’ solution of the sine-Gordon equation. Such solutions

were first described by Seidel and Suen [355] and are called oscillating soliton stars, or oscillatons.

Oscillaton solutions are again not trivial to construct, but we can give a brief overview [338]. Using the same line element as for boson stars, eqn. (2.1), the Einstein-Klein-Gordon equations must be solved to obtain equations for the metric components  $\nu'$ ,  $\lambda'$  and  $\dot{\lambda}$ , and the scalar field  $\phi(r, t)$ . One then constructs periodic expansions for  $e^\nu$ ,  $e^\lambda$  and  $\phi(r, t)$ .

$$e^{\nu(r,t)} = 1 + \sum_{j=0}^{\infty} N_{2j}(r) \cos(2j\omega_0 t) \quad (2.5)$$

$$e^{\lambda(r,t)} = 1 + \sum_{j=0}^{\infty} g_{2j}(r) \cos(2j\omega_0 t) \quad (2.6)$$

$$\phi(r, t) = \sum_{j=1}^{\infty} \phi_{2j-1}(r) \cos((2j-1)\omega_0 t) \quad (2.7)$$

Ureña-López [301] was the first to consider the weak field limit of oscillatons, with the motivation that boson stars and oscillatons are predicted by scalar field dark matter models. This author also considered the weak field limit of oscillatons with a self-interacting  $\phi^4$  term. Another paper [356] follows up by considering the formation of oscillatons from the gravitational collapse of scalar field configurations.

## 2.6 Penrose and the Quantum State Reduction Problem

The bound state of the Schrödinger-Poisson system has been considered by Penrose and others, motivated interestingly by the problem of *state reduction*, or *wavefunction collapse* in quantum mechanics. For a comprehensive discussion of these concepts see Wheeler and Zurek [357] or Giulini et al. [358].

Confronted by the results of the double slit experiment, the EPR paradox, Bell's inequalities and the Schrödinger's cat thought experiment and its variants, we are forced to consider the nature of the wavefunction in quantum mechanics. We can take the example of a charge of an electron represented by a wavefunction. Does the wavefunction

merely represent the probability distribution of a point charge, or is the charge actually distributed in space?

The issue of mathematical interpretation returns. The *Copenhagen interpretation* of Bohr and Heisenberg suggests that the wavefunction of a system should not be considered a real entity, but rather an abstract concept which allows the calculation of probabilities for the outcome of a measurement. The wavefunction in a sense represents the ‘maximal state of our knowledge’, with the notion of probability necessary because a complete knowledge of the state of a system is prevented by the Heisenberg uncertainty principle.

At the other extreme of interpretation comes the *many worlds theory*, suggesting that each probability distribution is actually realised, so that all outcomes actually exist. This interpretation poses the problem of why one particular scenario presents itself to us.

Integral to the issue of interpretation is the problem of the observer; whether an observer is indeed necessary for wavefunction collapse, thus defining the reality around him, or if the collapse is a purely objective phenomena.

Weinberg [359] suggests that resolution may lie in treating all the components of the system consistently. The quantum system, the measuring apparatus and the observer all require a description in terms of quantum mechanics.

Penrose has argued for an objective collapse of the wavefunction, in terms of a gravitational influence. His argument suggests that for a superposition of states representing two different mass distributions (the position of a particle confined by the Heisenberg uncertainty principle, for example), there should be an associated superposition of gravitational fields produced by the particle. If there is a significant mass displacement between the two states, each of which would be stationary on their own, the energy associated with the maintenance of dual gravitational fields may become larger than one or other of the component states. The system is unstable, and the wavefunction collapses, without ever invoking an external observer.

Penrose suggests that the timescale  $T$  of the instability would be inversely proportional to the gravitational self-energy associated to the difference between the mass distribu-

tions of the two states,  $E_G$ ,

$$T \simeq \frac{\hbar}{E_G}. \quad (2.8)$$

He also suggests that this statement is not a theory of quantum state reduction, but ‘rather a statement of the level at which deviations from standard linear Schrödinger (unitary) evolution are to be expected, owing to gravitational effects’ [360] pg. 584.

The final stationary states, for appropriate mass and velocity ranges, should then be represented by stationary solutions of the Schrödinger equation, coupled to an appropriate gravitational term arising from the mass density given by the expectation value of the mass distribution in the appropriate state. This leads to the Schrödinger-Newton equations [361], which we have referred to as the Schrödinger-Poisson system,

$$i\hbar \frac{\partial \Psi}{\partial t} = -\frac{\hbar^2}{2m} \nabla^2 \Psi + m\Phi \Psi, \quad (2.9)$$

$$\nabla^2 \Phi = 4\pi G m |\Psi|^2. \quad (2.10)$$

Bound, stationary solutions of this system have been investigated by Penrose, Moroz, Tod and Harrison [362, 363, 364, 365]. Relation to earlier boson star work is only mentioned in passing with a brief reference to Ruffini and Bonazzola’s paper [337].

## 2.7 Discussion

In this chapter we have attempted to give a thorough overview of the role of the Schrödinger-Poisson system in going beyond the standard Cold Dark Matter model. We implicitly motivated the nonlinear Schrödinger equation by discussing how problems of the CDM model may be circumvented by allowing dark matter particles to self-interact. After discussing some of the advantages of a classical approach to the Schrödinger equation in modelling structure formation, we then switched to a purely quantum description by discussing a dark matter condensate consisting of a Bose-Einstein condensate. Scalar fields provide a useful tool for modelling, as the specific properties of the matter can be left fairly general. The evolution equations for a gravitationally coupled scalar field are the Einstein-Klein-Gordon equations, or in the weak field limit, the Schrödinger-Poisson system. Scalar fields are also amenable to Bose-Einstein condensation, as they describe particles that obey boson statistics. We also

saw some of the bound solitonic solutions that exist for these systems, and how some authors have tried to identify them with galactic dark matter structure. We gave a brief overview of the construction of these ‘exotic’ objects, and finished with a discussion of the role of the Schrödinger-Poisson system in the quantum state reduction problem.

## Chapter 3

# The nonlinear Schrödinger Equation in Condensed Matter and Cosmology

In this chapter, we apply the nonlinear Schrödinger equation to various situations in cosmology. We start by looking at its use in condensed matter physics, where it is used to model the macroscopic properties of Bose-Einstein condensates. We look at its derivation, and some of the standard techniques used to relate the Gross-Pitaevskii equation to the fluid equations, as well as the description of quantum vortices.

We then return to ideas mentioned in Section 2.2 concerning the use of the Schrödinger equation in modelling structure formation, and note the role of the *Madelung transformation*, a concept from condensed matter theory. In a cosmological context, gravitational effects are included by coupling the Schrödinger equation to the Poisson equation.

In the final section, we use the quantum-mechanical version of this coupled system to model a novel dark matter candidate, in which the dark matter particles reside in a Bose-Einstein condensate. In particular we discuss the possibility that a rotating dark matter Bose-Einstein condensate halo might contain quantised vortices. Using known solutions for the density profiles of such vortices, we consider the gravitational self-interactions in such halos, in order to estimate some of the parameters of a dark matter particle in such a model.

### 3.1 The Bose-Einstein Condensate

We first outline the concept of Bose-Einstein condensation, and the criteria necessary for it to occur.

Integer-spin particles obey Bose-Einstein statistics and are not subject to any exclusion principle like that of fermions. As such, an unlimited number of particles may occupy any single-particle state. Any particles not in an excited state are accommodated in the single-particle ground state, which can hold an unlimited number, and the system is said to have a *Bose-Einstein condensate*.

The condensate temperature  $T_c$  is the highest temperature at which a condensate exists. That is, the highest temperature at which the single-particle ground state is occupied. At temperatures higher than this, all particles are excited into higher states.

The number of particles in an excited state can be given by

$$N_{\text{ex}} = \int_0^{\infty} d\epsilon g(\epsilon) f(\epsilon), \quad (3.1)$$

where  $g(\epsilon)$  is the density of states, and  $f(\epsilon)$  is the Bose-Einstein distribution function, which describes the mean occupation number of the single particle state  $i$ , for a noninteracting gas in thermodynamic equilibrium. It is given by

$$f_{\text{BE}}(\epsilon_i) = \langle n_i \rangle = \frac{1}{e^{\beta(\epsilon_i - E_v)} - 1} \quad (3.2)$$

where  $\beta = 1/k_B T$ , and  $\epsilon_i$  is the energy of the single particle state for a particular trapping potential.

The quantity  $E_v$  is known as the *chemical potential*, and is defined within the *Grand Canonical Ensemble* as a way of parameterising a changing particle number. The chemical potential can be thought of as the energy change of the system if one particle is added, at constant entropy and volume. It also acts as a Lagrange multiplier, as we will see in Section 3.2. In relativistic systems, each conserved quantity, and hence symmetry of the system, can be associated with a chemical potential. We will discuss this further in Section 4.2. The chemical potential is also generally a function of particle number  $N$ , and temperature  $T$ .

The number of excited particles  $N_{\text{ex}}$  is maximised for  $E_v = 0$ , and the transition temperature is the temperature at which all the particles are in excited states,  $N = N_{\text{ex}}$ .

Any lower, and the single-particle ground state will start to become occupied, and a condensate will form.

The density of states can be written in a general form in terms of powers of the energy

$$g(\epsilon) = C_\alpha \epsilon^{\alpha-1}, \quad (3.3)$$

where  $C_\alpha$  is a constant, and  $\alpha$  is a parameter dependent on the properties of the system, such as the trapping potential. By defining the dimensionless variable  $x = \epsilon/k_B T_c$ , and evaluating a nasty integral, the condensate temperature can be shown to be

$$k_B T_c = \frac{N^{1/\alpha}}{(C_\alpha \Gamma(\alpha) \xi(\alpha))^{1/\alpha}}, \quad (3.4)$$

where  $\Gamma(\alpha)$  is the gamma function, and  $\xi(\alpha)$  is the Riemann-zeta function. Below the condensate temperature, the number of excited particles is just

$$k_B T = \frac{N_{\text{ex}}^{1/\alpha}}{(C_\alpha \Gamma(\alpha) \xi(\alpha))^{1/\alpha}}. \quad (3.5)$$

So we can define the number of particles in the condensate  $N_0 = N - N_{\text{ex}}$  as

$$N_0 = N \left( 1 - \left( \frac{T}{T_c} \right)^\alpha \right). \quad (3.6)$$

For the particular examples of a gas confined to a three-dimensional box of volume  $V_{\text{ol}}$ , for which  $\alpha = 3/2$ , then

$$k_B T_c \approx 3.31 \hbar^2 \frac{n^{2/3}}{m}, \quad (3.7)$$

with the number density  $n = N/V_{\text{ol}}$ , while the condensation temperature for a gas trapped by a three-dimensional harmonic oscillator potential is given by

$$k_B T_c \approx 0.94 \hbar \bar{\omega} N^{1/3}, \quad (3.8)$$

where  $\alpha = 3$ , and  $\bar{\omega}$  is the geometric mean of the oscillator frequencies in each orthogonal direction. The corresponding condensate particle number can be obtained from eqn. (3.6).

The criterion for Bose-Einstein condensation then, is that the occupation number for one of the single particle levels should be macroscopic. This derivation does not include interactions between particles. Generally the depletion of the condensate due to interactions is small enough to be neglected. See, for example, comments in Section

6.1 of Pethick and Smith [328]. A generalisation of this condensation criterion for bulk systems has been proposed by Penrose [366] and Landau and Lifshitz [194], and elaborated by Penrose and Onsager [367] and Yang [368]. The Gross-Pitaevskii equation discussed in the next section includes the effects of interactions.

We can make a convenient approximation to the condensation temperature by simply comparing the thermal de Broglie wavelength to the interparticle separation, as suggested in Section 2.3. The thermal de Broglie wavelength can be thought of as the average de Broglie wavelength of particle in an ideal gas at temperature  $T$ . When the thermal de Broglie wavelength approaches the mean inter-particle spacing, quantum effects will become important, and the gas must be treated as a degenerate Bose gas, or condensate. The thermal de Broglie wavelength is given by

$$\lambda_T = \left( \frac{2\pi\hbar^2}{mk_B T} \right)^{\frac{1}{2}}, \quad (3.9)$$

for which  $\lambda_T \approx n^{-1/3}$  for a condensate, giving

$$k_B T_c \approx 2\pi\hbar^2 \frac{n^{2/3}}{m}, \quad (3.10)$$

which we see is a good approximation to eqn. (3.7). This simple but effective estimation can be useful in many scenarios including the early Universe. Particle mass, number density and the temperature at various epochs can all be determined, allowing a calculation of whether or not a particular particle species forms a condensate.

We now come to the Gross-Pitaevskii equation. We will see that typically, in the limit of large particle number the density distribution of the condensate can be described by a macroscopic wavefunction that is considered to be a quantum field. This field is manipulated by the Gross-Pitaevskii equation, or nonlinear Schrödinger equation, rather than working with the usual creation and annihilation operators of quantum mechanics. The density distribution of the condensate can be represented by a macroscopic wavefunction of the same form as the ground state wavefunction of a single particle. The momentum distribution of the condensate is obtained by taking the Fourier transform of this wavefunction and, in an experimental setup, the occurrence of a Bose-Einstein condensate is confirmed by a sharp peak in the momentum space distribution of the gas of particles. This is a good model for the condensate of Cooper pairs in a superconductor, or for helium atoms in a superfluid [328]. This procedure is also analogous

to classical electrodynamics, where electric and magnetic fields are used, rather than the creation and annihilation operators for photons.

In quantum field theory, a condensate corresponds to a non-zero expectation value for some operator in the vacuum and, in the limit of large quantum number, this condensate can be considered to be a classical field. The Higgs field, for example, has a vacuum expectation value, and interaction with this condensate leads to the gauge bosons acquiring mass. Similar mechanisms operate in the chiral and gluon condensates in QCD. The concept has also been applied to hypothetical particles such as axions or ghosts [369]. In this context, the axion field, for example, is coherent and has relatively small spatial gradients. The gradient energy can be interpreted as particle momenta, which will be the same and small for each particle, giving a sharp peak in the momentum-space distribution as in the case of the more familiar Bose-Einstein condensate described previously. The condensation of axions from a ‘standard’ condensed matter point of view has also been considered [370].

The relation to field theory will be described in more detail in Chapter 4.

## 3.2 The Gross-Pitaevskii Equation

The nonlinear Schrödinger equation is typically known in condensed matter parlance as the Gross-Pitaevskii equation. This equation represents the macroscopic properties of a many-body quantum-mechanical system, and is in some sense a semi-classical description. It seeks to describe the properties of a bulk material by including a term representing the interaction between particles. In a many body system, this gives a good description of the properties of the bulk fluid on scales where quantum effects become important, such as at boundaries, or in vortex cores. To move from a microscopic description of individual atoms to a wavefunction describing the macroscopic properties of the bulk material requires us to replace quantum operators with non-operator numbers. This is the Bogoliubov prescription, which we will describe shortly. All these concepts are further elaborated in, for example, Pethick and Smith [328] and Pitaevskii and Stringari [371]. To an extent, we also follow the notation and conventions set out in Roberts and Berloff [372].

We first deal with interactions within the Bose-Einstein condensate fluid. Rather than try and describe interactions in terms of a potential that will depend in a complicated way on the inter-particle distance, we instead make an approximation to the interaction potential that is proportional to the scattering length,  $a_s$ . To first order in an interaction, the wavefunction is dominated by a contribution from the scattering length. In the Born approximation, the scattering length is given by

$$a_{s(\text{Born})} = \frac{m_{\text{red}}}{2\pi\hbar^2} \int d\mathbf{r} V(\mathbf{r}), \quad (3.11)$$

where  $m_{\text{red}}$  is the reduced mass, and  $V(\mathbf{r})$  is the potential between atoms (see any good standard quantum mechanics text, such as Bransden and Joachain [373]). In the case of equal mass particles, we see that the Born approximation scattering length matches the true scattering length if we use the effective interaction potential

$$\int d\mathbf{r} V_{\text{eff}}(\mathbf{r}) = \frac{4\pi\hbar^2 a_s}{m} \equiv V_0. \quad (3.12)$$

For an effective interaction potential proportional to the scattering length, we can then write

$$V_{\text{eff}}(\mathbf{r}, \mathbf{r}') = V_0 \delta(\mathbf{r} - \mathbf{r}'). \quad (3.13)$$

We now look at the whole Bose-Einstein condensate. The effective Hamiltonian of this system can be written as

$$H = \sum_{i=1}^N \left[ \frac{\mathbf{p}_i^2}{2m} + V_{\text{ext}}(\mathbf{r}_i) \right] + V_0 \sum_{i<j} \delta(\mathbf{r}_i - \mathbf{r}_j), \quad (3.14)$$

where  $i$  labels each of the  $N$  particles, with the delta function taking care of interaction between each one.  $V_{\text{ext}}$  couples the system to some external potential. In a condensate, each of the  $N$  particles is in the same single-particle state  $\phi(\mathbf{r}_i)$ , and the energy functional of the system can be written as the expectation value of the above Hamiltonian

$$E = N \int d\mathbf{r} \left[ \frac{\hbar^2}{2m} |\nabla\phi(\mathbf{r})|^2 + V_{\text{ext}}(\mathbf{r}) |\phi(\mathbf{r})|^2 + \frac{(N-1)}{2} V_0 |\phi(\mathbf{r})|^4 \right], \quad (3.15)$$

where  $N(N-1)/2$  is the number of pairs of bosons. We take the particle number to be  $N \gg 1$ , and define the particle density to be  $n = N/V_{\text{ol}}$ . Introducing the wavefunction of the condensed state

$$\psi(\mathbf{r}) = N^{\frac{1}{2}} \phi(\mathbf{r}), \quad (3.16)$$

and noting that for a uniform system of volume  $V_{0l}$  the wavefunction of the system is  $1/V_{0l}^{1/2}$ , we find that the particle density is defined by

$$n(\mathbf{r}) = |\psi(\mathbf{r})|^2, \quad (3.17)$$

and we can rewrite the energy functional as

$$E(\psi) = \int d\mathbf{r} \left( \frac{\hbar^2}{2m} |\nabla\psi(\mathbf{r})|^2 + V_{\text{ext}}(\mathbf{r})|\psi(\mathbf{r})|^2 + \frac{1}{2} V_0 |\psi(\mathbf{r})|^4 \right). \quad (3.18)$$

Using the method of Lagrange multipliers, we can minimise this energy functional with the condition that the total number of particles in the system

$$N = \int d\mathbf{r} |\psi(\mathbf{r})|^2, \quad (3.19)$$

remain constant. We do this by minimising the quantity  $E - E_v N$  at fixed  $E_v$ , where  $E_v$  is the chemical potential, to obtain the time-independent Gross-Pitaevskii equation

$$-\frac{\hbar^2}{2m} \nabla^2 \psi(\mathbf{r}) + V_{\text{ext}}(\mathbf{r})\psi(\mathbf{r}) + V_0 |\psi(\mathbf{r})|^2 \psi(\mathbf{r}) = E_v \psi(\mathbf{r}). \quad (3.20)$$

We can generalise this to the time-dependent form by writing

$$i\hbar \frac{\partial}{\partial t} \Psi(\mathbf{r}, t) = -\frac{\hbar^2}{2m} \nabla^2 \Psi(\mathbf{r}, t) + V_{\text{ext}}(\mathbf{r}, t)\Psi(\mathbf{r}, t) + V_0 |\Psi(\mathbf{r}, t)|^2 \Psi(\mathbf{r}, t), \quad (3.21)$$

noting that, to be consistent with the time-independent form above, the evolution of  $\Psi$  must go as  $\Psi(\mathbf{r}, t) = \psi(\mathbf{r}, t) \exp(-iE_v t/\hbar)$ . The Gross-Pitaevskii equation we use for analysis, then, is

$$i\hbar \frac{\partial}{\partial t} \psi(\mathbf{r}, t) = -\frac{\hbar^2}{2m} \nabla^2 \psi(\mathbf{r}, t) + V_{\text{ext}}\psi + V_0 |\psi(\mathbf{r}, t)|^2 \psi(\mathbf{r}, t) - E_v \psi(\mathbf{r}, t). \quad (3.22)$$

We could also be slightly more rigorous in moving from the quantum description to the macroscopic system described by a classical wavefunction. We consider the Heisenberg equation of motion

$$i\hbar \frac{\partial}{\partial t} \hat{\Psi}(\mathbf{r}, t) = [\hat{\Psi}(\mathbf{r}, t), \hat{H}], \quad (3.23)$$

where the square brackets represent the commutator, or quantum-mechanical Poisson bracket. The Hamiltonian for this system can be written

$$\hat{H} = \int \left( \frac{\hbar^2}{2m} \nabla \hat{\Psi}^\dagger(\mathbf{r}, t) \nabla \hat{\Psi}(\mathbf{r}, t) \right) d\mathbf{r} + \frac{1}{2} \int \hat{\Psi}^\dagger(\mathbf{r}, t) \hat{\Psi}^{\dagger'}(\mathbf{r}, t) V(\mathbf{r}' - \mathbf{r}) \hat{\Psi}(\mathbf{r}, t) \hat{\Psi}'(\mathbf{r}, t) d\mathbf{r}' d\mathbf{r}, \quad (3.24)$$

which we substitute into the Heisenberg equation of motion to obtain,

$$i\hbar \frac{\partial}{\partial t} \hat{\Psi}(\mathbf{r}, t) = \left( -\frac{\hbar^2}{2m} \nabla^2 + \int \hat{\Psi}^\dagger(\mathbf{r}', t) V(\mathbf{r}' - \mathbf{r}) \hat{\Psi}(\mathbf{r}', t) d\mathbf{r}' \right) \hat{\Psi}(\mathbf{r}, t). \quad (3.25)$$

The field operators can be expressed as

$$\hat{\Psi}^{(\dagger)}(\mathbf{r}, t) = \sum_{\alpha} \Psi_{\alpha}(\mathbf{r}) a_{\alpha}^{(\dagger)}, \quad (3.26)$$

where  $\Psi_{\alpha}$  is the single particle wavefunction, and  $a_{\alpha}^{(\dagger)}$  are the annihilation (creation) operators. For a uniform gas, the field operators can be written

$$\hat{\Psi}(\mathbf{r}, t) = \frac{1}{\sqrt{V_{ol}}} \sum_{\mathbf{p}} \hat{a}_{\mathbf{p}} e^{i\mathbf{p}\cdot\mathbf{r}/\hbar}. \quad (3.27)$$

In the field operator, we separate out the condensate part of the wavefunction,  $\alpha = 0$

$$\hat{\Psi}^{(\dagger)}(\mathbf{r}, t) = \Psi_0(\mathbf{r}) \hat{a}_0 + \sum_{\alpha \neq 0} \Psi_{\alpha}(\mathbf{r}) \hat{a}_{\alpha}^{(\dagger)}. \quad (3.28)$$

Returning to the unperturbed system, we have

$$\hat{a}_0^{\dagger} | N_0 \rangle = \sqrt{N_0 + 1} | N_0 + 1 \rangle \quad \text{and} \quad \hat{a}_0 | N_0 \rangle = \sqrt{N_0} | N_0 - 1 \rangle. \quad (3.29)$$

In the large  $N$  limit, the case of a condensate with a macroscopic occupation of the ground state for example,  $N_0 \pm 1 \simeq N_0$  and we can identify

$$\hat{a}_0 \simeq \hat{a}_0^{\dagger} \simeq \sqrt{N_0}. \quad (3.30)$$

This is the Bogoliubov prescription, where an operator has been replaced with a standard number, in the limit of large particle number. The ground-state wavefunction, or zero-momentum mode, in eqn. (3.27) can be written as

$$\hat{\Psi}(\mathbf{r}) = \frac{1}{\sqrt{V_{ol}}} \hat{a}_0 = \left( \frac{N_0}{V_{ol}} \right)^{\frac{1}{2}} = \psi(\mathbf{r}, t), \quad (3.31)$$

with the final identification the same as we made previously, eqn. (3.17). This is equivalent to treating the condensed (macroscopically occupied) part of the field operator as a classical wavefunction. In general, to consider quantum fluctuations about a large  $N$  state in which all the atoms are in a single quantum state, we could write

$$\hat{\Psi}(\mathbf{r}, t) = \psi(\mathbf{r}, t) + \delta\hat{\psi}(\mathbf{r}, t), \quad (3.32)$$

where  $\psi(\mathbf{r}, t) = \langle \hat{\Psi}(\mathbf{r}, t) \rangle$ , as given in eqn. (3.31) above. Ignoring the quantum fluctuations and substituting this into eqn. (3.25) leads again to the Gross-Pitaevskii equation

$$i\hbar \frac{\partial}{\partial t} \Psi(\mathbf{r}, t) = -\frac{\hbar^2}{2m} \nabla^2 \Psi(\mathbf{r}) + V_0 |\Psi(\mathbf{r})|^2 \Psi(\mathbf{r}). \quad (3.33)$$

We take the time evolution as before  $\Psi(\mathbf{r}, t) = \psi(\mathbf{r}, t) \exp(-iE_v t/\hbar)$ , and we could also couple this system to an external potential, to again obtain the Gross-Pitaevskii equation,

$$i\hbar \frac{\partial}{\partial t} \psi(\mathbf{r}, t) = -\frac{\hbar^2}{2m} \nabla^2 \psi(\mathbf{r}, t) + V_{\text{ext}} \psi(\mathbf{r}, t) + V_0 |\psi(\mathbf{r}, t)|^2 \psi(\mathbf{r}, t) - E_v \psi(\mathbf{r}, t). \quad (3.34)$$

There are a few other properties of the condensate that we need to look at. We can find an expression for the stationary equilibrium state, by considering eqn. (3.34) at a distance far from any disturbance. We find

$$\psi_\infty = \left( \frac{E_v}{V_0} \right)^{\frac{1}{2}}. \quad (3.35)$$

When the condensate wavefunction reaches a boundary, such as the wall of a container, or the core of a vortex is being considered, we can define a distance over which the wavefunction changes from zero to its bulk value, or where quantum effects become important. We can do this by comparing the kinetic and interaction energies over the scales at which the wavefunction is rapidly changing. The interaction energy goes as  $\sim V_0 |\psi|^2$ , while if the scale over which the wavefunction is varying is given by  $\xi$ , then the kinetic energy term is given by  $\sim \hbar^2/2m\xi^2$ . When the two energies are equal, this defines for us a length scale

$$\xi = a_0 = \frac{\hbar}{(2mE_v)^{\frac{1}{2}}}, \quad (3.36)$$

where we have used eqn. (3.35). This is known as the *coherence length*, or *healing length*, as it is the distance over which the wavefunction requires ‘healing’, in the vicinity of a boundary, for example.

The *Thomas-Fermi* approximation we mentioned in Section 2.3.1, provides a way of obtaining tractable solutions to the Gross-Pitaevskii equation for the case where a condensate is confined within a potential, but in the limit that the spatially varying part of the wavefunction is negligible. The Gross-Pitaevskii equation in this case becomes

$$V_{\text{ext}} \psi + V_0 |\psi|^2 \psi - E_v \psi = 0, \quad (3.37)$$

which has solution

$$|\psi|^2 = n = \frac{E_\nu - V_{\text{ext}}}{V_0}. \quad (3.38)$$

This gives a condensate cloud whose radius is defined by  $V_{\text{ext}} = E_\nu$ . As the Thomas-Fermi approximation is valid for a smooth spatially varying wavefunction, the validity is such that the size of the cloud is much larger than the healing length. In this way, individual vortices can be ‘patched in’ to the body of the cloud, without affecting the overall profile. This was important in Böhmer and Harko’s dark matter model, see Section 2.3.1, and we will apply it to our later model.

### 3.2.1 The Madelung Transformation

The Madelung transformation is well known among those working in the field of condensed matter, but we note that among cosmologists, the concept of a Madelung transformation to relate the Schrödinger equation and the fluid equations has been elucidated by Coles [267, 269, 270] in the context of structure formation only as recently as 2000.

Using standard quantum mechanical techniques, we can recast eqn. (3.34) in the form of a continuity equation,

$$\frac{\partial |\psi|^2}{\partial t} + \nabla \cdot (n\mathbf{v}) = 0, \quad (3.39)$$

with velocity

$$\mathbf{v} = \frac{\hbar}{2mi} \frac{(\psi^* \nabla \psi - \psi \nabla \psi^*)}{|\psi|^2}. \quad (3.40)$$

We have seen how the square of the wavefunction can be identified as the boson number density, so that  $\rho = mn = m|\psi|^2$ . The quantum nature of the fluid can be made more evident with the application of a *Madelung transformation*

$$\psi = \alpha \exp(i\phi_\omega), \quad (3.41)$$

so that from eqn. (3.40), we obtain an expression for the velocity of the condensate

$$\mathbf{v} = \frac{\hbar}{m} \nabla \phi_\omega, \quad (3.42)$$

where  $\phi_\omega$  is the velocity potential. Substituting the Madelung transformation into eqn. (3.34), with the identification  $\phi_\omega' = \hbar\phi_\omega/m$ , yields the familiar fluid equations:

the continuity equation

$$\frac{\partial(\alpha^2)}{\partial t} + \nabla \cdot (\alpha^2 \nabla \phi_{\omega}') = 0, \quad (3.43)$$

and the (integrated) Euler equation

$$\frac{\partial \phi_{\omega}'}{\partial t} = \frac{\hbar^2}{2m^2} \frac{\nabla^2 \alpha}{\alpha} - \frac{(\nabla \phi_{\omega}')^2}{2} - \frac{V_0}{m} \alpha^2 + \frac{E_v}{m}. \quad (3.44)$$

The quantum nature of the fluid manifests itself in the first term on the right hand side of the Euler equation. This is known as the *quantum pressure* term, although dimensionally it is a chemical potential. This term is relevant only on small scales, where quantum effects become important, such as in a vortex core, or where the condensate meets a boundary. The identification made above eqn. (3.43) rather hides the quantum nature of the fluid with respect to the fluid velocity, which will become particularly relevant when we start talking about vortices.

### 3.2.2 Vortices

We have already seen that the velocity of the condensate is given by

$$\mathbf{v} = \frac{\hbar}{m} \nabla \phi_{\omega}, \quad (3.45)$$

and one would then expect that the condensate would be irrotational as

$$\nabla \times (\nabla f) = 0, \quad (3.46)$$

for any scalar,  $f$ . This restricts the motion of the condensate much more than a classical fluid. The circulation around any contour then, should also be zero. By Stokes' theorem

$$\Gamma = \oint_l \mathbf{v} \cdot d\mathbf{l} = \int_A (\nabla \times \mathbf{v}) \cdot d\mathbf{A} = 0 \quad (3.47)$$

This condition, defining the so-called Landau state, was first derived in an analysis of superfluid He II [374], and suggests that rotation of such a condensate should be impossible. Experiments by Osbourne [375] indicated that the condensate did indeed experience rotation. Feynman [376], building on the independent work of Onsager [377], suggested that rotation and hence non-zero circulation could be explained by assuming that the condensate is threaded by a lattice of parallel vortex lines. It is possible to have circulation surrounding a region from which the condensate is excluded

and in this case, this would be the vortex core. To see this, we note that the condensate wavefunction must be single valued, and so around any closed contour, the change in the phase of the wavefunction,  $\Delta\phi$ , must be a multiple of  $2\pi$ .

$$\Delta\phi_\omega = \oint \nabla\phi_\omega \cdot d\mathbf{l} = 2\pi l \quad (3.48)$$

where  $l$  is an integer. We immediately see that the circulation is quantised in units of  $h/m$

$$\Gamma = \oint \mathbf{v} \cdot d\mathbf{l} = \frac{\hbar}{m} 2\pi l = l \frac{h}{m}. \quad (3.49)$$

To obtain vortex solutions, we work in cylindrical coordinates  $(r, \chi, z)$ , and look for a static solution of the nonlinear Schrödinger equation, eqn. (3.34). To satisfy the requirement of single-valuedness, the condensate wavefunction must vary as  $\exp(in\chi)$ , with  $n$  integer. We make the vortex ansatz

$$\psi(r, \chi) = R(r) \exp(in\chi). \quad (3.50)$$

This procedure is very similar to that used in obtaining Nielsen-Olesen vortices [378], or *cosmic string* solutions in the Abelian Higgs model, which was first investigated by Abrikosov [379] in the context of superconductivity. We will return to this in Chapter 4. This analogy will be useful shortly for obtaining an expression for the vortex density profile. We can obtain an expression for the velocity profile of a vortex by substituting the vortex ansatz, eqn. (3.50), into eqn. (3.40)

$$\mathbf{v}_\omega = \frac{\hbar n}{r} \frac{1}{m} \hat{\chi}, \quad (3.51)$$

and we note again the discrete nature of the allowed values of velocity. From now on we will consider only  $n = 1$  vortices. From energy considerations, vortices with  $n > 1$  are generally expected to be unstable, and will break up into several  $n = 1$  vortices to form a vortex lattice. We can see this by inserting the vortex ansatz

$$\psi(r, \chi) = R(r) \exp(in\chi) \quad (3.52)$$

into the energy functional, eqn. (3.18). We find the energy per unit length of a vortex,

$$E_z = \int_0^{r'} 2\pi r dr' \left[ \frac{\hbar^2}{2m} \left( \frac{dR(r)}{dr} \right)^2 + n^2 \frac{\hbar^2}{2m} \frac{R(r)^2}{r^2} + \frac{V_0}{2} R(r)^4 \right]. \quad (3.53)$$

The term corresponding to the energy of the orbital motion diverges, in a similar way to the energy of a global string, which has no gauge terms to cancel it. To deal with this

divergence, a cutoff  $r'$  is introduced, which may correspond to the extent of the system, or for a multi-vortex system, the distance between individual vortices. To obtain the energy purely associated with the vortex, we subtract the energy per unit length of a cylinder of the uniform condensate. Then, the energy per unit length associated with the vortex can be shown to be

$$E_{z(\text{vor})} = \int_0^{r'} 2\pi r dr' \left[ \frac{\hbar^2}{2m} \left( \frac{dR(r)}{dr} \right)^2 + n^2 \frac{\hbar^2}{2m} \frac{R(r)^2}{r^2} + \frac{V_0}{2} (R_\infty^2 - R(r)^2)^2 \right]. \quad (3.54)$$

This can be integrated to obtain

$$E_{z(\text{vor})} \approx \pi R_\infty^2 n^2 \frac{\hbar^2}{m} \ln \left( \frac{r'}{\xi} \right). \quad (3.55)$$

From this expression, we can see that the energy of a single vortex with winding number  $n > 1$  would have a higher energy than the same configuration of  $n$  vortices, each with winding number  $n = 1$ .

We also note that cosmic strings with winding numbers  $n > 1$  are also unstable to perturbations [380]. Such defects break down to several  $n = 1$  configurations in both a condensed matter environment, and a high-energy field-theoretic one.

Feynman initially introduced quantised vortices as a purely theoretical tool with which to explain the rotation of the condensate, but the experimental verification of the quantisation of rotational velocities (e.g. by Packard and Sanders [381]) demonstrated that these vortices were indeed real.

By substituting the vortex ansatz, eqn. (3.50) into eqn. (3.34), we obtain

$$-\frac{\hbar^2}{2mE_v} \left[ \frac{d^2 R(r)}{dr^2} + \frac{1}{r} \frac{dR(r)}{dr} - \frac{R(r)}{r^2} \right] + \frac{V_0}{E_v} R(r)^3 - R(r) = 0, \quad (3.56)$$

which defines for us the density profile of a vortex (with  $\rho(r) = m|R(r)|^2$ ). From eqn. (3.35) we see that the density far from the vortex is given by

$$\rho_\infty = mR_\infty^2 = m \frac{E_v}{V_0}. \quad (3.57)$$

Analytic solutions of this equation are not known so it must be solved numerically. For our analyses we will use the approximation

$$R(r) \simeq \left( \frac{E_v}{V_0} \right)^{1/2} [1 - \exp(-r/a_0)], \quad (3.58)$$

as discussed next.

### 3.2.3 Approximations to the Density Profile

The numerical solution to the nonlinear Schrödinger equation can be cumbersome to work with, so we provide some discussion of some approximations that can be used. It is possible to scale the the variables  $r$  and  $R(r)$  in eqn. (3.56) to obtain a scale-free equation. Scaling  $r$  by the healing length,  $r' = r/a_0$ , and  $R(r)$  by the steady state value,  $R'(r') = R(r)/R_\infty$  we obtain

$$\frac{d^2 R'(r')}{dr'^2} + \frac{1}{r'} \frac{dR'(r')}{dr'} - \frac{R'(r')}{r'^2} - R'(r')^3 + R'(r') = 0. \quad (3.59)$$

Our approximation method appeals to the field of high energy vortices, specifically cosmic strings in the Abelian-Higgs model, in order to start elucidating the relationships between high-energy field theory and condensed matter. In Chapter 4 we will find that the profile of the Higgs field in a Nielsen-Olesen vortex can be written, in a similarly scaled way, as

$$\frac{d^2 R'(r')}{dr'^2} + \frac{1}{r'} \frac{dR'(r')}{dr'} - \frac{R'(r')}{r'^2} (A(r') - 1)^2 - \frac{\lambda}{2} R'(r') (R'(r')^2 - 1) = 0 \quad (3.60)$$

Here  $A(r)$  is a gauge term arising from the coupling to electromagnetism, and  $\lambda$  is determined by the potential term of the theory. It is possible to linearise eqn. (3.60) to obtain a modified Bessel function as the first order approximation to  $R'(r')$  - the zeroth order being 1. This happens in the string case, because the gauge contributions serve to cancel one of the terms, leaving a modified Bessel's equation. The linearised version of eqn. (3.59) does not quite reduce to a modified Bessel's equation, but taking our lead from the cosmic string example, we write

$$R'(r') \sim 1 - \exp(-r'). \quad (3.61)$$

Another approximation, which might seem to be more accurate, was developed by Berloff [382] in a condensed matter context. A Padé approximation has the same asymptotics at  $r = 0$  and  $r = \infty$  as the function one is trying to approximate. The Padé approximation in this case gives

$$R'(r') \sim \sqrt{\frac{r'^2(0.3437 + 0.0286r'^2)}{1 + 0.3333r'^2 + 0.0286r'^4}}. \quad (3.62)$$

This solution is plotted in Fig. 3.1 along with the numeric solution given by eqn. (3.59), and the previous approximation, eqn. (3.61). The Padé approximation is indeed more

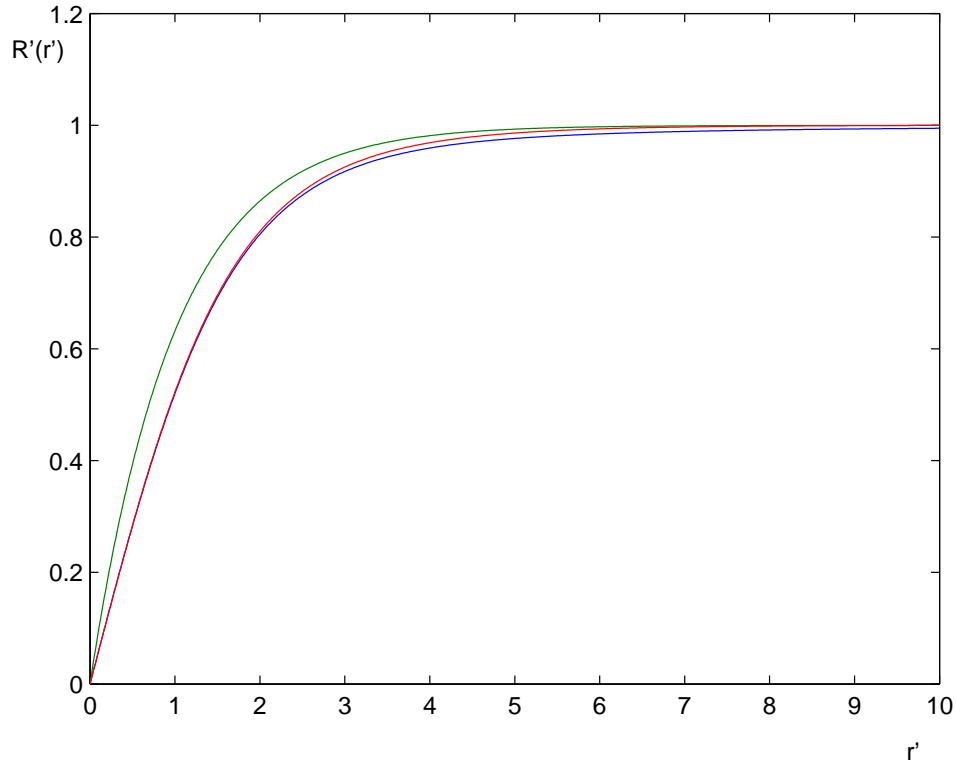


**Figure 3.1:** Numeric solution to eqn. (3.59) (blue), the Padé approximation, eqn. (3.62) (red), and the scaled approximation used in this analysis, eqn. (3.61) (green).

accurate in the small and large  $r$  regions. However, the Padé approximation has the tendency to overestimate the density in the central region, producing a density function whose derivative is negative in this region. Later in this chapter, we will find that the gravitational potential is proportional to the density, and so the gravitational force will be proportional to the derivative of the density function. If we chose to use the Padé approximation for our density profile, we could be potentially misled by its behaviour in the central region.

We will use the approximation

$$R(r) = \left( \frac{E_v}{V_0} \right)^{\frac{1}{2}} (1 - \exp[-r/a_0]). \quad (3.63)$$

### 3.3 The Wave Mechanical Approach to Structure Formation

It is interesting to note that the Euler and continuity equations, without the quantum pressure term, when coupled to the Poisson equation, are the full set of equations required to model structure formation in the early Universe. See, for example, Coles and Lucchin [383]. With the application of a Madelung transformation, one can then use the coupled Schrödinger-Poisson system in a *classical* context to describe the evolution of structure. In this case,  $\hbar$  is replaced by an adjustable parameter which controls the *spatial resolution* of the simulation involved. This idea is investigated more thoroughly in Short and Coles [268]. In the classical case, there is no form of pressure support as CDM is pressureless. The nonlinear Schrödinger equation has been used in a classical context to model gas pressure [270].

In Sections 1.1.3 and 2.2 we discussed the possibility of using the Schrödinger equation to model structure formation. Now that we have introduced the Gross-Pitaevskii equation, its application in describing the macroscopic properties of a system, and the relation to the equations of fluid mechanics, we can elaborate further on the wave-mechanical approach.

We consider a curl-free fluid (so that  $\mathbf{v} = \nabla\phi'_\omega$ , as above), evolving under gravity. A curl-free fluid is acceptable, as there are no sources of vorticity in this system of equations. Also, any vortical perturbation modes that may have been present in the early Universe will decay with expansion. The equations required for investigating structure formation are: the continuity equation,

$$\frac{\partial\rho}{\partial t} + \nabla \cdot (\rho\nabla\phi'_\omega) = 0, \quad (3.64)$$

the first integral of the Euler equation (the Bernoulli equation),

$$\frac{\partial\phi_\omega}{\partial t} + \frac{1}{2}(\nabla\phi'_\omega)^2 = -\Phi, \quad (3.65)$$

which is coupled to the Poisson equation, in order to model the effects of gravity,

$$\nabla^2\Phi = 4\pi G\rho. \quad (3.66)$$

We can again make a Madelung transformation of the form

$$\psi = \alpha \exp(i\phi_\omega/\nu), \quad (3.67)$$

to rewrite eqns. (3.64) and (3.65) as

$$i\nu \frac{\partial \psi}{\partial t} = -\frac{\nu^2}{2} \nabla^2 \psi + \Phi \psi + \frac{\nu^2}{2} \frac{\nabla \alpha}{\alpha}. \quad (3.68)$$

We again have a Schrödinger-like equation coupled to the Poisson equation. As we mentioned in Section 2.2, this is no longer a quantum mechanical system, and the parameter  $\nu$  has taken the place of  $\hbar$ . The parameter  $\nu$  is now an adjustable parameter that can be changed according to the resolution of the simulation required. For the formalism used by Coles, Short and Spencer [269, 267, 268, 266, 270]  $\nu = \hbar/m$ , giving the correct dimensions for Planck's constant, and the de Broglie relation  $\lambda = \nu/\nu$ . We note that the quantum pressure term currently appears in the above Schrödinger equation. Generally, in the wave-mechanical approach, one evolves the 'standard' Schrödinger equation in simulations. If one performs a Madelung transformation on this equation, we find that the quantum pressure term instead appears in the Bernoulli equation. In this sense, adjusting the parameter  $\nu$  in the Schrödinger equation controls the range over which the new pressure term in the Bernoulli equation is effective.

This approach circumnavigates two of the problems of the standard perturbation approach to structure formation that we mentioned in Section 1.1.3. Firstly, due to the form of the Madelung transformation,  $\rho \sim |\psi|^2$ , and so the density distribution will always be positive. Secondly, because we are not dealing with point-like particles, shell-crossing is not as catastrophic as in the Zel'dovich approximation, and caustics will never be formed. More complex representations of the wavefunction can allow for multi-streaming solutions to occur [265]. It is also possible to add the effects of gas dynamics to this approach by considering the nonlinear Schrödinger equation [270], in this case simulating the evolution of a polytropic fluid under gravity.

### 3.4 Gravitational Stability of Vortices in Bose-Einstein Condensate Dark Matter

In Section 1.1 we have seen the motivation for a Cold Dark Matter component to the Universe, as well as some of the problems that the CDM model faces in reproducing observations. In Chapter 2.3 we saw that some authors proposed a resolution to these problems by exploiting the quantum-mechanical nature of ultralight matter, so that the de Broglie wavelength of this matter might manifest itself on astrophysical scales, leading to naturally smoother and less centrally concentrated galaxy halos than in the CDM case. Silverman & Mallett [279] suggested a symmetry-breaking mechanism for such an ultralight particle, based upon a real scalar field, and while in this case the symmetry-breaking mechanism provides a nice example of particle production in a universe with a cosmological constant, symmetry breaking with a real scalar field generically produces a catastrophic domain wall problem [380] and we shall see in Section 4.4 that this model is no exception. Silverman & Mallett [279] also considered the rotation of a galactic-scale dark matter halo. Using a phenomenological description taken directly from condensed matter, they concluded that a galactic halo should be threaded by a lattice of quantised vortices, as a consequence of the rotation of the galaxy exceeding the critical rotation rate required for quantised vortices to form. Indeed, from studies of rotating Bose-Einstein condensates and quantum turbulence [384, 103], it would seem to be difficult to prevent such vortices from forming. Classical vortices may also be of importance in an astrophysical environment. Their role in planet formation, for example, has been discussed [385].

The effects of the interaction of gravity with a coherent state of matter, such as a Bose-Einstein condensate, have certainly been considered previously [386, 387], and prompted the question of whether it is actually possible for dark matter to be in a coherent quantum state if the only interaction with visible matter is gravitational. In Section 2.6 we saw how Penrose has used the Schrödinger-Poisson system during his ‘quantum state reduction’ research program.

Böhmer and Harko [276] considered a model of a galactic halo consisting of a Bose-Einstein condensate. In condensed matter scenarios, the Thomas-Fermi approximation

is used to describe a Bose-Einstein condensate cloud, confined by a potential. In the galactic case, the confining potential is supplied by the gravitational interaction, and the dark matter density takes the form of a spherical halo that drops to zero outside the confining potential, as expected from investigations of dark matter halos in the Universe [130] and Bose-Einstein condensates in the laboratory (see, for example, Abo-Shaeer et al. [388]). Conventionally, a vortex, or an array of vortices, can then be ‘patched’ into the Thomas-Fermi envelope, with the approximation for the cloud remaining valid for all regions except that of the vortex cores. If dark matter does consist of a Bose-Einstein condensate, Silverman’s paper [279] suggests it would seem to be difficult to prevent vortex arrays from forming in galactic halos. Detection of these vortices and investigation of their properties, for example, with gravitational lensing, could give considerable insight into the nature of dark matter.

In this section we seek to determine the properties of a dark matter particle from considerations of an array of quantised vortices residing in a dark matter Bose-Einstein condensate. We investigate the properties of the individual vortices in the galactic Thomas-Fermi envelope, in order to determine ranges for the parameters describing a dark matter condensate particle, such as its mass. For the purposes of this investigation, we presume that the dark matter does indeed consist of a Bose-Einstein condensate, formed at an earlier stage of cosmological history and described by the coupled nonlinear Schrödinger-Poisson system, and that vortices are present, and stable, in this cosmological fluid.

To consider Bose-Einstein condensates on scales relevant to structure formation in the Universe, we must necessarily include gravitational effects. Bose-Einstein condensates are typically sufficiently dilute that the mass densities are not very large, and so a Newtonian approximation is valid. Gravitational effects can be added to the Bose-Einstein condensate by including a term in the nonlinear Schrödinger equation that couples to the Poisson equation. We then have a pair of equations modelling a gravitationally coupled fluid.

$$i\hbar\dot{\psi} = -\frac{\hbar^2}{2m}\nabla^2\psi + V_0|\psi|^2\psi - E_v\psi + m\Phi\psi \quad (3.69)$$

$$\nabla^2\Phi = 4\pi G\rho = 4\pi Gm|\psi|^2. \quad (3.70)$$

We have already seen how this system can emerge, either as the weak field limit of the

Einstein-Klein-Gordon system (Chapter 2 and Appendix A), or in different approaches to various phenomena, such as a wave-mechanical approach to structure formation (Section 3.3), or in Penrose's work (Section 2.6).

### **3.4.1 Vortices in Gravitationally Coupled Bose-Einstein Condensates**

We can now consider how to determine the properties of a dark matter particle from observations of a vortex in a galactic dark matter condensate. We see that, from the above coupled equations, (3.69) and (3.70), and the relation for the healing length, eqn. (3.36), the density,  $\rho = m|\psi|^2$ , is entirely determined by the mass  $m$ , the healing length  $a_0$ , and the interparticle potential  $V_0$ . If we could provide a measurement of  $a_0$ , possibly from gravitational lensing observations of a vortex in a dark matter Bose-Einstein condensate halo, then it is only the  $(V_0, m)$  parameter space that remains to be constrained. It is the goal of this section to place some bounds on this parameter space using some simple physical arguments.

As we have previously mentioned, the dark matter halo we are considering is well described by the Thomas-Fermi approximation. Vortices reside within this envelope and, to a good approximation, provide only a small perturbation to it. We will consider the properties of single vortices within this halo. The size of the vortex radius compared to the size of the dark matter halo is small, and so we can consider the vortex to be residing in a constant density background, so that the vortex density profile obtained by solving eqn. (3.56) and approximated by eqn. (3.58) is valid.

If we could solve the above coupled equations using the standard vortex ansatz, eqn. (3.50), to obtain a density profile for a gravitationally coupled vortex, then we only need specify a sensible value of  $a_0$  and the background density in a dark matter halo to give us a relation between  $V_0$  and  $m$ . Unfortunately, it is not tractable to solve for the density profile,  $R(r)$ , by substituting the vortex ansatz  $\psi = R(r) \exp(i\chi)$  into eqns. (3.69) and (3.70). The vortex ansatz assumes that the density profile is static, thus providing no force terms, from rotation for example, to counter the gravitational interaction. Coupling the equation for the density profile to a gravitational potential

that is diverging, as it is for a constant density background, is then inconsistent. We anticipate in any case that the vortex density profile will not be altered dramatically, as the particle densities within the region of the vortex will be fairly low.

### **3.4.2 Vortex Stability in Gravitationally Coupled Bose-Einstein Condensates**

Instead of solving the coupled eqns. (3.69) and (3.70) for a vortex directly, we make an argument regarding the stability of a gravitationally coupled Bose-Einstein condensate vortex, and consequently give some bounds on the parameters that describe it. Our analysis is based upon the consideration of the radial velocity profile of a Bose-Einstein condensate vortex,  $v_\omega(r)$ , and the radial velocity induced from gravitational attraction,  $v_G(r)$ . In other words,  $v_\omega(r)$  is the velocity that the vortex density distribution is moving at, for a particular  $r$ , while  $v_G(r)$  would be the velocity experienced by a test particle orbiting that density distribution, at a distance  $r$ . To sustain a vortex,  $v_\omega(r)$  must be greater than  $v_G(r)$ , otherwise the quantum-mechanical forces that produce the vortex are not sufficiently strong to hold the vortex up against gravitational collapse. That is, the vortex is spinning too slowly to provide enough centripetal force to balance the gravitational force. Particles in the condensate will then gravitate into the core, destroying the vortex. For stability, we therefore have the bound,

$$v_\omega(r) \geq v_G(r). \tag{3.71}$$

We can use this bound to eliminate some regions of the  $(V_0, m)$  parameter space, as we now demonstrate.

#### **Gravitational Field of a Cylindrically Symmetric System**

We have already seen that  $v_\omega(r)$  can be given by

$$\mathbf{v}_\omega = \frac{\hbar}{r} \frac{1}{m} \hat{\chi}. \tag{3.72}$$

To obtain  $v_G(r)$ , we turn to Gauss's law to determine the gravitational field of a cylindrically symmetric mass distribution, and hence obtain the radial gravitational velocity

of a test particle moving in the field of that system. Gauss's law is

$$\oint \mathbf{g} \cdot d\mathbf{A} = -4\pi G M_{\text{encl}}. \quad (3.73)$$

The mass enclosed is the density pervading a cylinder of radius  $r$  and length  $L$ :

$$M_{\text{encl}} = L \int_0^r 2\pi r \rho(r) dr. \quad (3.74)$$

The density,  $\rho(r) = m|R(r)|^2$ , is already determined in terms of the cylindrical  $r$  coordinate, as it is a solution of the vortex equation. The left-hand side of Gauss's law, in cylindrical coordinates, is

$$\int g r d\chi dz, \quad (3.75)$$

where the integral over the  $z$  coordinate is again  $L$ , the length of the vortex. Gauss's law, then, gives us

$$g r (2\pi L) = -4\pi G (2\pi L) \int_0^r \rho(r) r dr, \quad (3.76)$$

giving

$$g = -\frac{4\pi G m}{r} \int_0^r |R(r)|^2 r dr. \quad (3.77)$$

The sign is negative, because we have chosen an outward-pointing surface normal in our formulation of Gauss's law, eqn. (3.73), which indicates that the gravitational flux will always be towards the origin. This leads to the slightly counter-intuitive conclusion that a hole (the vortex) in a constant mass density background would seem to produce a gravitational force towards it. We instead view it like this; the static vortex configuration will want to act to collapse in, and close the hole. We believe that this is related to the complications in solving for the density profile that we mentioned in Section 3.4.1. This need not concern us further, as it is the magnitude that is required for our argument. The magnitude of the induced centripetal force is

$$g = \frac{v_G^2}{r}, \quad (3.78)$$

and the gravitational circular velocity profile  $v_G$  is given by,

$$v_G(r)^2 = 4\pi G \int_0^r \rho(r) r dr = 4\pi G m \int_0^r |R(r)|^2 r dr. \quad (3.79)$$

### 3.4.3 Bounds on Parameters

We now have expressions for  $v_G(r)$  and  $v_\omega(r)$ , eqns. (3.72) and (3.79), to go in the bound given by eqn. (3.71). In Fig. 3.2 we plot, as an example,  $v_\omega(r)$  and  $v_G(r)$  and the density profile for comparison. For this example we use an ultralight boson, with parameter values of  $m = 3.56 \times 10^{-59}$  kg ( $2 \times 10^{-23}$  eV),  $E_v = 2.5 \times 10^{-49}$  J ( $1.56 \times 10^{-30}$  eV) and  $V_0 = 4.45 \times 10^{-84}$  Jm<sup>3</sup> ( $3.7 \times 10^{-45}$  eV<sup>-2</sup>). These values are obtained using considerations of vortices in galactic Bose-Einstein condensates with an ultralight boson, as investigated in Silverman and Mallett [279]. These values are explained in more detail in the following subsection. These particular values are used simply to demonstrate the behaviours of the velocity profiles, and are not used again in our analysis.

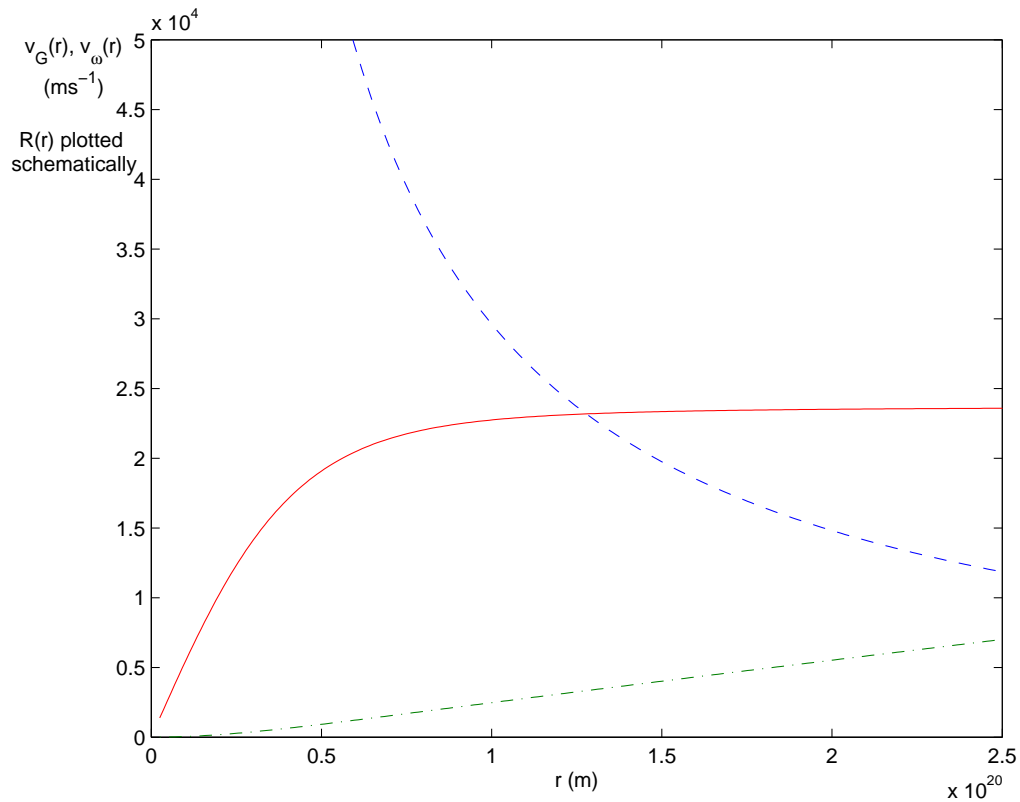


**Figure 3.2:** Velocity Profiles for  $v_G$  (green, dot dash) and  $v_\omega$  (blue, dash). Density profile plotted schematically for comparison (red, solid).

The bound on stability,  $v_\omega(r) \geq v_G(r)$ , will always be violated at some point, as outside the vortex core  $v_\omega(r) \sim 1/r$  and  $v_G(r) \sim r$ . We must specify what might be an

acceptable value of  $r$  for  $v_\omega(r)$  and  $v_G(r)$  to meet, such that the vortex configuration is not destroyed. We want the vortices to exist, and so the vortex density profile should be fully established. We interpret this to mean that the density has essentially reached the level of the background. From the scaled density profile discussed previously, and plotted in Fig. 3.1, we see that the density reaches its background level at a value of about ten times the healing length. This is the minimum number of healing lengths at which we will allow the bound to be violated, otherwise the vortex cannot be established. Using the approximation to the density profile, eqn. (3.58), in the expression for the gravitational circular velocity  $v_G$ , eqn. (3.79), we then substitute our expressions for  $v_G$  and  $v_\omega$  into the bound given by eqn. (3.71), to obtain

$$\frac{\sqrt{2\pi}}{2} \left( \frac{G\hbar^2}{V_0 a_0^2} \left[ 2r^2 + 8ra_0 e^{-\frac{r}{a_0}} + 8a_0^2 e^{-\frac{r}{a_0}} - 2ra_0 e^{-\frac{2r}{a_0}} - a_0^2 e^{-\frac{2r}{a_0}} \right] \right)^{\frac{1}{2}} \leq \frac{\hbar}{mr}. \quad (3.80)$$

We have also eliminated  $E_v$  using eqn. (3.36). This allows us to plot a line indicating an allowed region of  $(V_0, m)$  parameter space. We will consider a range of physically reasonable healing lengths  $a_0$  from considerations of galactic scales. We consider  $r$  to be the length scale at which the bound is violated, and so express  $r$  in terms of an integer number of healing lengths,  $r = na_0$ , with the minimum being  $n = 10$  as outlined above. Eqn. (3.80) then becomes

$$V_0 \geq \frac{\pi}{2} Gm^2 n^2 \left( 2n^2 a_0^2 + 8na_0^2 e^{-n} + 8a_0^2 e^{-n} - 2na_0^2 e^{-2n} - a_0^2 e^{-2n} \right), \quad (3.81)$$

or, to leading order,

$$V_0 \geq \pi Gm^2 a_0^2 n^4. \quad (3.82)$$

### **Approximations for Parameters Defining the Bose-Einstein Condensate**

We take a brief diversion to consider how we approximated the values necessary to obtain the velocity profiles in the previous subsection. These values are merely to provide an idea of the forms of the velocity profiles and are not used again in our analysis.

To enable us to obtain velocity and density profiles, we must provide values for the parameters  $m$ ,  $V_0$ , and  $E_v$ . The properties of dark matter particles are, by their very nature, unknown, so we must make some approximations. We use the analysis in

Silverman and Mallet [279] to provide us with some data values. The mass of the Bose-Einstein condensate dark matter particle in that paper is  $3.56 \times 10^{-59}$  kg ( $2 \times 10^{-23}$  eV) (Silverman and Mallett unfortunately use a mix of natural and S.I. units). Their analysis is based on the mass and angular rotation of the Andromeda galaxy. The mean density is given as  $2 \times 10^{-24}$  kg m<sup>-3</sup>, and they estimate that the vortex line density in the galaxy would be about 1 vortex per 208 kpc<sup>2</sup>. This gives a vortex radius of  $r_\omega \sim 2.5 \times 10^{20}$  m ( $\sim 8.1$  kpc). This is a slightly strange result, as previous analysis in their paper (which we will return to in Section 4.4) suggests a coherence length of  $\sim 30$  kpc, meaning that their vortex core is bigger than their vortex.

We continue with the suggested vortex radius of  $r_\omega \sim 2.5 \times 10^{20}$  m, and turn to vortex lattices in condensed matter systems to provide us with some further estimates of the vortex properties in a Bose-Einstein condensate.

Taking the distance between two vortices to be twice the vortex radius, we note from experimental observations of vortex lattices in a Bose-Einstein condensate that the vortex density reaches the normal density at about half the vortex radius; see, for example, Fig. 9.3 in Pethick and Smith [328], taken from Coddington et al. [389]. From Fig. 3.1, we also see that the vortex density reaches the normal condensate density at around five healing lengths. This gives us an estimate of  $r_\omega/2 = 5a_0$ . We then use  $r_\omega \sim 2.5 \times 10^{20}$  m,  $a_0 = \hbar/(2mE_v)^{1/2}$ , and  $\rho_\infty = mE_v/V_0$  to give estimates for  $E_v$  and  $V_0$ . With these approximations we find values of  $E_v = 2.5 \times 10^{-49}$  J ( $1.56 \times 10^{-30}$  eV) and  $V_0 = 4.45 \times 10^{-84}$  J m<sup>3</sup> ( $3.7 \times 10^{-45}$  eV<sup>-2</sup>). A better approximation of the inter-vortex separation could be made by considering the forces acting on a vortex lattice within the system we are studying. However, as we mentioned at the start of this section, these approximations are used only in obtaining Fig. 3.2 to give an idea of the forms of the profiles for  $v_\omega(r)$  and  $v_G(r)$ .

### Other Bounds

We can obtain some other bounds to cut off other bits of parameter space. The asymptotic vortex density is given by

$$\rho_\infty = m \left( \frac{E_v}{V_0} \right). \quad (3.83)$$

If the vortex exists as a component of a galaxy, then there is a minimum and maximum density that the vortex can have, given by the maximum and minimum known values of mass density within a galaxy,

$$\rho_{\min} \leq \rho_{\infty} \leq \rho_{\max}. \quad (3.84)$$

The value of  $E_v$  in eqn. (3.83) is fixed (as we are fixing the healing length), and so the bound on the density becomes a bound on  $V_0$ .

$$\frac{\hbar^2}{2a_0^2\rho_{\max}} \leq V_0 \leq \frac{\hbar^2}{2a_0^2\rho_{\min}}. \quad (3.85)$$

Eqn. (3.81) gives a lower bound on  $V_0$ , so to obtain an upper bound, we use the second half of the above relation.

$$V_0 \leq \frac{\hbar^2}{2a_0^2\rho_{\min}}. \quad (3.86)$$

Another bound is provided because the vortex velocity should never exceed the speed of light,

$$v_{\omega} = \frac{\hbar}{mr} \leq c. \quad (3.87)$$

It can be seen from eqn. (3.72) that the vortex velocity increases with decreasing radius. This relation breaks down within the vortex core,  $a_0$ , where the vortex velocity diverges. Finding an appropriate description is a topic of some interest in condensed matter theory [390]. We evaluate the maximum vortex velocity at a distance of  $r = 5a_0$  from the origin, i.e. in a regime where we are sure the relation holds. This gives a bound on the mass.

$$m \geq \frac{\hbar}{5ca_0}. \quad (3.88)$$

### Values

To see how the restriction on  $m$  and  $V_0$  varies, we can think of a range of healing lengths that cover all possible scales in a galaxy.

$$1 \times 10^{10} \text{ m} \quad (3.2 \times 10^{-10} \text{ kpc}, \quad \sim 7 \times 10^{-2} \text{ AU}) \leq a_0 \quad (3.89)$$

$$a_0 \leq 1 \times 10^{22} \text{ m} \quad (324 \text{ kpc}) \quad (3.90)$$

This range of scales takes us from sub solar system, to that of the largest known galaxies (e.g. IC 1101 in the Abell 2029 cluster [391]). The two ends of this parameter

range are extreme cases for cosmological vortices, but we have chosen them to include all possible scales, to make our bounds as conservative as possible. At fixed  $a_0$  we will also cover a large range of  $n$ ; the number of healing lengths where the velocity profiles cross.

For the bound given in eqn. (3.86), we take the minimum density found within a galaxy to be the cosmological density. This minimum must necessarily be close to the critical density of the universe,

$$\rho_{\min} = \rho_c = \frac{3H_0^2}{8\pi G}. \quad (3.91)$$

With  $H_0 = 70 \text{ km s}^{-1} \text{ Mpc}^{-1}$ , this gives a value of  $\rho_{\min} = 9.2 \times 10^{-27} \text{ kg m}^{-3}$ .

### 3.4.4 Results

In Fig. 3.3, we show a region of the  $(V_0, m)$  parameter space for the healing length  $a_0 = 1 \times 10^{16} \text{ m}$  ( $\sim 1\text{pc}$ ). The lines bounding the region of allowed parameter values are given by eqns. (3.81), (3.88) and (3.86).

The lower bound on  $V_0$  is given when  $v_\omega$  and  $v_G$  cross at a value of ten times the healing length,  $n = 10$ . A vortex could be considered more stable if  $v_\omega$  and  $v_G$  cross at a greater value of  $n$ . Higher values of  $n$  will then move the bounding diagonal line upwards in the  $(V_0, m)$  parameter space. A value of  $n = 10^6$  is also plotted to demonstrate this. It is clear then, that higher  $n$  values (the more stable vortices) are more restrictive in the values that the parameters  $V_0$  and  $m$  can take. We will now just consider vortices with  $n = 10$  in order to be conservative in ruling out possible parameter ranges.

Fig. 3.4 shows allowed regions for various healing lengths, all at a value of  $n = 10$ . We see that as we move to smaller values of  $a_0$ , the allowed bounds on  $m$  and  $V_0$  both move up, as expected from eqns. (3.86) and (3.88). More physically, as the mass of the particle is increased, the repulsive potential  $V_0$  must increase to balance the stronger gravitational force.

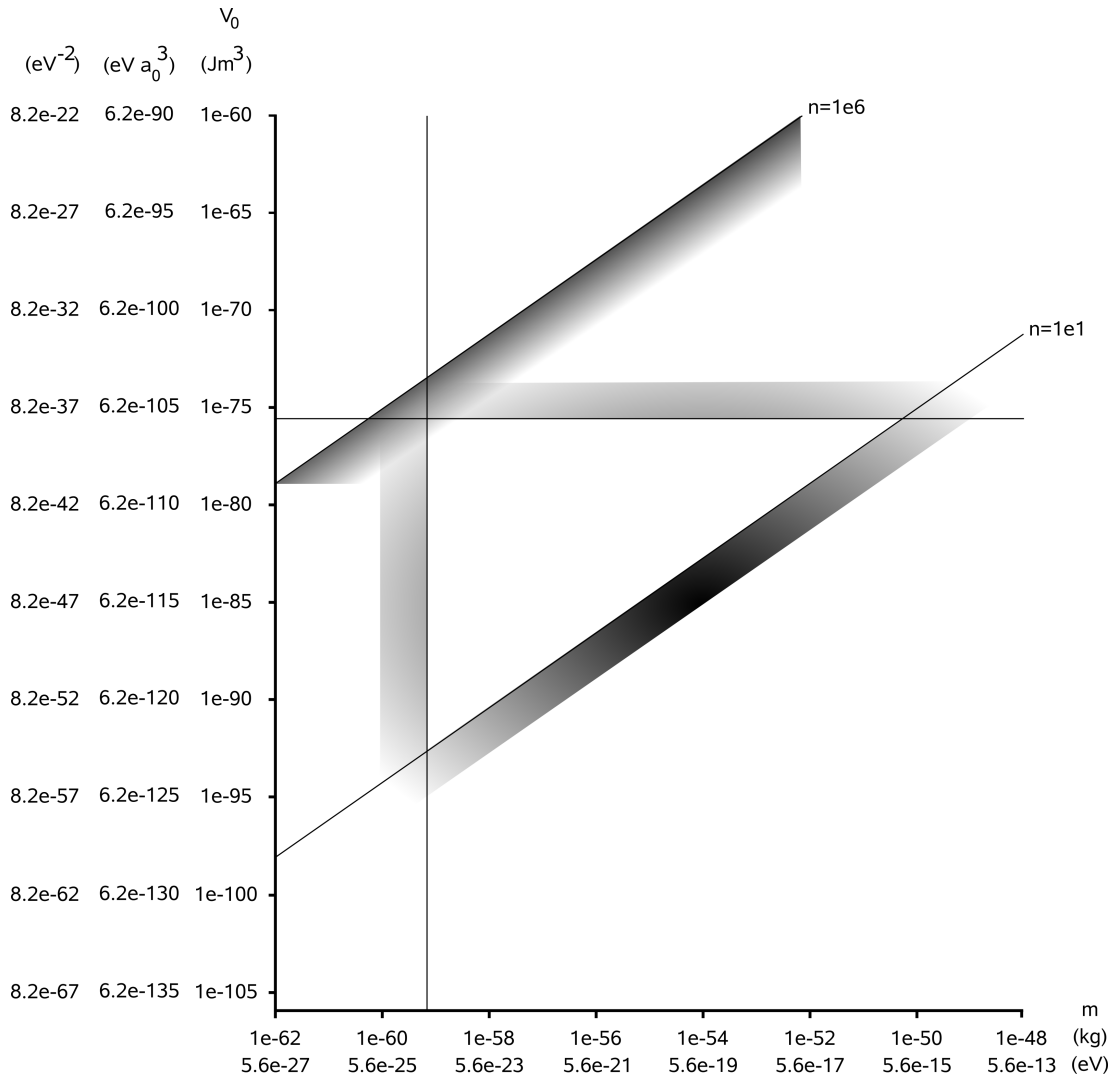


**Figure 3.3:** Allowed region in  $(V_0, m)$  parameter space, for a healing length of  $a_0 = 1 \times 10^{16} \text{ m}$  ( $\sim 1$  parsec).

### 3.5 Discussion

In this chapter we have presented, in some detail, techniques from condensed matter physics and discussed how they might be used in a cosmological setting. We first looked at the phenomenon of Bose-Einstein condensation, and derived the Gross-Pitaevskii, or nonlinear Schrödinger equation, enabling us to present the inherently quantum-mechanical phenomenon of quantised vortices. We used the Madelung transformation to relate the Schrödinger equation to the fluid equations, and also saw how it could be used in a purely classical context to circumvent some of the problems of standard approaches to structure formation, as mentioned in Section 2.2. We then returned to the quantum case in order to describe a Bose-Einstein condensate dark matter

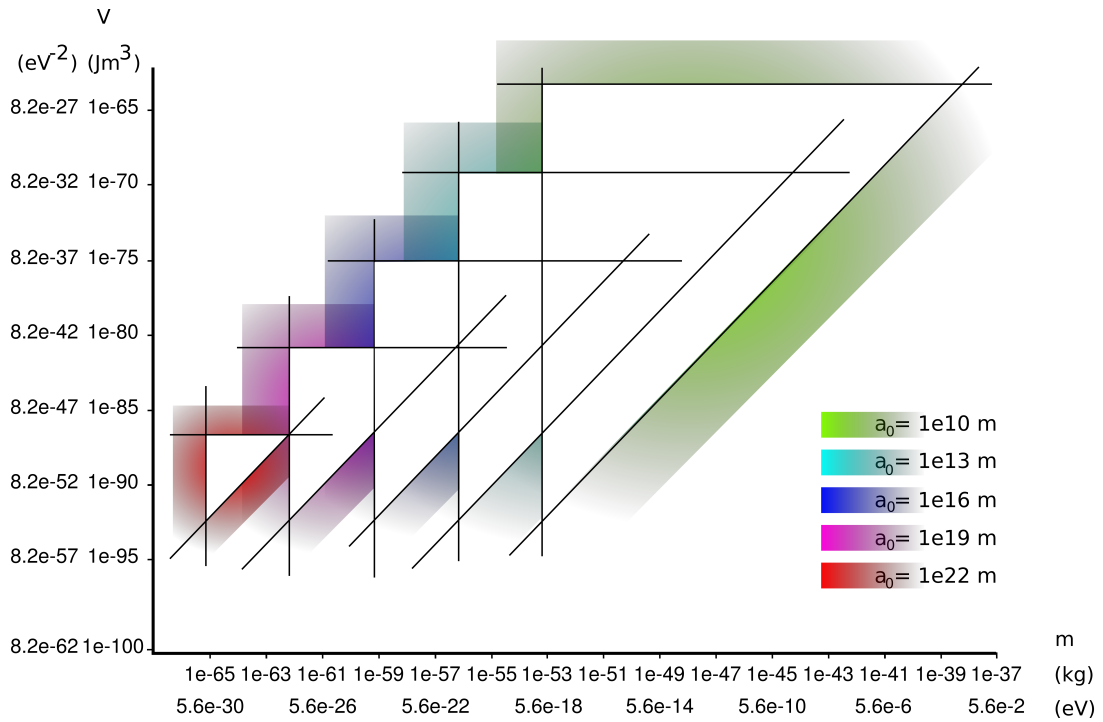


**Figure 3.4:** Allowed regions in  $(V_0, m)$  parameter space, with  $n = 10$ . Healing lengths as labelled.

candidate, where a galaxy dark matter halo is threaded by quantised vortices. The gravitationally coupled nonlinear Schrödinger equation is a complex system to solve. In the case of a laboratory Bose-Einstein condensate, self-gravitational forces are not important and even here analytical progress is limited. However, using a simple physical argument, we have shown how limits on the consistency of such a model can be imposed. Considering sensible values for the size of a galactic Bose-Einstein condensate vortex places constraints on the values that the interaction potential, mass and hence the chemical potential can take. There remain sizeable regions of parameter space in which a model of dark matter comprising a Bose-Einstein condensate appears to be viable. If the parameters of a dark matter particle can be established from experiment, or predicted from theory, the model we have presented facilitates an easy comparison for deciding whether it is possible for a galactic scale Bose-Einstein condensate vortex to exist. Suggestions have been made to test the hypothesis of a galactic Bose-Einstein condensate with gravitational lensing [276], possibly, in the case of vortices, from rotationally induced frame-dragging effects [279]. It has also already been shown that the quantum mechanical properties of such a dark matter model may eliminate the problems of cuspy density cores and the overproduction of substructure that the CDM

model seems to predict [275]. Our analysis shows there are regions where both light galactic Bose-Einstein condensate particles,  $\sim 1$  eV [322, 327], and ultralight particles,  $\sim 10^{-23}$  eV [279, 275, 296, 303], are viable. From regions of our parameter space, it can be seen that while ultralight bosonic particles are not ruled out, the allowed regions are far more constrained for the lighter mass particles.

The relations between cosmology and condensed matter also facilitate a comparison with cosmic strings and the bounds placed on them by the Cosmic Microwave Background. Global strings have an energy per unit length associated with them, whose equation (in natural units) is

$$\mu_T \approx 2\pi\eta^2 \ln\left(\frac{r'}{\delta}\right), \quad (3.92)$$

where  $\mu_T$  is the string energy per unit length, or *tension*,  $\eta$  is the symmetry breaking scale, which we will discuss fully in Chapter 4,  $\delta$  is the string core width, or equivalently, the coherence length, and  $r'$  is a cut-off distance that must be imposed to stop the expression diverging. This may be the curvature of the string, or the inter-string separation. We can see that this expression is identical to that for the energy per unit length of a Bose-Einstein vortex, given by eqn. (3.55).

In the cosmic string literature, the string energy per unit length is typically expressed as a dimensionless number, given by the combination  $G\mu_T$ . In the early universe, strings with a high tension can typically give rise to a certain amount of anisotropy in the CMB. It can be shown, see Section 10.2 of Vilenkin and Shellard [380] and references therein for example, that in order to be consistent with observations of the CMB anisotropy, then

$$G\mu_T \lesssim 2 \times 10^{-6}, \quad (3.93)$$

or, in S.I. units,

$$\mu_T \lesssim 2.4 \times 10^{-38} \text{ Jm}^{-1}. \quad (3.94)$$

We can make a simple comparison with the results obtained from the allowed regions in Fig. 3.4. We remember from eqn. (3.55) that the energy per unit length of a vortex is given by

$$E_{z(\text{vor})} \approx \pi R_\infty^2 n^2 \frac{\hbar^2}{m} \ln\left(\frac{r'}{a_0}\right).$$

Using eqn. (3.57)

$$\rho_\infty = mR_\infty = m\frac{E_v}{V_0},$$

and the expression for the healing length,

$$a_0 = \frac{\hbar}{(2mE_v)^{\frac{1}{2}}},$$

we can rewrite the expression for the energy per unit length in terms of  $m$  and  $V_0$ , the parameter space that we have been dealing with, and  $a_0$ ,

$$E_{z(\text{vor})} \approx \frac{\pi}{4} \frac{\hbar^6}{m^3 V_0^2 a_0^4} \ln\left(\frac{r'}{a_0}\right). \quad (3.95)$$

We have already suggested an inter-vortex separation of  $r_\omega = r' = 10a_0$ , giving

$$E_{z(\text{vor})} \approx 1.8 \frac{\hbar^6}{m^3 V_0^2 a_0^4}. \quad (3.96)$$

Using Fig. 3.4, we can simply read off approximate values of  $V_0$  and  $m$ , for different values of the healing length, to get an idea of the energy per unit length of each vortex.

The results are given in Table 3.1.

$a_0$ (m)	$m$ (kg)	$V_0$ (Jm <sup>3</sup> )	$E_{z(\text{vor})}$ (Jm <sup>-1</sup> )	$E_{z(\text{vor})}$ ( $G\mu_T$ )
10 <sup>10</sup>	10 <sup>-48</sup>	10 <sup>-70</sup>	$2.5 \times 10^{40}$	$2 \times 10^{-4}$
10 <sup>13</sup>	10 <sup>-52</sup>	10 <sup>-75</sup>	$2.5 \times 10^{50}$	$2 \times 10^{06}$
10 <sup>16</sup>	10 <sup>-56</sup>	10 <sup>-80</sup>	$2.5 \times 10^{60}$	$2 \times 10^{14}$
10 <sup>19</sup>	10 <sup>-60</sup>	10 <sup>-85</sup>	$2.5 \times 10^{70}$	$2 \times 10^{16}$
10 <sup>22</sup>	10 <sup>-64</sup>	10 <sup>-90</sup>	$2.5 \times 10^{80}$	$2 \times 10^{24}$

**Table 3.1:** Vortex Energy per Unit Length.

When we compare these values with the bounds placed on Cosmic Strings

$$G\mu_T \lesssim 2 \times 10^{-6},$$

it would seem that this analysis would start to cast significant doubt on galactic Bose-Einstein condensate vortices existing at all. We see that smaller vortices could be consistent with CMB observations, but also note from eqn. (3.95) that any attempt to separate the vortices further would exacerbate the problem. Timescales of galaxy formation also complicate the picture. It may be possible that such vortices would form *after* any interaction with the CMB.

A more detailed analysis is required to resolve the problems demonstrated here.

In future work, it would seem to be of fundamental importance to investigate further whether a dark matter candidate could reside in a coherent quantum state, if the only interaction was gravitational. This is the topic of a wide ranging research program, as mentioned in Section 3.4.

A less ambitious undertaking would be to find a numerical solution to the coupled equations, in order to describe the density profile of a gravitationally coupled vortex. This may be difficult in the case of an infinite background, progress may be able to be made by considering a cutoff in the background density, imposed by the physical extent of the Thomas-Fermi cloud modelling the galaxy halo.

We could develop this model further by also considering the possibility of instability and collapse of the vortex in the axial direction. This could provide further constraints on the dark matter particle parameters, and the existence of vortices in dark matter Bose-Einstein condensates. In both cases, the system to be solved would be subject to a more complete numerical method than we have been able to implement so far.

# Chapter 4

## Relations to Field Theory

As already alluded to throughout this thesis, there are a number of strong links between high-energy field theory, and the models used to describe phenomena in condensed matter. We have already come across concepts such as condensates, and quantised vortices. Chapter 3 addressed these ideas from a condensed matter standpoint, and in this chapter we will focus on the field theory point of view, particularly with regard to phenomena that the two areas have in common, as well as elucidating some more mathematical concepts.

We start with a comparison of models describing features in field theory and condensed matter, and their analogous characteristics. We focus in particular on the role of spontaneous symmetry breaking, looking at some related phenomena such as soliton solutions, examples of which are present in both condensed matter and cosmology. We also discuss the relation between spontaneous symmetry breaking and Bose-Einstein condensation.

We also mention a hypothetical particle that embodies most of the concepts in this chapter. The axion is an example of a particle that can be produced as a result of spontaneous symmetry breaking, and is relevant to this thesis as it is a nonrelativistic low mass particle ( $m \sim 10^{-5}$  eV), which is born as a Bose-Einstein condensate and has been considered as a promising dark matter candidate.

We finish with an example of one of the problems associated with the production of topological defects in the early Universe, in the context of a Bose-Einstein condensate

dark matter model mentioned previously in this thesis.

## 4.1 Comparison of Related Models

We start by looking pedagogically at some models that are highly relevant to the ideas within this thesis: the Abelian-Higgs model, the Goldstone model, the Landau-Ginzburg theory, and the model of Bose-Einstein condensation encapsulated by the Gross-Pitaevskii equation. This also allows us to introduce many concepts that are common to all, such as topological defects, symmetry breaking, and the Higgs mechanism.

### 4.1.1 The Abelian-Higgs Model

The Abelian-Higgs model is the typical pedagogical example for demonstrating mass generation via spontaneous symmetry breaking. It is expected to play a major role in the standard model, and the detection of the associated particle, the *Higgs boson*, is one of the primary goals of the LHC. We have already mentioned many of the concepts and the historical background in Chapter 1. The model consists of a complex scalar field, coupled to electromagnetism. In the context of the early Universe, this field is usually considered to be primordial in origin, and fundamental, though we have again suggested in Chapter 1 that this may not be the case. The potential in which the Higgs field moves evolves with the Universe's decreasing temperature, to a potential that exhibits spontaneous symmetry breaking. We will describe the evolution of the potential with temperature in Section 4.2. For now it will be sufficient to consider models with a potential that exhibit spontaneous symmetry breaking.

The Abelian-Higgs Lagrangian (density) is given by

$$\mathcal{L} = (\partial_\mu + ieA_\mu)\bar{\phi}(\partial^\mu - ieA^\mu)\phi - \frac{1}{4}F_{\mu\nu}F^{\mu\nu} - V(\phi). \quad (4.1)$$

Here,  $F_{\mu\nu}$  is the electromagnetic field strength tensor,  $F_{\mu\nu} = \partial_\mu A_\nu - \partial_\nu A_\mu$ , with the gauge vector field  $A_\mu$ , and the coupling constant of electromagnetism  $e$ . This Lagrangian is invariant under the transformations

$$\phi(x) \rightarrow \phi'(x) = e^{i\alpha(x)}\phi(x), \quad A_\mu(x) \rightarrow A'_\mu(x) = A_\mu(x) + \frac{1}{e}\partial_\mu\alpha(x). \quad (4.2)$$

The potential takes the form

$$V(\phi) = -\mu^2|\phi|^2 + \frac{\nu}{2}|\phi|^4. \quad (4.3)$$

If the parameter  $\mu^2$  in eqn. (4.3) is positive, then the field  $\phi$  has a non-zero vacuum expectation value. There is a circle of degenerate minima at

$$|\phi| = \frac{\mu}{\sqrt{\nu}} = \phi_0. \quad (4.4)$$

We can expand around this vacuum, as such redefining some of the variables, to provide some intuition into the properties of the model. As the potential is symmetric, we can fix the gauge so that  $\phi$  is real, rewriting the field as  $\phi = \phi_0 + \phi_1/\sqrt{2}$ . Substituting this into the Lagrangian, eqn. (4.1), gives

$$\mathcal{L} = \frac{1}{2}(\partial_\mu\phi_1)^2 + \frac{1}{2}M^2A_\mu A^\mu - \frac{1}{2}N^2\phi_1^2 + \mathcal{L}_{\text{int+vac}}, \quad (4.5)$$

with

$$M = \sqrt{2}e\phi_0 \quad N = \sqrt{2}\mu. \quad (4.6)$$

$\mathcal{L}_{\text{int+vac}}$  contains terms that mix  $A_\mu$  and  $\phi_1$ , the ‘interaction’ terms, terms which are higher than second-order in  $\phi_1$ , and a vacuum offset  $\mathcal{L}_{\text{vac}} = \mu^4/2\nu$ , which arises due to the form of the potential we are using. The potential has a quadratic form in the real direction, and perturbations up and down this potential give rise to a massive  $\phi_1$  field. The vector field also becomes massive. This Lagrangian, eqn. (4.5), no longer respects the U(1) symmetry, and the symmetry is said to be *spontaneously broken*. We see that spontaneous symmetry breaking has given rise to particle mass.

We can define two length scales from the Compton wavelengths of the particle masses.

$$d = M^{-1} = \frac{1}{\sqrt{2}e\phi_0} \quad \xi = N^{-1} = \frac{1}{\sqrt{2}\mu} \quad (4.7)$$

The significance of these length scales will become apparent later.

These results are particular to models invariant under a *local* transformation, i.e. one where the parameter  $\alpha$  is dependent on the *local* coordinate  $x$ ,  $\alpha = \alpha(x)$ , rather than a *global* one, where the parameter  $\alpha$  independent of any such coordinate. A similar procedure can be performed on the Goldstone model discussed later, which is invariant under the global transformation  $\phi(x) \rightarrow \phi'(x) = e^{i\alpha}\phi(x)$ . In this case, we would

produce a massive boson, and a massless scalar particle, a *Goldstone* boson. Goldstone bosons were first described by Nambu [392], in the context of superconductivity, and demonstrated in field theory by Goldstone soon after [393]. When breaking a local symmetry, massless Goldstone particles do not appear, as the corresponding degree of freedom is absorbed by the vector field, giving rise to massive gauge bosons.

The Lagrangian, eqn. (4.1), gives rise to the equations of motion

$$(\partial_\mu - ieA_\mu)(\partial^\mu - ieA^\mu)\phi - \mu^2\phi + \nu|\phi|^2\phi = 0, \quad (4.8)$$

$$\partial_\mu F^{\mu\nu} = ie(\phi\partial^\nu\bar{\phi} - \bar{\phi}\partial^\nu\phi) - 2e^2A^\nu|\phi|^2 = j^\nu, \quad (4.9)$$

where  $j^\mu$  is the four-current. With the rescaling

$$\phi \rightarrow \phi' = \frac{\phi}{\phi_0}, \quad (4.10)$$

$$x^\mu \rightarrow x'^\mu = e\phi_0 x^\mu, \quad (4.11)$$

$$A^\mu \rightarrow A'^\mu = \frac{A^\mu}{\phi_0}, \quad (4.12)$$

the field equations become

$$(\partial'_\mu - iA'_\mu)(\partial'^\mu - iA'^\mu)\phi' - \frac{\nu}{e^2}\phi'(1 - |\phi'|^2) = 0, \quad (4.13)$$

and

$$\partial'_\mu F'^{\mu\nu} = i(\phi'\partial'^\nu\bar{\phi}' - \bar{\phi}'\partial'^\nu\phi') - 2A'^\nu|\phi'|^2 \quad (4.14)$$

so that the model depends only upon the parameter  $\nu/e^2$ . This is the ratio of the square of the Compton wavelengths of the two particles defined previously. From now on we will drop the primes from discussions of eqns. (4.13) and (4.14).

## Solitons

One of the phenomena that brings together the models we describe is the appearance of soliton solutions. Solitons can be broadly defined as stable configurations of local energy density, and can be split into two categories: topological and non-topological. Generally, topological solitons occur when different degenerate vacuum configurations exist in a model. A topological defect is required to interpolate between the two different vacuum states. Within the interpolating region exists the energy density associated

with ‘undoing’ the defect. We can see that the formation of topological defects is intimately related to symmetry-breaking phenomena. In a model exhibiting spontaneous symmetry breaking with a number of degenerate vacua, then topological defects will usually be present, often with some associated particle production. The topology of the vacuum manifold also ensures the stability of the soliton, as the topology cannot be continuously transformed to a topologically trivial solution.

Non-topological solitons exist only in nonlinear models, as nonlinear effects are required to cancel dissipative effects that will usually destroy the configuration. We have already seen examples of non-topological solitons; the boson stars and oscillatons that we encountered in Chapter 2. We will not comment further on these solutions.

### Vortices

In the case of the Abelian-Higgs model, the topological defects produced are line-like *string* solutions, the Nielsen-Olesen vortex lines [378]. To look for vortex solutions in the system, we make a vortex ansatz in cylindrical coordinates  $(r, \chi, z)$ , similar to that in Section 3.2.2.

$$\phi(\mathbf{r}) = e^{in\chi} R(r), \quad (4.15)$$

$$A(\mathbf{r}) = A_\chi(r) = nA(r). \quad (4.16)$$

Or, in Cartesian coordinates,

$$A(\mathbf{r}) = \left( -\frac{y}{r^2} nA(r), \frac{x}{r^2} nA(r), 0 \right). \quad (4.17)$$

Substituting this ansatz into equations (4.13) and (4.14), we obtain the equations

$$\frac{d^2 R(r)}{dr^2} + \frac{dR(r)}{dr} \frac{1}{r} - \frac{n^2}{r^2} R(r) (A(r) - 1)^2 - \frac{\nu}{e^2} R(r) (R(r)^2 - 1) = 0, \quad (4.18)$$

and

$$\frac{d^2 A(r)}{dr^2} - \frac{1}{r} \frac{dA(r)}{dr} - 2R(r)^2 (A(r) - 1) = 0. \quad (4.19)$$

As before, explicit solutions to these equations are not known, and they must be solved numerically. The solutions can be thought of as representing a scalar and a vector flux tube, with widths corresponding to the Compton wavelength of the scalar and vector bosons,  $r_A \sim M^{-1}$  and  $r_{\phi_1} \sim N^{-1}$ .

The ratio of the Compton wavelengths defines for us the parameter we had mentioned previously,

$$\beta = \left( \frac{M^{-1}}{N^{-1}} \right) = \frac{\nu}{e^2}, \quad (4.20)$$

and we can then split the solutions into two types.

$$\beta < 1 \quad \Rightarrow \quad N^{-1} > M^{-1} \quad (\text{Type I}) \quad (4.21)$$

$$\beta > 1 \quad \Rightarrow \quad N^{-1} < M^{-1} \quad (\text{Type II}) \quad (4.22)$$

We label them in this way to facilitate a comparison with the condensed matter solutions that will be discussed later.

### 4.1.2 The Goldstone Model

The Goldstone model can be considered to be the Abelian-Higgs model without the coupling to electromagnetism. The introduction we give here will be brief, but the reason for introducing it will hopefully become evident later in the chapter.

The Goldstone model describes a real scalar field, not coupled to electromagnetism. The Lagrangian can be written

$$\mathcal{L} = \frac{1}{2}(\partial_\mu\phi)(\partial^\mu\phi) + \mu^2\phi^2 - \frac{\nu}{2}\phi^4. \quad (4.23)$$

This model also exhibits spontaneous symmetry breaking, and if we follow a similar procedure to that of the Abelian-Higgs model, expanding around one of the minima of the potential, we would uncover a massless scalar (Goldstone) particle, and a boson with mass  $N = \sqrt{2}\mu$ , as before. The equations of motion from the Goldstone Lagrangian are

$$\partial_\mu\partial^\mu\phi - 2\mu^2\phi + 2\nu\phi^3 = 0. \quad (4.24)$$

We recognise this as having the form of the nonlinear Klein-Gordon equation, with the negative term due to the symmetry-breaking form of the potential we are using. The Goldstone model also exhibits a topological defect. For simplicity, we take the one-dimensional case, where there is a static solution to the equations of motion,

$$\phi(z) = \frac{\mu}{\nu^{\frac{1}{2}}} \tanh(\mu z). \quad (4.25)$$

This is a kink, or *domain wall* solution, as it separates two domains of the potential with different values of the degenerate minima. We notice that this suggests a length scale defined previously by eqn. (4.7). We can rewrite eqn. (4.25) as

$$\phi(z) = \phi_0 \tanh\left(\frac{z}{\sqrt{2}\xi}\right). \quad (4.26)$$

In this case  $\xi$  has an interpretation as the width of the domain wall.

### 4.1.3 The Landau-Ginzburg Model

The Landau-Ginzburg model is the macroscopic equivalent to BCS theory, used to model the behaviour of superconductors. Some of the history of this subject was presented in Section 1.2. Landau and Ginzburg first constructed a theory of second-order phase transitions, and then coupled this theory to electromagnetism. The Lagrangian they obtained describes the evolution of a complex scalar and as such, is identical to the Lagrangian of the Abelian-Higgs model, eqn. (4.1). In contrast with the field theory literature however, the theory is not usually presented in a covariant way. While the same mathematics can be applied to the two different theories, the interpretation is of course, very different. The wavefunction in the Abelian-Higgs model represents a fundamental scalar field in the early Universe, while the wavefunction in the Landau-Ginzburg is a phenomenological order parameter describing how deep into the superconducting phase the material is, or the density of Cooper pairs. Since we can apply the same mathematical techniques, we start again from the Lagrangian eqn. (4.1) in order to make some comments about the theory of superconductivity.

For simply connected domains the Lagrangian, and the equations of motion, are again invariant under the local gauge transformations, eqn. (4.2). With this transformation, the four-current, eqn. (4.9) becomes

$$j^\mu = -2e^2 A^\nu |\phi|^2. \quad (4.27)$$

The spatial part of this equation is known in the condensed matter literature as London's equation [371]. This equation can be used to explain the exclusion of magnetic flux from a superconductor. This is known as the *Meissner effect*. We take the curl of the London equation

$$\nabla \times \mathbf{j} = -2e^2 |\phi|^2 \nabla \times \mathbf{A}, \quad (4.28)$$

and the curl of the fourth Maxwell equation

$$\nabla \times \mathbf{B} = \mathbf{j} + \frac{\partial \mathbf{E}}{\partial t}, \quad (4.29)$$

along with the identity  $\nabla \times (\nabla \times \mathbf{B}) = \nabla(\nabla \cdot \mathbf{B}) - \nabla^2 \mathbf{B}$ . Putting all this together, we obtain

$$\nabla^2 \mathbf{B} = 2e^2 n \mathbf{B}, \quad (4.30)$$

where  $n = |\phi|^2$ , the number density of charge carriers. The solution to this equation is

$$\mathbf{B} = \mathbf{B}_0 e^{-\frac{x}{d}}. \quad (4.31)$$

We see that a magnetic field entering a distance  $x$  into a superconductor is exponentially suppressed, and dies away within a penetration region  $d$ , of depth  $d = 1/\sqrt{2e^2 n}$ . We note that this is exactly the quantity given in eqn. (4.7), where we interpreted it as the Compton wavelength of the gauge boson associated with the spontaneously broken symmetry. This penetration depth is a direct consequence of the symmetry-breaking potential, and can be considered as the acquisition of mass by a gauge boson. The gauge boson in this case is the photon, and in going from being massless to massive, the force that it mediates goes from having an infinite range to having a finite range within the superconductor.

In terms of a superconductor then, the two quantities in eqn. (4.7) have an immediate interpretation as the penetration depth, and the coherence length of the wavefunction within the superconductor. If the coherence length is smaller than the penetration depth, then at high enough external fields, magnetic flux lines can penetrate the superconductor. In this case, the flux lines arrange themselves into narrow tubes, or vortices, with a core of the non-superconducting phase carrying the magnetic flux. These magnetic flux tubes were first described by Abrikosov [379]. Again, we recognise this phenomenon. It corresponds to the regime  $\beta > 1$ , as given in eqn. (4.22), and is known as a type II superconductor. In the condensed matter case,  $\beta$  is known as the Landau-Ginzburg parameter. Magnetic flux cannot penetrate type I superconductors, and so magnetic flux tubes do not exist within them.

We saw in Section 3.2 that the representation of the superfluid velocity as the gradient of a phase can lead to vortices with quantised circulation. This happens analogously for superconductors.

To see how the magnetic flux quantum arises, we can consider a type II superconductor, which we have seen allows the presence of magnetic flux, but prevents it penetrating beyond a distance  $d$ . We again consider the equation for the current, eqn. (4.9). We write the wavefunction as  $\phi = |\phi| \exp(in\chi)$ , and consider a contour that is far enough away from the vortex core that no magnetic field penetrates, so the current  $j^\mu$  is zero. The spatial part of eqn. (4.9) becomes,

$$n \oint_L \nabla\chi \cdot d\mathbf{l} = e \oint_L \mathbf{A} \cdot d\mathbf{l} \quad (4.32)$$

For the wavefunction to be single-valued, the integral around the contour must be equal to  $2\pi$ , and the right-hand side becomes an integral over a surface, via Stokes' theorem, giving the magnetic flux,

$$2\pi n = e \int_S \mathbf{B} \cdot d\mathbf{A} = e\Phi, \quad (4.33)$$

so that the flux is quantised in multiples of  $2\pi$ ,

$$\Phi = \frac{2\pi n}{e}. \quad (4.34)$$

This expression also holds for cosmic strings in the Abelian-Higgs model.

### Critical Coupling

The  $\beta = 1$  case is of some special interest. As well as being the transition between type I and type II superconductivity, it is important analytically as the often difficult-to-solve second-order equations of motion can be reduced to two first-order equations [394]. Fields satisfying these equations also satisfy what is known as the *Bogomolny bound*, which states that the energy of the field configuration is a minimum, and so the soliton solution is inherently stable.

This *critical coupling* is also of importance to supersymmetry [395], where BPS states, solutions which saturate the Bogomolny bound, are important as supersymmetries of the theory are automatically preserved. See, for example, Tong [396, 397].

#### 4.1.4 The Gross-Pitaevskii Equation

We have looked at the Goldstone model, which can be considered to be the 'uncharged' version of the Abelian-Higgs model, that is, does not include electromagnetism. In

the same way, in the nonrelativistic versions, the Landau-Ginzburg theory describes condensate phenomena that is electromagnetically coupled, while the Gross-Pitaevskii equation describes condensate phenomena that is not.

Generally, when discussing the Landau-Ginzburg theory, the equations used are not in the covariant form that we have been using. The equations of motion depend on the first derivative, with respect to the time coordinate, rather than the second, as is present in the Klein-Gordon equation. All the phenomena we have described so far have been time independent, so this has not been a concern. In Appendix A, we discuss how to reduce the relativistic nonlinear Klein-Gordon equation to the nonlinear Schrödinger equation, and similar techniques can be employed to move from the Abelian-Higgs to the Landau-Ginzburg theory.

We remind ourselves of the Gross-Pitaevskii equation, eqn. (3.34),

$$i\hbar \frac{\partial}{\partial t} \psi(\mathbf{r}, t) = -\frac{\hbar^2}{2m} \nabla^2 \psi(\mathbf{r}, t) + V_{\text{ext}} \psi(\mathbf{r}, t) + V_0 |\psi(\mathbf{r}, t)|^2 \psi(\mathbf{r}, t) - E_v \psi(\mathbf{r}, t).$$

This equation also admits soliton solutions. We have already seen the vortex solutions in Section 3.2.2, but there is also a one-dimensional solution, analogous to the domain wall solution in the Goldstone model. To construct a solution, we can consider the condensate bounded by a container, so that the potential behaves as

$$V_{\text{ext}} = \infty \quad \text{for } x < 0 \quad (4.35)$$

$$V_{\text{ext}} = 0 \quad \text{for } x > 0. \quad (4.36)$$

The solution to the Gross-Pitaevskii equation is then

$$\psi(x) = \psi_\infty \tanh\left(\frac{x}{\sqrt{2}\xi}\right). \quad (4.37)$$

This solution for the case of a condensate with a boundary can also be extended to all space. In this case, the solution describes a static soliton. It is also possible to find moving solitons of this type, whose profile typically depends on their velocity. See, for example, Pethick and Smith [328]. The soliton solution above is known as a *dark* soliton, as it describes an underdensity in a constant density background (recall  $\rho \propto |\psi|^2$ ). There are also soliton solutions for attractive interaction potentials,  $V_0 < 0$ . These are referred to as *bright* solitons, as they correspond to an overdensity. We came across one such model in a cosmological context at the end of Section 2.4.1. As

we noted there, attractive interactions generally lead to negative values of the particle scattering length, and an imaginary sound speed. The dark soliton solution given above is identical to eqn. (4.26). Again  $\xi$  is interpreted as the width of the domain wall, or a coherence length over which the wavefunction varies, given by

$$\xi = \frac{\hbar}{(2mE_v)^{\frac{1}{2}}}, \quad (4.38)$$

agreeing with the previous argument for the coherence length we gave in eqn. (3.36).

## 4.2 The Relationship between Bose-Einstein Condensation and Spontaneous Symmetry Breaking, and the Role of Temperature

Very often in high-energy field theory literature, it is suggested that the symmetry of the theory being described is spontaneously broken by the appearance of a condensate. See, for example, pg. 39 of Vilenkin and Shellard [380], pg. 272 and pg. 428 of Kolb and Turner [398], and many others [399, 400, 401, 402]. This statement is an equivalent way of describing the process of mass generation via spontaneous symmetry breaking. The Higgs mechanism, for example, generates a Bose-Einstein condensate of Higgs particles, while the particle produced as a result of the spontaneously breaking the Peccei-Quinn symmetry, the axion, is also produced in a zero-momentum Bose-Einstein condensate. We can pause for a moment to see why these two descriptions are equivalent.

We have already seen the Bogoliubov prescription, which describes, in the limit of large occupation numbers, how the creation and annihilation operators can be replaced by a non-quantum number, in this case the root of the number of particles occupying the ground state. In field theory, the field wavefunction  $\phi$  acquires a classical expectation value, which can equivalently be described as  $\phi$  particles sitting at the bottom (macroscopically occupying the lowest energy state) of the potential  $V(\phi)$ . In this way, the appearance of a non-zero vacuum expectation value in field theory also corresponds to the appearance of a condensate. In a thermodynamic system, the onset of Bose-Einstein condensation, and the appearance of a non-zero vacuum expectation

value arising from a spontaneously broken vacuum can be considered two parts of the same process, both occurring at some critical temperature.

It is expected that the symmetry groups corresponding to the standard model were unified at some higher temperature, earlier in the Universe's history. As the temperature decreased, the potential of the model moved from a symmetric one, to one exhibiting spontaneous symmetry breaking. We can demonstrate this using the Goldstone model. In spontaneous symmetry-breaking phenomena in the early Universe, the scalar field  $\phi$  is a quantum field, and hence the classical potential  $V(\phi)$  is modified by *radiative corrections*. We can introduce an *effective potential* that is treated in the normal way, but is derived by including quantum corrections to the potential. The effective potential can be built up by summing the  $n$ -loop contributions, and was first described rigorously by Coleman [403] and Weinberg [119]. Weinberg was awarded the 1979 Nobel prize for his work with Salam and Glashow on the electroweak interaction. The development of a effective potential allowed a large amount of progress on a low energy limit of QCD. It is possible to show that the calculation of the quantum corrections is the same as computing the free energy. See Vilenkin and Shellard [380], for example. The effective potential then, can be shown to be

$$V_{\text{eff}}(\phi, T) = V(\phi) + \frac{1}{24} \mathcal{M}^2(\phi) T^2 - \frac{\pi^2}{90} \mathcal{N} T^4, \quad (4.39)$$

where

$$\begin{aligned} \mathcal{M}^2 &= \sum_{\text{B}} m_n^2 + \frac{1}{2} \sum_{\text{F}} m_n^2 \\ \mathcal{N} &= \mathcal{N}_{\text{B}} + \frac{7}{8} \mathcal{N}_{\text{F}} \end{aligned} \quad (4.40)$$

are the mass and number of bosonic and fermionic spin states.

We remind ourselves of the form of the potential we have been using, eqn. (4.3),

$$V(\phi) = -\mu^2 |\phi|^2 + \frac{v}{2} |\phi|^4.$$

We split the complex field into two real fields,

$$\phi = \frac{1}{\sqrt{2}} (\phi_1 + i\phi_2), \quad (4.41)$$

so that  $|\phi|^2 = \frac{1}{2}(\phi_1^2 + \phi_2^2)$  and the masses of the associated particles are given by the eigenvalues of the matrix

$$m_{\text{eff}}^2 = \frac{\partial^2 V(\phi)}{\partial \phi_i \partial \phi_j} \quad (4.42)$$

so

$$m_1^2(\phi) = -\mu^2 + 3\nu|\phi|^2 \quad (4.43)$$

$$m_2^2(\phi) = -\mu^2 + \nu|\phi|^2. \quad (4.44)$$

Note that if we are on the vacuum manifold,  $|\phi|^2 = \frac{\mu^2}{\nu}$ , then

$$m_1^2 = 2\mu^2 \quad (4.45)$$

$$m_2^2 = 0 \quad (4.46)$$

as we derived in Section 4.1.2. With  $\mathcal{M}^2 = m_1^2 + m_2^2$ , and  $\mathcal{N} = 2$  (two bosons), eqn. (4.39) becomes

$$V_{\text{eff}}(\phi) = -\mu^2|\phi|^2 + \frac{\nu}{2}|\phi|^4 + \frac{1}{24}(-2\mu^2 + 4\nu|\phi|^2)T^2 - \frac{\pi^2}{45}T^4. \quad (4.47)$$

Defining  $\frac{1}{2}m_{\text{eff}}^2$  to be the coefficient of  $|\phi|^2$ , we find

$$\frac{1}{2}m_{\text{eff}}^2 = \frac{\nu}{6} \left( T^2 - 6\frac{\mu^2}{\nu} \right). \quad (4.48)$$

This defines for us a critical temperature,

$$T_{\text{crit}}^2 = \frac{6\mu^2}{\nu}. \quad (4.49)$$

If  $T > T_{\text{crit}}$ , then  $m_{\text{eff}}^2 > 0$ , and the effective potential takes a quadratic form with a single minimum. This corresponds to the parameter  $\mu^2$  in the potential, eqn. (4.3), being negative. If however, the temperature drops below the critical temperature,  $T < T_{\text{crit}}$  (the parameter  $\mu^2$  is positive, as we assumed in our initial demonstrations of symmetry breaking), then  $m_{\text{eff}}^2 < 0$ , the effective potential develops two degenerate minima, and exhibits spontaneous symmetry breaking. We recall that for the potential we have been using for our symmetry-breaking models,  $\phi_0 = \mu/\sqrt{\nu}$  (eqn. (4.4)), and see from eqn. (4.49) that the critical temperature  $T_{\text{crit}}$  is comparable to the symmetry-breaking scale  $\phi_0$ . This is generally the case.

A similar process exists in condensed matter physics. If the temperature in a superfluid or superconductor is raised, then the proportion of condensed phase decreases

until some critical temperature  $T_{\text{crit}}$  where the fluid is completely in the normal phase. Kirzhnits pointed out that symmetries in particle physics models can be restored in a similar way [404, 405], and this is known as *symmetry restoration at high temperature*.

From the temperature of the symmetry-breaking scale then, one can predict the mass of the associated particle, or vice versa. For each symmetry of the theory, there is also a conserved charge. This is Noether's theorem [223]. For each conserved charge, it is also possible to associate a chemical potential. We saw in Section 3.2 the use of the chemical potential as a Lagrange multiplier, which led to a description of a Bose-Einstein condensate, with the associated conserved quantity being the particle number. We can demonstrate the role of a chemical potential in spontaneous symmetry breaking, to reinforce again the equivalence of spontaneous symmetry breaking and Bose-Einstein condensation.

Bose-Einstein condensation as a broken symmetry phenomenon was first pointed out by Bogoliubov [406], and later extended in seminal papers by Bernard [407], Kapusta [408] and Haber and Weldon [409]. The full derivation requires the use of a complex functional integral calculation, integrating out the canonical momenta in the process. This elegant calculation is fairly involved, and we can summarise their argument by considering the effect of a chemical potential, in a similar way to our derivation of the Gross-Pitaevskii equation, eqn. (3.20), in Section 3.2.

We consider a model similar in form to those we are familiar with. We take a real scalar field  $\phi_i$ , with two components  $i = 1, 2$  (we could consider the two components to be the two parts of a complex field), and a conserved charge. We write the Hamiltonian density,

$$\mathcal{H} = -\frac{1}{2}\pi_i\pi_i - \frac{1}{2}(\nabla\phi_i)(\nabla\phi_i) + \mu^2\phi_i\phi_i + \frac{\nu}{2}(\phi_i\phi_i)^2, \quad (4.50)$$

and conserved charge

$$Q = \int d^3\mathbf{x}j^0 = \int d^3\mathbf{x}(\phi_1\pi_2 - \phi_2\pi_1), \quad (4.51)$$

where  $\pi$  is the momentum density conjugate to  $\phi$ .

We can demonstrate the effect of this background charge by considering  $H - E_\nu Q$ . In our example in Section 3.2, we considered  $E_\nu$  to be a Lagrange multiplier, one of which can be assigned to each conserved quantity, or symmetry of the system. The conserved

charge for the Gross-Pitaevskii equation was particle number,  $N$ .

The corresponding  $E_v$ -dependent Hamiltonian density may be written as

$$\mathcal{H}(E_v) = \mathcal{H} - E_v j^0 = \mathcal{H} - E_v(\phi_1 \pi_2 - \phi_2 \pi_1), \quad (4.52)$$

giving

$$\mathcal{H}(E_v) = -\frac{1}{2}\pi_i \pi_i - \frac{1}{2}(\nabla \phi_i)(\nabla \phi_i) + \mu^2 |\phi|^2 + \frac{\nu}{2} |\phi|^4 - E_v(\phi_1 \pi_2 - \pi_2 \phi_1). \quad (4.53)$$

From Hamilton's equations, we find

$$\dot{\phi}_1 = \frac{\partial}{\partial \pi_1} \mathcal{H}(E_v) = -\pi_1 - E_v \phi_2, \quad \dot{\phi}_2 = \frac{\partial}{\partial \pi_2} \mathcal{H}(E_v) = -\pi_2 + E_v \phi_1. \quad (4.54)$$

The Lagrangian can be written

$$\mathcal{L}(E_v) = \pi_i \dot{\phi}_i - \mathcal{H}(E_v). \quad (4.55)$$

Substituting our expression for  $\mathcal{H}(E_v)$ , eqn. (4.53), and Hamilton's equations, eqn. (4.54), into the above equation, we find the Lagrangian

$$\mathcal{L}(E_v) = |\partial_\mu \phi|^2 - V(\phi) + E_v(\phi_1 \dot{\phi}_2 - \phi_2 \dot{\phi}_1), \quad (4.56)$$

where the potential is given by

$$V(\phi) = (\mu^2 - E_v^2) |\phi|^2 + \frac{\nu}{2} |\phi|^4. \quad (4.57)$$

Generally, the chemical potential is temperature dependent,  $E_v = E_v(T)$ , and we can see that if the chemical potential evolves in such a way to move from  $E_v^2 < \mu^2$  to  $E_v^2 > \mu^2$  at some critical temperature  $T_{\text{crit}}$ , then the potential given in eqn. (4.57) evolves into a potential exhibiting symmetry breaking, with the same form as eqn. (4.3). We see that symmetry breaking in the presence of a background charge effectively forms a Bose-Einstein condensate. We should not be surprised then, that a theory including a chemical potential, eqn. (4.56), can also be written in the form of a gauge theory,

$$\mathcal{L} = |D_\mu \phi|^2 - \mu^2 |\phi|^2 - \frac{\nu}{2} |\phi|^4, \quad (4.58)$$

where

$$D_\mu \phi = \partial_\mu \phi - i A_\mu \phi, \quad A_\mu = (E_v, 0, 0, 0). \quad (4.59)$$

These results have also been formalised for high temperature systems [410, 411], relativistic systems [412, 318], and extended to cosmological systems [317, 413], and Yang-Mills theories in QCD [414]. Quark or gluon condensates, the result of breaking a *chiral* symmetry in QCD may be responsible for producing hadron masses. Chiral condensates are an example of a fermionic condensate. Fermionic condensates are possible as fermions combine into Cooper pairs to produce a particle that behaves, statistically, as a boson. The first fermionic condensate was produced in the laboratory by Deborah Jin's group in 2003 [415, 416]. Condensates are also exhibited in theories in which ghosts are present. See, for example, Arkani-Hamed et al. [369]. As an interesting link to gravitational physics, Schiff and Barnhill [417, 418] showed that the electric field inside a conductor does not vanish when a gravitational field is present. DeWitt [419] described a similar result for magnetic fields inside superconductors, and showed that the vector potential associated with frame dragging can be formally associated with the vector potential for a superconductor.

Axions can also be produced as the result of a symmetry-breaking phenomenon in QCD, and reside in a Bose-Einstein condensate.

### 4.3 The Axion

The axion appears as a result of a proposed resolution to the *strong CP problem* in *Quantum Chromodynamics* (QCD), the theory of the strong interaction. The particle appears as a result of symmetry-breaking phenomena producing a (pseudo) Goldstone boson. The axion is not massless, as Goldstone bosons are, as quantum effects also produce a small explicit broken symmetry, providing a unique vacuum.

We have already demonstrated some examples of symmetry breaking, leading to particle production and the creation of topological defects, and these concepts can be straightforwardly applied to the symmetry-breaking potential that is used to solve the strong CP problem.

### The Strong CP Problem, and a Dark Matter Candidate

Charge-Parity (CP) symmetry is a postulated symmetry of nature that suggests that a particle with opposite charge and parity should be indistinguishable from the original particle. The combination of charge and parity was originally suggested as a symmetry, winning Lee and Yang the Nobel prize in 1957 for their theoretical work, after parity alone was found to be violated in some weak interactions [420, 421]. In fact the CP symmetry is still violated in weak decay [422], a discovery which won James Cronin and Val Fitch the 1980 Nobel prize.

When QCD was first being developed, the theory apparently had no CP violating terms. As the details were expanded upon, 't Hooft [423, 424] realised that the vacuum structure of QCD is more complicated than initially thought. This additional structure allows CP violating terms, characterised by a term in the Lagrangian known as the  $\theta$ -parameter. CP violation is not observed in experimental tests of the strong interaction, and in addition, the CP violating terms give rise to an electric dipole moment of the neutron. Measurements of CP violation in QCD and of the neutron electric dipole moment require the  $\theta$ -parameter to be less than  $10^{-10}$ , with CP being preserved exactly for a value of  $\theta = 0$ . This amounts to an unpalatable amount of fine-tuning for theorists. This is the *strong CP problem*.

To resolve this fine tuning problem, Peccei and Quinn [425, 426] postulated a new U(2) chiral symmetry in the QCD Lagrangian. This chiral symmetry can be decomposed into the symmetry groups  $SU(2) \times U(1)$ , a chiral symmetry and a global axial symmetry. At some energy scale, corresponding to a certain temperature in the early Universe, as we have already mentioned, the potential of the global U(1) can evolve to one that exhibits spontaneous symmetry breaking, giving a vacuum expectation value to the associated scalar field. The  $\theta$ -parameter can then be viewed as the phase of the complex scalar field around the bottom of the global U(1) 'Mexican hat' potential, similar to the potential described in our explanation of the Higgs mechanism. We have already seen that this form of symmetry breaking gives rise to a massless Goldstone boson, and in this case, this is the axion. In fact, there is a small explicit breaking of the symmetry from *QCD instanton* effects. This has the effect of 'tipping' the potential slightly, providing a unique vacuum for the potential at  $\theta = 0$ , preserving CP

symmetry, and giving a small mass to the axion, making it a *pseudo*-Goldstone boson. As with the temperature-dependent symmetry-breaking mechanism we described previously, the axion mass is set by the energy scale at which the symmetry breaking occurs.

This energy scale is usually represented by the parameter  $f_a$ , and the axion mass is given by

$$m_a \simeq 0.6 \text{ eV} \frac{10^7 \text{ GeV}}{f_a}. \quad (4.60)$$

Typically, one seeks to detect the axion through its decay to two photons, and so the axion-photon-photon interaction

$$g_{a\gamma\gamma} = \frac{\alpha g_\gamma}{\pi f_a}, \quad (4.61)$$

is of interest. Here,  $\alpha$  is the fine structure constant, and  $g_\gamma$  is a dimensionless, model-dependent parameter, typically of order unity.

Based upon experimental evidence of other QCD and astrophysical processes, one can place limits on the symmetry-breaking scale and axion mass. The upper limit on the axion mass from astrophysical considerations is currently  $3 \times 10^{-3}$  eV. For further detail, see Carosi [427], Turner [172], and Sikivie [428].

It is also possible that the instanton effects occur at a later time than the spontaneous breaking of the U(1) global symmetry. This would result in an *axionic* string, a topological defect produced as the result of breaking a U(1) symmetry, as we have already seen. It is also possible that the primary energy loss mechanism for axionic strings may be the radiation of axions, rather than gravitational waves, and in this case, axionic string decay may be the primary source of axion production, rather than the symmetry-breaking mechanism [429].

The axion is predicted to be electrically neutral, with a low interaction cross-section for the strong and weak forces. Theoretical bounds and bounds placed by experimental results, some of which we saw in Section 1.1.4, suggest a low particle mass,  $\sim 10^{-5}$  eV. These parameters made the axion an ideal dark matter candidate, but unfortunately, no further experimental evidence has been forthcoming.

Condensates of axions have also been considered as dark matter halos [370, 430], and within these halos, quantised vortices have been investigated [431] and found to

produce phenomenological rotation curves in a similar vein to those produced by scalar field dark matter that we discussed in Chapter 2.

## 4.4 The Domain Wall Problem in a Model of Bose-Einstein Condensate Dark Matter

In this section, we consider in more detail one of the models set out in a paper that we mentioned in Sections 2.3.1 and 3.4. After giving an overview, we note what we perceive to be one of the problems associated with it.

The paper “*Dark Matter as a Cosmic Bose-Einstein Condensate and Possible Superfluid*” by Silverman and Mallett [279], is adapted from an essay that received an honourable mention from the Gravity Research Foundation in 2001 [432]. The model considers a real scalar field in the early Universe, in which particles making up the dark matter component arise from the breaking of a  $Z_2$  symmetry. This paper provides a nice example of particle production as a result of spontaneous symmetry breaking, with the additional result of the emergence of a cosmological constant.

We look at one of the phenomena generic to the breaking of a  $Z_2$  symmetry; the production of domain walls. These are the kink solutions that we saw in the Goldstone model. Depending on the energy scale of formation, these walls can come to dominate the energy density of the Universe, and/or cause problems with the observed isotropy of the Universe at decoupling.

We briefly introduce the model in Section 4.4.1 and examine the existence of domain walls within it in Section 4.4.2. We discuss the possible Cosmological constraints on the existence of domain walls in Section 4.4.3 and in Section 4.4.4 we compare these to the estimates of particle mass and symmetry-breaking scale made by Silverman and Mallett. Some final remarks are made in Section 4.4.5.

### 4.4.1 The Model

In the Silverman-Mallett model, a real scalar field is coupled to General Relativity. The Lagrangian takes the form

$$\mathcal{L} = \frac{R}{\kappa^2} + \frac{1}{2}(\partial_\mu\phi)(\partial^\mu\phi) - V(\phi), \quad (4.62)$$

where  $\kappa^2 = \frac{16\pi G}{c^4}$ , and  $R$  is the Ricci scalar.

The potential takes the form

$$V(\phi) = \frac{1}{2}(a\phi^2 + b\phi^4), \quad (4.63)$$

and the parameter  $a$  evolves from positive to negative as the temperature passes through some critical temperature.

We have already seen in Section 4.1.2 how this type of setup can lead to domain wall solutions. The Ricci tensor in Silverman and Mallett's setup will give the Einstein equations, as well as the nonlinear Klein-Gordon equations of motion for the scalar field that we have already seen, eqn. (4.24).

The parameters in the Silverman and Mallett model are related to the parameters that we have been using to define the potential by

$$a = -2\mu^2, \quad \text{and} \quad b = \nu. \quad (4.64)$$

We will continue with Silverman and Mallett's notation for this section. We also note that Silverman and Mallett model keeps factors of  $\hbar$ ,  $c$  and  $G$  explicit, while we have previously been using natural units.

Expanding around the vacuum, with  $\phi = \phi_0 + \bar{\phi}$ , in a similar way to that described in Section 4.1.1, gives a Lagrangian

$$\mathcal{L} = \frac{R}{\kappa^2} + \frac{a^2}{8b} + \frac{1}{2}\partial_\mu\bar{\phi}\partial^\mu\bar{\phi} + a\bar{\phi}^2 - 2b\phi_0\bar{\phi}^3 - \frac{b}{2}\bar{\phi}^4. \quad (4.65)$$

The coefficient of the kinetic term gives an expression for the mass of the particle. The field  $\phi^2$  has units of  $\text{Jm}^{-1}$ , so keeping factors of  $\hbar$  and  $c$  explicit, gives

$$a = -\frac{m^2 c^2}{2 \hbar^2}. \quad (4.66)$$

In their paper, the mass parameter is frequently related to the reduced Compton wavelength,  $\lambda_c$ ,

$$\frac{mc}{\hbar} = \sqrt{-2a} = \frac{1}{\lambda_c}, \quad (4.67)$$

and the vacuum offset is identified with the Lagrangian term one would expect for a cosmological constant ( $\mathcal{L}_\Lambda = 2\Lambda/\kappa^2$ ), obtaining

$$\Lambda = \frac{\kappa^2 a^2}{16b} = \left( \frac{\kappa\phi_0}{4\lambda_c} \right)^2. \quad (4.68)$$

#### 4.4.2 Existence of Domain Walls in the Silverman-Mallett Model

Domain walls arise generically in models that exhibit spontaneously broken discrete symmetries [205]. We have already seen in Section 4.1.2 a particular case of domain wall formation from the breaking of a  $Z_2$  symmetry, and we briefly remind ourselves of the results of that section, using the notation conventions set out in Silverman and Mallett 4.64.

The equations of motion are

$$\partial_\mu \partial^\mu \phi + a\phi + 2b\phi^3 = 0, \quad (4.69)$$

remembering that the parameter  $a$  is negative below the critical temperature. The one-dimensional static solution to these equations of motion is

$$\phi(z) = \left( -\frac{a}{2b} \right)^{\frac{1}{2}} \tanh \left( \left( -\frac{a}{2} \right)^{\frac{1}{2}} z \right), \quad (4.70)$$

and can be rewritten as

$$\phi(z) = \phi_0 \tanh \left( \frac{z}{2\lambda_c} \right). \quad (4.71)$$

#### 4.4.3 Cosmological Constraints on the Existence of Domain Walls

We now turn to some constraints provided by the CMB on the existence of domain walls and their related symmetry-breaking scale, in anticipation of a comparison of estimates of these parameters provided by the Silverman-Mallett model. The argument we present here is adapted from Vilenkin and Shellard [380].

The contribution to the energy density of the Universe from domain walls is expected to be

$$\rho_W \sim \frac{\sigma R^2}{R^3} \sim \frac{\sigma}{R}, \quad (4.72)$$

where  $R$  is the mean radius of curvature of the wall, and  $\sigma$  is the surface energy density, or mass per unit area of the wall. If we consider only one domain wall, stretched across the Universe, so its radius of curvature is approximately equal to the Hubble length, or in natural units, the Hubble time, then

$$\rho_W \sim \frac{\sigma}{t_0}. \quad (4.73)$$

Using the relation  $\rho_{r,m} \sim 1/Gt^2$ , which holds in matter and radiation dominated universes, when we would expect the domain wall to form, it is possible to write

$$\frac{\rho_W}{\rho} \sim \sigma G t_0 \quad (4.74)$$

We can estimate the surface energy density from parameters that we already know. The vacuum energy at the centre of the wall is approximately equal to the offset between the potential at the bottom of the well, and the value of the potential at  $V(\phi = 0)$ . The form of our potential defines

$$V(0) = 0, \quad (4.75)$$

so that

$$V(\phi_0) = -\frac{b}{2}\phi_0^4. \quad (4.76)$$

The magnitude of the energy at the centre of the wall is then

$$\rho \sim \frac{b}{2}\phi_0^4. \quad (4.77)$$

The width of the wall  $\xi$ , is approximately equal to the Compton wavelength of the pseudo Nambu-Goldstone boson,

$$\xi \sim \lambda_c \sim \frac{1}{\sqrt{-a}} \sim \frac{1}{\phi_0 \sqrt{b}}. \quad (4.78)$$

The surface energy density then, is

$$\sigma \sim \rho \delta \sim \sqrt{b}\phi_0^3. \quad (4.79)$$

This can be shown more precisely by integrating the  $t - t$  component of the energy-momentum tensor

$$\sigma = \int T_0^0 dz, \quad (4.80)$$

where

$$T_{\mu\nu} = \partial_\mu \phi \partial_\nu \phi - g_{\mu\nu} \mathcal{L}, \quad (4.81)$$

and the domain wall solution, eqn. (4.71), is used.

The final relation we require is

$$Gt_0 \sim \left( \frac{10^{20}}{m_{\text{pl}}} \right)^3. \quad (4.82)$$

Putting all the above together, we then have an expression relating the density fluctuations we observe, to the symmetry-breaking scale  $\phi_0$ ,

$$\frac{\delta\rho}{\rho} \sim G\sigma t_0 \sim 10^{60} \left( \frac{\phi_0}{m_{\text{pl}}} \right)^3. \quad (4.83)$$

Temperature fluctuations in the CMB are related to density perturbations by

$$\frac{\delta\rho}{\rho} \sim \frac{\delta T}{T}, \quad (4.84)$$

and CMB observations constrain  $\delta T/T \lesssim 10^{-5}$ . This means that models predicting topologically stable domain walls with

$$\phi_0 \gtrsim 1 \text{ MeV}, \quad (4.85)$$

should be ruled out.

#### 4.4.4 Mass and Symmetry-Breaking Parameters in the Silverman-Mallett Model

Silverman and Mallett make some estimates of the mass of their dark matter candidate using considerations from Jeans' stability analysis, and comparing the resultant quantities with parameters in their symmetry-breaking model. They suggest that the energy of a gravitationally bound quantum particle can be given by

$$E(\xi) \approx \frac{p^2}{2m} + m\Phi(\xi) = \frac{h^2}{2m\xi^2} - \frac{GMm}{\xi}. \quad (4.86)$$

The equilibrium ( $dE/d\xi = 0$ ) between quantum pressure and gravitational attraction leads to a minimum size; the coherence length,

$$\xi_c = \frac{h^2}{GMm^2} = \left( \frac{3h^2}{4\pi Gm^2\bar{\rho}} \right)^{\frac{1}{2}}, \quad (4.87)$$

where the mean density has been defined as  $\bar{\rho}$  as  $M = 4\pi\xi_c^3\bar{\rho}/3$ .

They then compare this to the Jeans length for a fluid. The Jeans length is a critical scale which determines whether a density fluctuation grows or decays. Simple arguments can be made to determine its size. A density fluctuation with length scale  $\lambda$ , mass  $M$ , and average density  $\bar{\rho}$ , will grow if the attractive gravitational force per unit mass,  $F_G$ , is greater than the opposing force per unit mass from gas pressure,  $F_p$ , where

$$F_G \simeq \frac{GM}{\lambda} \simeq \frac{G\bar{\rho}\lambda^3}{\lambda^2}, \quad F_p \simeq \frac{p\lambda^2}{\bar{\rho}\lambda^3} \simeq \frac{v^2}{\lambda}. \quad (4.88)$$

The balance of the two forces leads to the tipping-point length scale, the Jeans length,

$$\lambda_J = \frac{v}{\sqrt{G\bar{\rho}}}. \quad (4.89)$$

This approximation can also be derived by equating the hydrodynamic time, the time scale for the gas pressure to respond,  $\tau_{\text{pres}}$ , to the time-scale for gravitational collapse,  $\tau_{\text{grav}}$ ,

$$\tau_{\text{pres}} \simeq \frac{\lambda}{v}, \quad \tau_{\text{grav}} = \frac{1}{\sqrt{G\bar{\rho}}}. \quad (4.90)$$

In a classical fluid the speed  $v$ , is the sound speed. Silverman and Mallett suggest that the relevant speed in the case of a dark matter Bose-Einstein condensate is given by the de Broglie wavelength of the particles,  $v = h/m\lambda$ . They substitute this into the expression for the Jeans length to find an expression for the ‘quantum’ Jeans length,

$$\lambda_Q \simeq \left( \frac{h^2}{Gm^2\bar{\rho}} \right)^{\frac{1}{2}}. \quad (4.91)$$

This is equivalent, up to a numerical factor, to the coherence length of a gravitationally bound quantum fluid, eqn. (4.87). Thus, the minimum gravitationally stable length scale in an astrophysical system is equivalent to the quantum coherence length of the particles making up that system. There is one point we pick up on about this derivation, which they also note themselves. In an ideal Bose-Einstein condensate, with no interactions, the sound speed (also referred to as *first sound* [328]) is zero, and so the

Jeans length should also be expected to be zero. They resolve this by suggesting that the Bose-Einstein dark matter condensate is not a true condensate due to the gravitational interaction that must be taken into account. This brings us back to issues that were mentioned in Section 3.4 about the existence of a gravitationally interacting condensate. This matter is unfortunately not pursued any further in this paper, and they continue with their analysis.

Taking the ‘real-life’ example of the Andromeda galaxy, M31, they suggest that the luminous core is approximately the largest gravitationally stable scale, and equate this to the boson’s coherence length. The luminous core of M31 is taken to be  $\xi_c \sim 30$  kpc. From the rotation curve of M31 and the Andromeda Atlas [433], the mass density of the Andromeda halo is estimated to be  $\bar{\rho} \sim 2 \times 10^{24}$  kg/m<sup>3</sup>.

Substituting these values into eqn. (4.87) they obtain a particle mass of  $\sim 3 \times 10^{-59}$  kg, and a boson Compton wavelength of  $\lambda_c \sim 7$  lightyears ( $\sim 7 \times 10^{16}$  m). A value of  $\Lambda = (0.7)8\pi G\rho_c/c^2 \sim 1 \times 10^{-52}$  m<sup>-2</sup> has also been used. From eqn. (4.68), the magnitude of the symmetry-breaking scale is estimated to be  $1.5 \times 10^{21}$  (eV/m)<sup>1/2</sup>. In natural units, this is  $\phi_0 \sim 7 \times 10^8$  GeV.

Returning to the bound we set on the symmetry-breaking scale, set by observations of temperature fluctuations in the CMB, eqn. (4.85), we see that the value set by Silverman and Mallett  $\phi_0 \gtrsim 1$  MeV is far beyond this range.

#### 4.4.5 Final Remarks

We have briefly reviewed a model of Bose-Einstein condensate dark matter. This particular model draws heavily on the mechanism of symmetry breaking in order to produce a condensate of ultra-light particles. We have demonstrated the problem of domain wall domination in the early Universe which is present in this model, and in fact is a generic feature of discrete symmetry-breaking models where the symmetry-breaking scale is  $\gtrsim 10^6$  eV [434, 380].

There are a few mechanisms by which a model containing domain walls may be acceptable. If the formation of domain walls is followed by a period of inflation, then the domination of the energy density can be avoided. We described in Section 1.1.2 how

this mechanism was originally introduced to eliminate the monopole problem, and the solution work analogously for domain walls.

Restoration of the broken symmetry at a lower temperature would also avoid domain wall domination. See Section 3.2.5 of Vilenkin and Shellard, [380], for example.

If the vacuum states separated by the domain wall have slightly differing vacuum levels, then the domain wall network will be unstable and subsequently break up. This may occur after inflation for real scalar fields that are sufficiently weakly coupled that they are not in thermal equilibrium [435, 436].

If the discrete symmetry responsible for producing domain walls is embedded in a continuous symmetry group, then the domain walls become bounded by strings. These are known as *hybrid defects*. Defects in hybrid models decay before they can dominate the energy density of the Universe [437, 438].

A vacuum phase transition in the early Universe after the decoupling of matter from the CMB would allow the bound from the CMB observations to be substantially weakened [439].

Some axionic models also have domain walls present within them, and many authors have proposed solutions [440, 441, 442].

## 4.5 Discussion

In this chapter, we have elucidated many concepts that we previously alluded to. We particularly wanted to establish the relationships between condensed matter and field theory that may be applied to early Universe cosmology. To this end, we looked at models that contain ideas central to the ideas in this thesis: the Abelian-Higgs model, and its condensed matter counterpart, the Landau-Ginzburg theory, and their ‘uncharged’ versions, the Goldstone model and the Gross-Pitaevskii equation.

We described the phenomena of symmetry breaking in the Abelian-Higgs model, and how the acquisition of mass by the photon produced a natural explanation of the Meissner effect in superconductors, described by Landau-Ginzburg theory. We found that the Compton wavelengths of particles produced also had equivalent descriptions in terms

of a penetration depth, a coherence length, or a length scale for topological defects in both theories.

Topological defects are often present in models whose potentials exhibit spontaneous symmetry breaking, and we described two types of this kind of defect. Nielsen-Olesen vortices describe cosmic strings in the early Universe scenario, or magnetic flux tubes in Type II superconductors in the condensed matter scenario. Vortices in superfluids were modelled by the Gross-Pitaevskii equation. This particular example is familiar to us from our work in Chapter 3, but we are now aware of their analogue in high-energy field theory; the global cosmic string. Domain walls were also shown to exist in cosmological and condensed matter scenarios. We mentioned the possibility of experimental tests of cosmological branes with topological defects from condensed matter in Section 1.2.

We then looked at how potentials exhibiting spontaneous symmetry breaking might be implemented in the early Universe, and saw that potentials evolving with temperature provide a natural way to do this. The restoration of symmetry at high temperature is an important concept for particle cosmology and was, as we have now often seen, first applied in condensed matter scenarios. We also described the equivalence of spontaneous symmetry breaking and Bose-Einstein condensation, or equivalently, how Bose-Einstein condensation could be formulated as a gauge theory exhibiting spontaneous symmetry breaking.

For an example of a model that brought all these concepts together, as well as ideas about dark matter that we investigated previously, we described the axion. The axion is a light dark matter candidate that can be produced as a Bose-Einstein condensate, as a result of a symmetry-breaking phenomenon. There are also topological defects associated with the symmetry breaking, such as domain walls and axionic strings.

We then looked in more detail at a model that similarly embodies all these concepts, and described one of the problems associated with it. Silverman and Mallett's Bose-Einstein condensate dark matter model describes a particle formed as the result of a discrete symmetry-breaking potential. Generically, models such as these contain domain wall solutions in order to interpolate between the different degenerate vacua, and this is no exception. In cosmological scenarios, such solutions are generally fatal,

at best destroying the homogeneity of the CMB, and at worst overclosing the Universe as a result of their huge energy distributions. This model nicely embodies the concepts we have described however, and we finished by describing some possible ways to overcome the cosmological domain wall problem.

# Chapter 5

## Conclusions and Further Work

In this thesis, we have looked at some of the examples where phenomena in condensed matter and cosmology overlap, and seen that the novel application of techniques from one field may help in understanding aspects of the other.

We first looked at the standard cosmology, detailing some of the historical narrative to provide a sense of how the subject came to be where it is today. We gave some thought to the relationship between mathematics and physics, the necessity of experimental data to drive forward theoretical understanding, and the process of scientific ‘revolution’, in which old theories are not usually replaced by new, but are rather recovered in some limit. We concentrated to some extent on modern cosmology, borne to large extent as a result of technological advancements allowing ever more accurate measurement. We detailed the emergence and success of the concordance model of cosmology, and introduced traditional approaches to structure formation, as well as describing the potential roles of scalar fields and the part that particle physics plays. We also looked in more detail at the modelling of dark matter, and the status of experimental searches, which, at this point, can be considered to be in their early stages. We then introduced the interface between cosmology and condensed matter, and gave some early examples of where one has informed the other. Both disciplines are in a position where cutting-edge technological advancement is required to make experimental progress, and this is demonstrated by the only relatively recent production of a Bose-Einstein gas, and the onset of the era of ‘precision cosmology’. The relationships then, are often ingrained more deeply in the theoretical overlap. As examples of this we introduced

the ‘Higgs-Anderson’ and the ‘Kibble-Zurek’ mechanisms, and a more speculative analogy proposed by Volovik, involving the group structure of theories describing the Universe, and liquid Helium. In the final part of the introduction, we discussed the future of multi-disciplinary research, with exciting theoretical progress being made in the form of the mathematically rigorous, but as yet unphysical, AdS/CFT correspondence. Progress is also being made experimentally, where Hawking radiation, the results of the first attempts to combine General Relativity and Quantum Field Theory, may well be demonstrated in the laboratory, rather than in an astrophysical environment as one might expect.

Chapter 2 was a somewhat more technical overview of the role of the linear and non-linear Schrödinger-Poisson systems and their relativistic counterparts, the linear and nonlinear Klein-Gordon-Einstein equations, in describing cosmological phenomena. In addition to reasons detailed in Chapter 1, we motivated further the need to go beyond the Cold Dark Matter model, possibly by introducing an interacting dark matter candidate. We suggested that the nonlinear Schrödinger equation can be thought of as describing an interacting particle system, a  $\phi^4$  theory in Quantum Field Theory, and that this is equivalent to the Gross-Pitaevskii equation in condensed matter physics. We looked at some of the uses, both quantum and classical, of these systems, motivated primarily by models seeking to resolve some of the problems with the Cold Dark Matter model, such as cuspy density profiles and the overabundance of substructure. As the Gross-Pitaevskii and nonlinear Schrödinger equations are equivalent, it is almost natural to start thinking of dark matter models in which the dark matter candidate resides in a Bose-Einstein condensate.

In Chapter 3, we explicitly introduced the concept of a Bose-Einstein condensate, and derived the Gross-Pitaevskii equation. We also introduced concepts that we would return to often, such as the Madelung transformation and quantised vortices. We then demonstrated a classical use for these equations in a novel approach to modelling structure formation, which we introduced in Chapters 1 and 2. The rest of this chapter was dedicated to a model of a galactic dark matter halo, comprised of a Bose-Einstein condensate in which quantised vortices exist. By considering the gravitational stability of the dark matter vortices, we were able to place limits on parameters describing the

dark matter particle, hence placing ranges of validity on the possibility for quantised vortices to exist within a Bose-Einstein condensate dark matter model.

In the penultimate chapter, we considered some of the relations between condensed matter physics and the high-energy field theory used to describe particle interactions in the early Universe. We elucidated the relationships between the Abelian-Higgs, Landau-Ginzburg, Goldstone and Gross-Pitaevskii equations, particularly with regard to symmetry breaking, topological defect, and particle production phenomena. We also described condensates and vacuum expectation values, and looked at two models where all these concepts play a role: the axion, particularly as it has also been considered as a dark matter candidate, and a Bose-Einstein condensate dark matter model that we came across in Chapter 2 and 3, in which the dark matter candidate is produced as a result of a symmetry-breaking event. We saw how, in this case, the symmetry-breaking mechanism is accompanied by an unacceptable amount of topological defect production, leading to experimental predictions that would be in contradiction to observations of the Cosmic Microwave Background.

There are several ways in which this work could be continued or extended. As a general point, the historical perspectives presented in this thesis demonstrate the importance of clear communication between different disciplines in physics, in order for effective progress to be made. This will be of particular importance if highly technical concepts such as the AdS/CFT correspondence are to be applied and demonstrated in experimental condensed matter setups.

The wave-mechanical approach to structure formation can be extended to include a particle interaction, or pressure term, with the use of a (classical) nonlinear Schrödinger equation. Some promising preliminary analysis has already been done in this regard [270], and there is a lot of potential for this work to be extended, particularly to the level of rigour presented in earlier work dealing with the linear Schrödinger equation [266, 268]. The addition of a pressure term may enable models of galaxy formation to progress much further into the nonlinear regime, where hydrodynamical effects such as shocks and other gas physics come into play. It may be possible to study a pure dark matter model in this way, extending the properties of the dark matter candidate to become interacting in a similar way to models we mentioned at the start of Chapter 2,

such as those developed by Spergel and Steinhardt [263]. It may even be possible to study models that involve some combination of baryonic matter and interacting dark matter, as more recent analysis has demonstrated that the wave-mechanical formalism can be used to model multi-fluid systems [271].

The dark matter vortex model we described in Chapter 3 can also be extended. Firstly, it would be interesting to find a description of the density profile of a gravitationally coupled vortex. This may be able to be found by considering a cutoff in the background density that would prevent the gravitational potential from diverging. Such a cutoff may arise naturally in the Thomas-Fermi approximation where it would have a physical interpretation as the extent of a galaxy halo. A full solution for the density profile would also allow a more detailed exploration of the parameter space of quantum dark matter vortices. Knowing the sizes of the vortex core, and the density profile, it should be possible to analyse any observational effects such as those from gravitational lensing. A fuller analysis of the vortex could also investigate possible instability and collapse of the vortex in the axial direction.

A more ambitious project would be to try and establish whether it is possible for a Bose-Einstein condensate to exist when there is a gravitational interaction present. We have briefly hinted at this idea throughout this thesis, and further work is hinted at in Chapter 1 of Callender and Huggett [443].

Following on from models of dark matter and dark energy that were mentioned in Chapter 2, in which the two unknown constituents of the Universe are modelled as the condensed and normal components of one fluid, and the models of structure formation that we have mentioned, it may be of interest to investigate a structure formation model in which the dark and normal matter components are modelled as the two phases of a superfluid. The relative amounts of each component could be a temperature-dependent quantity, as it is in a standard superfluid, with the possibility of linking the relative amounts of dark and normal matter to the temperature of the Universe throughout various epochs. The possibility for the Schrödinger approach to handle multiple fluids has already been mentioned, and interactions in the two-fluid system may lead to the appearance of excitations such as *rotons*, which produce a very distinct dispersion relation, and a phenomena analogous to *mutual friction* [444]. It is difficult to see

what these excitations may correspond to in the wave-mechanical picture, while if we suggest that we are modelling a quantum superfluid, the measurement of such a dispersion relation in the galactic dark matter halo would provide convincing evidence of superfluid or condensate behaviour. In fact, the Gross-Pitaevskii equation struggles to describe the roton minimum in the dispersion relation of a superfluid, which is thought to be responsible for many of a superfluid's properties. In order to modify the Gross-Pitaevskii equation to produce an accurate dispersion relation, Berloff and Roberts [445, 446, 447] have included an interaction term based on Skyrme's model of nuclei interactions [448].

There is an interesting, but fairly tenuous link to note that Skyrme's more famous work is a model of topological solitons [449], in which the topological charge that we discussed in Chapter 4 is identified as baryon number. See Schechter and Weigel [450] and Wong [451] for further details of the model. The Skyrme model is also an effective model of QCD, and it is possible for Skyrmions to exist in a condensate [452].

Some fairly speculative work has also been done suggesting that the metric of a cosmic string spinning about its symmetry axis can describe the gravitational field of a vortex [453], in a model that postulates spacetime as a superfluid [454, 455].

Finally, in an alliance between two subject areas that has already given understandings as fundamental as the Higgs mechanism, it will be intriguing to what the next inter-disciplinary development will be. In the foreseeable future, it would seem that analogue experiments of gravity and, in particular, Hawking radiation, might be about to make their mark, while on the theoretical side, the AdS/CFT correspondence may be able to provide realistic descriptions of superconductor physics.

# Appendix A

## From Einstein-Klein-Gordon to Schrödinger-Poisson

We suggest many times in this thesis that the Landau-Ginzburg theory, which uses a scalar field to describe the order parameter for the transition to superconductivity, can be thought of as the non-relativistic limit of the Abelian-Higgs model, which describes a fundamental scalar field that may undergo a phase transition to generate mass.

We have also noted that the Gross-Pitaevskii, or non-linear Schrödinger equation, coupled to the Poisson equation can be thought of as the non-relativistic limit of the Einstein-Klein-Gordon system.

The limiting procedure is actually fairly non-trivial, and has been investigated in a number of papers [456, 457, 458, 459], some of which are highly mathematical. We will not go into all the detail here, but we can outline some approximation methods for getting from one system to the other.

In our method, drawn from Widrow and Kaiser [265], and Zinn-Justin [460], we start at the level of the Lagrangian of the system.

We consider the Lagrangian

$$\mathcal{L}_{\text{KG}} = \frac{1}{2}g^{\mu\nu}(\nabla_{\mu}\phi)(\nabla_{\nu}\phi) - \frac{1}{2}a^2\phi^2 - b\phi^4. \quad (\text{A.1})$$

We neglect gravitational coupling for now, and consider a flat metric,

$$g_{\mu\nu} = \text{diag}(1, -1, -1, -1). \quad (\text{A.2})$$

In this limit,  $\nabla_\mu \rightarrow \partial_\mu$ .

To obtain the equations of motion a Lagrangian, we can either minimise the action

$$S = \int \mathcal{L} d^4x, \quad (\text{A.3})$$

with respect to the field  $\phi$ , or we can use the Euler-Lagrange equations,

$$\partial_\mu \left( \frac{\partial \mathcal{L}}{\partial(\partial^\mu \phi)} \right) - \frac{\partial \mathcal{L}}{\partial \phi} = 0. \quad (\text{A.4})$$

Inserting the Lagrangian, eqn. (A.1) into the Euler-Lagrange equations, eqn. (A.4), we find

$$\partial_\mu \partial^\mu \phi + a^2 \phi^2 + 4b\phi^4. \quad (\text{A.5})$$

We see that this is the nonlinear Klein-Gordon equation, and with the variables  $a$  and  $b$  defined as  $a = \sqrt{2}\mu$  and  $b = \nu/2$ , this is the form of eqn. (4.24) given in Chapter 4, with a standard quadratic potential, rather than one exhibiting symmetry breaking.

To consider the non-relativistic limit, we return to the Lagrangian, eqn. (A.1). We write the field  $\phi$  in terms of two complex fields.

$$\phi(t, x) = \frac{1}{\sqrt{2a}} (\Psi e^{-iat} + \Psi^* e^{iat}). \quad (\text{A.6})$$

To take the non-relativistic limit, we assume that the space variation is small compared to the time variation,  $\nabla^2 \Psi \ll \partial_t \Psi$ , and the fields  $\Psi$ ,  $\Psi^*$  have slow time variation compared to the factors  $e^{iat}$ , so we can neglect terms that go like  $\partial_t^2 \Psi$ .

We substitute eqn. (A.6) into the Lagrangian, eqn. (A.1). In the ensuing manipulation, we note that terms of the form  $\Psi^{*r} \Psi^s$  are multiplied by a factor  $e^{ia(r-s)}$ , and for factors where  $r \neq s$ , the corresponding time integrals give small contributions due to the fast time oscillations. At leading order then, the only terms that survive are those with equal factors of  $\Psi$  and  $\Psi^*$ . After some manipulation, the Lagrangian now takes the form

$$\mathcal{L}_{\text{NLS}} = \frac{i}{2} (\Psi^* \partial_t \Psi - \Psi \partial_t \Psi^*) - \frac{1}{2a} \nabla \Psi \nabla \Psi^* - \frac{3b}{2a^2} \Psi \Psi \Psi^* \Psi^*. \quad (\text{A.7})$$

Inserting this Lagrangian into the Euler-Lagrange equations

$$\partial_t \left( \frac{\partial \mathcal{L}}{\partial (\partial_t \Psi^*)} \right) + \nabla \cdot \left( \frac{\partial \mathcal{L}}{\partial (\nabla \Psi^*)} \right) - \frac{\partial \mathcal{L}}{\partial \Psi^*} = 0, \quad (\text{A.8})$$

yields

$$i \frac{\partial \Psi}{\partial t} = -\frac{1}{2a} \nabla^2 \Psi + \frac{3}{a^2} b |\Psi|^2 \Psi. \quad (\text{A.9})$$

We recognise this as the nonlinear Schrödinger equation, and identifying the constants  $a$ ,  $b$  as  $a = m$  and  $b = m^2 V_0/3$  we note that this is precisely the Gross-Pitaevskii equation, eqn. (3.33) in Chapter 3.

To consider the coupling to the Poisson equation, we consider the Einstein-Hilbert Lagrangian,

$$\mathcal{L}_{\text{EH}} = \sqrt{-g} \frac{R}{2\kappa}, \quad (\text{A.10})$$

where  $g$  is the determinant of the spacetime metric,  $R$  is the Ricci scalar, as introduced in Section 1.1, and  $\kappa = 8\pi G$ .

To obtain the nonlinear Einstein-Klein-Gordon equation, we could construct a total Lagrangian density, by adding together the Einstein-Hilbert Lagrangian density to the Klein-Gordon Lagrangian density, eqn. (A.1), multiplied by a suitable constant, see Wald [461], pg. 455,

$$\mathcal{L}_{\text{EKG}} = \mathcal{L}_{\text{EH}} + c \mathcal{L}_{\text{KG}}. \quad (\text{A.11})$$

Varying the action

$$S = \int \mathcal{L}_{\text{EKG}} d^4 x, \quad (\text{A.12})$$

we would recover the coupled nonlinear Einstein-Klein-Gordon equations for a scalar field, with energy momentum tensor,

$$T_{\mu\nu} = \partial_\mu \phi \partial_\nu \phi - \frac{1}{4} g_{\mu\nu} (\partial_\kappa \phi \partial^\kappa \phi - a^2 \phi^2 - 4b\phi^4). \quad (\text{A.13})$$

Instead, we consider the weak field limit of the Einstein-Hilbert Lagrangian. In the weak field limit, the metric,  $g_{\mu\nu}$ , takes the form,

$$g_{\mu\nu} = \text{diag}(1 + 2\Phi, -1, -1, -1), \quad (\text{A.14})$$

and the Ricci tensor,  $R_{\mu\nu}$ , can be shown to be,

$$R_{\mu\nu} = R_{tt} = \nabla^2 \Phi. \quad (\text{A.15})$$

This result can be found in any standard General Relativity textbook. See, for example, Misner, Thorne and Wheeler [462], Chapter 17. The weak field Einstein-Hilbert Lagrangian then, can be shown to be

$$\begin{aligned}
 \mathcal{L}_{\text{EHw}} &= \frac{\sqrt{-g}R}{2\kappa} = \frac{\sqrt{-g}}{2\kappa}g^{\mu\nu}R_{\mu\nu} \\
 &= \frac{1}{2\kappa}(1+2\Phi)^{\frac{1}{2}}(1+2\Phi)^{-1}\nabla^2\Phi \\
 &= \frac{1}{2\kappa}(1-\Phi)\nabla^2\Phi.
 \end{aligned} \tag{A.16}$$

As total derivatives will vanish in the action, an equivalent form of the Lagrangian is

$$\mathcal{L}_{\text{EHw}} = \frac{\nabla\Phi\nabla\Phi}{2\kappa}. \tag{A.17}$$

For the weak field limit of the Klein-Gordon equation, we use our previous Lagrangian, eqn. (A.1), with  $\nabla_\mu \rightarrow \partial_\mu$ , and metric as given in eqn. (A.14). Following a similar procedure to before, and neglecting terms that go as  $\Phi\partial_t\Psi$ , we find the Lagrangian,

$$\mathcal{L}_{\text{NLSw}} = \frac{i}{2}(\Psi^*\partial_t\Psi - \Psi\partial_t\Psi^*) - a\Psi\Psi^*\Phi - \frac{1}{2a}\nabla\Psi\nabla\Psi^* - \frac{3b}{2a^2}\Psi\Psi\Psi^*\Psi^* \tag{A.18}$$

To consider the full system, we add the weak field Einstein-Hilbert Lagrangian, eqn. (A.17), to the weak field nonlinear Schrödinger equation, eqn. (A.18).

$$\mathcal{L}_{\text{NLSP}} = \mathcal{L}_{\text{EHw}} + c\mathcal{L}_{\text{NLSw}}. \tag{A.19}$$

We note that any choice of constant is acceptable, as any Lagrangian,  $\mathcal{L}$ , that satisfies the Euler-Lagrange equations will also be satisfied by  $c\mathcal{L}$ . For numerical factors to work out, the appropriate constant is chosen to be  $c = -1/2$ . The nonlinear-Schrödinger-Poisson Lagrangian is then,

$$\mathcal{L}_{\text{NLSP}} = \frac{\nabla\Phi\nabla\Phi}{2\kappa} - \frac{i}{4}(\Psi^*\partial_t\Psi - \Psi\partial_t\Psi^*) + a\Psi\Psi^*\Phi + \frac{1}{4a}\nabla\Psi\nabla\Psi^* - \frac{3b}{4a^2}\Psi\Psi\Psi^*\Psi^*. \tag{A.20}$$

Substituting this into the Euler-Lagrange equations, with respect to  $\Phi$  and  $\Psi^*$ , we find,

$$i\frac{\partial\Psi}{\partial t} = -\frac{1}{2a}\nabla^2\Psi + \frac{3}{a^2}b|\Psi|^2\Psi + a\Phi\Psi^*, \tag{A.21}$$

$$\nabla^2\Phi = 4\pi Gm|\Psi|^2; \tag{A.22}$$

the coupled nonlinear-Schrödinger-Poisson system.

# Bibliography

- [1] E. P. Wigner, *Comm. Pure. Applied. Mathematics.* **13** (1960) 1.
- [2] Aristotle, “*De Caelo*”, ~ 3rd cent. B.C.
- [3] Eudoxus works are lost. His ideas are mentioned in Aristotle’s “*Metaphysics XXI*, 8, and a commentary by Simplicius of Cilicia on the *De Caelo* [2].
- [4] Ptolemy, “*Almagest*”, ~ 2nd cent. A.D.
- [5] Ptolemy, “*Syntaxis*”, ~ 2nd cent. A.D.
- [6] Copernicus, “*De Revolutionibus orbium coelestium*”, (1543)
- [7] O. Neugebauer, “*The Exact Sciences in Antiquity*” 2nd ed. New York: Dover (1969), p 204.
- [8] J. Kepler, Kepler’s ideas are documented in “*Astronomia nova*” (1609) “*Harmonices Mundi*” (1619) “*Epitome of Copernican Astronomy*” (1617) and collected later in, for example, Newton’s “*Principia*”, [9]
- [9] I. Newton, “*Philosophiæ Naturalis Principia Mathematica*”, (1687)
- [10] J. Polkinghorne, “*Belief in God in an Age of Science (The Terry Lectures Series)*”, (Yale University Press (1999))
- [11] P. A. M. Dirac, *Proc. Roy. Soc. Lond. A* **126** (1930) 360.
- [12] Anderson, quoted by A. Pais, “*Inward Bound*”, (Oxford University Press, (1986) pg. 352)
- [13] K. Schwarzschild, *Sitzungsber. Preuss. Akad. Wiss. Berlin (Math. Phys. )* **1916** (1916) 189 [arXiv:physics/9905030].
- [14] K. Schwarzschild, *Sitzungsber. Preuss. Akad. Wiss. Berlin (Math. Phys. )* **1916** (1916) 424 [arXiv:physics/9912033].
- [15] S. W. Hawking and R. Penrose, *Proc. Roy. Soc. Lond. A* **314**, 529 (1970).
- [16] S. W. Hawking and G. F. R. Ellis, “*The Large scale structure of space-time*”, (Cambridge University Press, Cambridge, 1973)
- [17] W. Isaacson, “*Einstein: His Life and Universe*”, (Simon & Schuster (2007))
- [18] A. Friedman, *Z. Phys.* **10**, 377 (1922) [*Gen. Rel. Grav.* **31**, 1991 (1999)].

- [19] A. Friedmann, Z. Phys. **21**, 326 (1924) [Gen. Rel. Grav. **31**, 2001 (1999)].
- [20] G. Lemaitre, Gen. Rel. Grav. **29**, 641 (1997) [Annales Soc. Sci. Brux. Ser. I Sci. Math. Astron. Phys. A **53**, 51 (1933)].
- [21] E. P. Hubble, Astrophys. J. **64**, 321 (1926).
- [22] K. Crowell, “*The Alchemy of the Heavens*”, (Anchor Books, 1995)
- [23] E. Hubble, Proc. Nat. Acad. Sci. **15**, 168 (1929).
- [24] R. P. Kirshner, PNAS **101** (2004) 8
- [25] H. P. Robertson, Astrophys. J. **82** 248 (1935)
- [26] A. G. Walker, Proc. Lon. Math. Soc. **42** 90 (1937)
- [27] K. Land and J. Magueijo, Phys. Rev. Lett. **95** (2005) 071301 [arXiv:astro-ph/0502237].
- [28] K. Land and J. Magueijo, Mon. Not. Roy. Astron. Soc. **378** (2007) 153 [arXiv:astro-ph/0611518].
- [29] R. A. Matzner and B. R. Tolman, Phys. Rev. D **26**, 2951 (1982)
- [30] F. Zwicky, Helv. Phys. Acta **6** (1933) 110.
- [31] A. McKellar, Pub. Dom. Astrophys. Obs. **7** (1941) 251
- [32] R. H. Dicke, R. Beringer, R. Kyhl, A. B. Vane, Phys. Rev. **70** (1946) 340
- [33] G. Gamow, Phys. Rev. **74** (1948) 505.
- [34] G. Gamow, Nature **162** (1948) 608.
- [35] R. A. Alpher and R. Herman, Phys. Rev. **74** (1948) 1577
- [36] A. G. Doroshkevich and I. D. Novikov, Sov. Phys. Dok. **9**
- [37] A. A. Penzias and R. W. Wilson, Astrophys. J. Lett. **142** (1965) 1149.
- [38] R. H. Dicke, P. J. E. Peebles, P. G. Roll and D. T. Wilkinson, Astrophys. J. **142** (1965) 414.
- [39] A. A. Penzias and R. W. Wilson, Astrophys. J. **142** (1965) 419.
- [40] R. A. Alpher, H. Bethe and G. Gamow, Phys. Rev. **73** (1948) 803.
- [41] E. Komatsu *et al.* [WMAP Collaboration], Astrophys. J. Suppl. **180** (2009) 330 [arXiv:0803.0547 [astro-ph]].
- [42] J. R. Ellis, D. V. Nanopoulos and M. Quiros, Phys. Lett. B **174** (1986) 176.
- [43] B. de Carlos, J. A. Casas, F. Quevedo and E. Roulet, Phys. Lett. B **318**, 447 (1993) [arXiv:hep-ph/9308325].

- [44] T. Banks, D. B. Kaplan and A. E. Nelson, Phys. Rev. D **49**, 779 (1994) [arXiv:hep-ph/9308292].
- [45] A. A. Starobinsky, JETP Lett. **30** (1979) 682 [Pisma Zh. Eksp. Teor. Fiz. **30** (1979) 719].
- [46] A. A. Starobinsky, Phys. Lett. B **91** (1980) 99.
- [47] A. H. Guth, Phys. Rev. D **23** (1981) 347.
- [48] A. D. Linde, Phys. Lett. B **108** (1982) 389.
- [49] A. D. Linde, Phys. Lett. B **129** (1983) 177.
- [50] A. J. Albrecht, P. J. Steinhardt, M. S. Turner and F. Wilczek, Phys. Rev. Lett. **48** (1982) 1437.
- [51] G. Jungman, M. Kamionkowski and K. Griest, Phys. Rept. **267** (1996) 195 [arXiv:hep-ph/9506380].
- [52] R. Brustein, M. Gasperini, M. Giovannini, V. F. Mukhanov and G. Veneziano, Phys. Rev. D **51** (1995) 6744 [arXiv:hep-th/9501066].
- [53] A. Mennim and R. A. Battye, Class. Quant. Grav. **18**, 2171 (2001) [arXiv:hep-th/0008192].
- [54] M. J. Duff, B. E. W. Nilsson and C. N. Pope, Phys. Rept. **130**, 1 (1986).
- [55] J. D. Bekenstein, Phys. Rev. D **70** (2004) 083509 [Erratum-ibid. D **71** (2005) 069901] [arXiv:astro-ph/0403694].
- [56] K. Agashe, R. Contino and A. Pomarol, Nucl. Phys. B **719** (2005) 165 [arXiv:hep-ph/0412089].
- [57] D. B. Kaplan, H. Georgi and S. Dimopoulos, Phys. Lett. B **136** (1984) 187.
- [58] G. W. Gibbons, S. W. Hawking and S. T. C. Siklos, “*The Very Early Universe. Proceedings*”, (Cambridge, Uk: Univ. Pr. ( 1983) 480p)
- [59] J. M. Bardeen, P. J. Steinhardt and M. S. Turner, Phys. Rev. D **28**, 679 (1983).
- [60] A. H. Guth and S. Y. Pi, Phys. Rev. Lett. **49** (1982) 1110.
- [61] S. W. Hawking, Phys. Lett. B **115**, 295 (1982).
- [62] A. A. Starobinsky, Phys. Lett. B **117**, 175 (1982).
- [63] T. Padmanabhan, “*Structure Formation in the Universe*”, (Cambridge University Press, Cambridge)
- [64] R. Penrose, “*The Road to Reality*”, (Jonathan Cape, London, 2004)
- [65] T. Vachaspati and M. Trodden, Phys. Rev. D **61** (1999) 023502 [arXiv:gr-qc/9811037].

- [66] R. Lieu and T. W. B. Kibble, [arXiv:0904.4840] [astro-ph.CO].
- [67] N. Bartolo, E. Komatsu, S. Matarrese and A. Riotto, Phys. Rept. **402** (2004) 103 [arXiv:astro-ph/0406398].
- [68] E. Komatsu *et al.*, arXiv:0902.4759 [astro-ph.CO].
- [69] D. H. Lyth and Y. Rodriguez, Phys. Rev. D **71** (2005) 123508 [arXiv:astro-ph/0502578].
- [70] J. M. Maldacena, JHEP **0305** (2003) 013 [arXiv:astro-ph/0210603].
- [71] I. A. Strukov and D. P. Skulachev, Pis. Ast. Zhurnal, **10** (1984), 3 Sov. Ast. Lett. **10** (1984) 1 (Translation).
- [72] J. C. Mather *et al.*, Astrophys. J. **420** (1994) 439.
- [73] E. L. Wright *et al.*, Astrophys. J. **420**, 450 (1994).
- [74] D. J. Fixsen, E. S. Cheng, J. M. Gales, J. C. Mather, R. A. Shafer and E. L. Wright, Astrophys. J. **473**, 576 (1996) [arXiv:astro-ph/9605054].
- [75] G. F. Smoot *et al.*, Astrophys. J. **396** (1992) L1.
- [76] I. A. Strukov, A. A. Brukhanov, D. P. Skulachev and M. V. Sazhin, Phys. Lett. B **315** (1993) 198.
- [77] A. D. Miller *et al.*, Astrophys. J. **524**, L1 (1999) [arXiv:astro-ph/9906421].
- [78] A. Miller *et al.*, Astrophys. J. Suppl. **140**, 115 (2002) [arXiv:astro-ph/0108030].
- [79] S. Hanany *et al.*, Astrophys. J. **545** (2000) L5 [arXiv:astro-ph/0005123].
- [80] A. E. Lange *et al.* [Boomerang Collaboration], Phys. Rev. D **63** (2001) 042001 [arXiv:astro-ph/0005004].
- [81] C. B. Netterfield *et al.* [Boomerang Collaboration], Astrophys. J. **571** (2002) 604 [arXiv:astro-ph/0104460].
- [82] M. Bucher, A. S. Goldhaber and N. Turok, Phys. Rev. D **52** (1995) 3314 [arXiv:hep-ph/9411206].
- [83] A. D. Linde, Phys. Lett. B **351**, 99 (1995) [arXiv:hep-th/9503097].
- [84] G. F. R. Ellis and P. Coles, Nature **370**, (1994) 609
- [85] P. J. E. Peebles, Astrophys. J. **284** (1984) 439
- [86] G. Efstathiou, W. J. Sutherland, S. J. Maddox, Nature **348**, (1990) 705
- [87] L. M. Krauss and M. S. Turner, Gen. Rel. Grav. **27** (1995) 1137 [arXiv:astro-ph/9504003].
- [88] J. P. Ostriker and P. J. Steinhardt, Nature **377**, 600 (1995).

- [89] S. Perlmutter *et al.* [Supernova Cosmology Project Collaboration], *Astrophys. J.* **517** (1999) 565 [arXiv:astro-ph/9812133].
- [90] S. Perlmutter *et al.* [Supernova Cosmology Project Collaboration], *Nature* **391** (1998) 51 [arXiv:astro-ph/9712212].
- [91] A. G. Riess *et al.* [Supernova Search Team Collaboration], *Astron. J.* **116** (1998) 1009 [arXiv:astro-ph/9805201].
- [92] A. G. Riess *et al.* [Supernova Search Team Collaboration], *Astrophys. J.* **560** (2001) 49 [arXiv:astro-ph/0104455].
- [93] J. L. Tonry *et al.* [Supernova Search Team Collaboration], *Astrophys. J.* **594** (2003) 1 [arXiv:astro-ph/0305008].
- [94] E. J. Copeland, M. Sami and S. Tsujikawa, *Int. J. Mod. Phys. D* **15** (2006) 1753 [arXiv:hep-th/0603057].
- [95] W. J. Percival *et al.* [The 2dFGRS Collaboration], *Mon. Not. Roy. Astron. Soc.* **327** (2001) 1297 [arXiv:astro-ph/0105252].
- [96] M. Colless *et al.* [The 2DFGRS Collaboration], *Mon. Not. Roy. Astron. Soc.* **328** (2001) 1039 [arXiv:astro-ph/0106498].
- [97] M. Tegmark *et al.* [SDSS Collaboration], *Phys. Rev. D* **69** (2004) 103501 [arXiv:astro-ph/0310723].
- [98] D. J. Eisenstein *et al.* [SDSS Collaboration], *Astrophys. J.* **633** (2005) 560 [arXiv:astro-ph/0501171].
- [99] T. R. Choudhury and T. Padmanabhan, *Astron. Astrophys.* **429** (2005) 807 [arXiv:astro-ph/0311622].
- [100] A. G. Riess *et al.* [Supernova Search Team Collaboration], *Astrophys. J.* **607** (2004) 665 [arXiv:astro-ph/0402512].
- [101] G. Hinshaw *et al.* [WMAP Collaboration], *Astrophys. J. Suppl.* **180**, 225 (2009) [arXiv:0803.0732 [astro-ph]].
- [102] M. R.olta *et al.* [WMAP Collaboration], *Astrophys. J. Suppl.* **180**, 296 (2009) [arXiv:0803.0593 [astro-ph]].
- [103] C. Short, “*A Wave Mechanical Approach to Structure Formation*” Ph.D Thesis, University of Nottingham, 2007
- [104] P. Coles and B. Jones, *Mon. Not. Roy. Astron. Soc.* **248** (1991) 1.
- [105] B. Jones *Mon. Not. Roy. Astron. Soc.* **307** (1999) 376-386.
- [106] Y. B. Zeldovich, *Astron. Astrophys.* **5**, 84 (1970).
- [107] S. F. Schandarin and Y. B. Zeldovich, *Rev. Mod. Phys.* **61**, 185 (1989).
- [108] M. S. Roberts and A. H. Rots, *Astr. and Astrophys.* **26**, 483 (1973)

- [109] J. P. Ostriker, P. J. E. Peebles and A. Yahil, *ApJ. Lett.* **193**, L1 (1974)
- [110] J. Einasto, A. Kaasik and E. Saar, *Nature* **250**, 309 (1974)
- [111] J. Einasto, A. Kaasik, E. Saar and A. D. Chernin, *Nature* **252**, 111 (1974)
- [112] V. C. Rubin, N. Thonnard and W. K. Ford Jr., *ApJ. Letters* **225**, L107 (1978)
- [113] T. S. van Albada, J. N. Bahcall, K. Begeman and R. Sancisi, *Astrophys. J.* **295** (1985) 305.
- [114] D. Zaritsky, R. Smith, C. Frenk and S. D. M. White, *Astrophys. J.* **478** (1997) 39 [arXiv:astro-ph/9611199].
- [115] P. J. E. Peebles, *Astrophys. J.* **263** (1982) L1.
- [116] G. R. Blumenthal, S. M. Faber, J. R. Primack and M. J. Rees, *Nature* **311** (1984) 517.
- [117] M. Davis, G. Efstathiou, C. S. Frenk and S. D. M. White, *Astrophys. J.* **292** (1985) 371.
- [118] M. Davis, F. J. Summers and D. Schlegel, *Nature* **359** (1992) 393.
- [119] S. Weinberg, *Phys. Rev. D* **7** (1973) 2887.
- [120] M. Persic, P. Salucci and F. Stel, *Mon. Not. Roy. Astron. Soc.* **281**, 27 (1996) [arXiv:astro-ph/9506004].
- [121] J. F. Navarro, C. S. Frenk and S. D. M. White, *Astrophys. J.* **490** (1997) 493 [arXiv:astro-ph/9611107].
- [122] V. Springel *et al.*, *Mon. Not. Roy. Astron. Soc.* **391** (2008) 1685 [arXiv:0809.0898 [astro-ph]].
- [123] B. Moore, T. Quinn, F. Governato, J. Stadel and G. Lake, *Mon. Not. Roy. Astron. Soc.* **310**, 1147 (1999) [arXiv:astro-ph/9903164].
- [124] B. Moore, F. Governato, T. R. Quinn, J. Stadel and G. Lake, *Astrophys. J.* **499**, L5 (1998) [arXiv:astro-ph/9709051].
- [125] A. V. Kravtsov, A. A. Klypin, J. S. Bullock and J. R. Primack, *Astrophys. J.* **502**, 48 (1998) [arXiv:astro-ph/9708176].
- [126] S. Ghigna, B. Moore, F. Governato, G. Lake, T. R. Quinn and J. Stadel, *Astrophys. J.* **544**, 616 (2000) [arXiv:astro-ph/9910166].
- [127] Y. P. Jing and Y. Suto, *Astrophys. J.* **529**, L69 (2000) [arXiv:astro-ph/9909478].
- [128] A. Klypin, A. V. Kravtsov, J. Bullock and J. Primack, *Astrophys. J.* **554**, 903 (2001) [arXiv:astro-ph/0006343].
- [129] T. Fukushige, A. Kawai and J. Makino, *Astrophys. J.* **606**, 625 (2004) [arXiv:astro-ph/0306203].

- [130] F. C. van den Bosch, B. E. Robertson, J. J. Dalcanton and W. J. G. de Blok, *Astron. J.* **119**, 1579 (2000) [arXiv:astro-ph/9911372].
- [131] W. J. G. de Blok, S. S. McGaugh, A. Bosma and V. C. Rubin, *Astrophys. J.* **552**, L23 (2001) [arXiv:astro-ph/0103102].
- [132] F. C. van den Bosch and R. A. Swaters, *Mon. Not. Roy. Astron. Soc.* **325**, 1017 (2001) [arXiv:astro-ph/0006048].
- [133] G. Battaglia *et al.*, *Mon. Not. Roy. Astron. Soc.* **364**, 433 (2005) [Erratum-ibid. **370**, 1055 (2006)] [arXiv:astro-ph/0506102].
- [134] J. F. Navarro *et al.*, *Mon. Not. Roy. Astron. Soc.* **349**, 1039 (2004) [arXiv:astro-ph/0311231].
- [135] J. F. Navarro, C. S. Frenk and S. D. M. White, *Astrophys. J.* **462**, 563 (1996) [arXiv:astro-ph/9508025].
- [136] J. F. Navarro and M. Steinmetz, [arXiv:astro-ph/9908114.]
- [137] C. Carignan, *ApJS*, **58**, 107 (1985)
- [138] L. Chemin, C. Carignan and P. Amram, [arXiv:0707.1479] [astro-ph].
- [139] R. A. Swaters, B. F. Madore and M. Trewhella, [arXiv:astro-ph/0001277.]
- [140] J. A. Tyson, G. P. Kochanski and I. P. Dell'Antonio, *Astrophys. J.* **498**, L107 (1998) [arXiv:astro-ph/9801193].
- [141] J. J. Binney and N. W. Evans, *Mon. Not. Roy. Astron. Soc.* **327**, L27 (2001) [arXiv:astro-ph/0108505].
- [142] R. Dave, D. N. Spergel, P. J. Steinhardt and B. D. Wandelt, *Astrophys. J.* **547** (2001) 574 [arXiv:astro-ph/0006218].
- [143] F. Stoehr, S. D. M. White, G. Tormen and V. Springel, *Mon. Not. Roy. Astron. Soc.* **335**, L84 (2002) [arXiv:astro-ph/0203342].
- [144] J. T. Kleyna, M. I. Wilkinson, G. Gilmore and N. W. Evans, *Astrophys. J.* **588**, L21 (2003) [Erratum-ibid. **589**, L59 (2003)] [arXiv:astro-ph/0304093].
- [145] C. Power *et al.*, *Mon. Not. Roy. Astron. Soc.* **338**, 14 (2003) [arXiv:astro-ph/0201544].
- [146] M. Ricotti, *Mon. Not. Roy. Astron. Soc.* **344**, 1237 (2003) [arXiv:astro-ph/0212146].
- [147] A. W. Graham, D. Merritt, B. Moore, J. Diemand and B. Terzic, "Empirical models for Dark Matter Halos. I. Nonparametric Construction of *Astron. J.* **132**, 2685 (2006) [arXiv:astro-ph/0509417].
- [148] A. A. Klypin, A. V. Kravtsov, O. Valenzuela and F. Prada, *Astrophys. J.* **522** (1999) 82 [arXiv:astro-ph/9901240].

- [149] B. Moore, S. Ghigna, F. Governato, G. Lake, T. R. Quinn, J. Stadel and P. Tozzi, *Astrophys. J.* **524** (1999) L19.
- [150] N. Dalal and C. S. Kochanek, *Astrophys. J.* **572**, 25 (2002) [arXiv:astro-ph/0111456].
- [151] J. P. Ostriker, *Ann. Rev. Astron. Astrophys.* **31** (1993) 689.
- [152] G. Toth and J. P. Ostriker, *ApJ.* **389**, 5 (1992)
- [153] A. S. Font, J. F. Navarro, J. Stadel and T. R. Quinn, [arXiv:astro-ph/0106268.]
- [154] M. Abdelqader and F. Melia, *AIP Conf. Proc.* **1115** (2009) 175 [arXiv:0806.0602 [astro-ph]].
- [155] V. P. Debattista and J. A. Sellwood, [arXiv:astro-ph/9710039.]
- [156] A. J. Romanowsky *et al.*, *Science* **301**, 1696 (2003) [arXiv:astro-ph/0308518].
- [157] M. Markevitch *et al.*, *Astrophys. J.* **606** (2004) 819 [arXiv:astro-ph/0309303].
- [158] A. Mahdavi, H. y. Hoekstra, A. y. Babul, D. y. Balam and P. Capak, arXiv:0706.3048 [astro-ph].
- [159] A. Dekel, F. Stoehr, G. A. Mamon, T. J. Cox and J. R. Primack, *Nature* **437** (2005) 707 [arXiv:astro-ph/0501622].
- [160] R. Minchin *et al.*, *Astrophys. J.* **622** (2005) L21 [arXiv:astro-ph/0502312].
- [161] M. D. Weinberg and N. Katz, *Astrophys. J.* **580** (2002) 627 [arXiv:astro-ph/0110632].
- [162] J. A. Sellwood, *Astrophys. J.* **587**, 638 (2003) [arXiv:astro-ph/0210079].
- [163] M. Milgrom, *Astrophys. J.* **270** (1983) 365.
- [164] J. D. Bekenstein and R. H. Sanders, [arXiv:astro-ph/0509519.]
- [165] J. W. Moffat, *JCAP* **0603** (2006) 004 [arXiv:gr-qc/0506021].
- [166] M. Milgrom and R. H. Sanders, *Astrophys. J.* **599** (2003) L25 [arXiv:astro-ph/0309617].
- [167] J. R. Brownstein and J. W. Moffat, *Mon. Not. Roy. Astron. Soc.* **382** (2007) 29 [arXiv:astro-ph/0702146].
- [168] S. Funkhouser, [arXiv:astro-ph/0503104.]
- [169] M. J. Jee *et al.*, *Astrophys. J.* **661** (2007) 728 [arXiv:0705.2171 [astro-ph]].
- [170] E. O. Kahya, *Class. Quant. Grav.* **25** (2008) 184008 [arXiv:0801.1984 [gr-qc]].
- [171] J. R. Ellis, *Phil. Trans. R. Soc. Lon.* **A34**, 475 (1986)
- [172] M. S. Turner, *Phys. Rept.* **197** (1990) 67.

- [173] C. Robilliard, R. Battesti, M. Fouche, J. Mauchain, A. M. Sautivet, F. Amiranoff and C. Rizzo, *Phys. Rev. Lett.* **99** (2007) 190403 [arXiv:0707.1296 [hep-ex]].
- [174] L. D. Duffy *et al.*, *Phys. Rev. D* **74** (2006) 012006 [arXiv:astro-ph/0603108].
- [175] C. Alcock *et al.* [MACHO Collaboration], *Astrophys. J.* **542** (2000) 281 [arXiv:astro-ph/0001272].
- [176] P. Tisserand *et al.* [EROS-2 Collaboration], *Astron. Astrophys.* **469** (2007) 387 [arXiv:astro-ph/0607207].
- [177] C. Savage, G. Gelmini, P. Gondolo and K. Freese, *JCAP* **0904** (2009) 010 [arXiv:0808.3607 [astro-ph]].
- [178] D. P. Finkbeiner, [arXiv:astro-ph/0409027.]
- [179] P. Jean *et al.*, *Astron. Astrophys.* **407** (2003) L55 [arXiv:astro-ph/0309484].
- [180] D. Hooper, D. P. Finkbeiner and G. Dobler, *Phys. Rev. D* **76** (2007) 083012 [arXiv:0705.3655 [astro-ph]].
- [181] I. Cholis, D. P. Finkbeiner, L. Goodenough and N. Weiner, [arXiv:0810.5344] [astro-ph].
- [182] I. Cholis, L. Goodenough and N. Weiner, [arXiv:0802.2922] [astro-ph].
- [183] D. Hooper, F. Ferrer, C. Boehm, J. Silk, J. Paul, N. W. Evans and M. Casse, *Phys. Rev. Lett.* **93**, 161302 (2004) [arXiv:astro-ph/0311150].
- [184] C. Boehm, D. Hooper, J. Silk, M. Casse and J. Paul, *Phys. Rev. Lett.* **92** (2004) 101301 [arXiv:astro-ph/0309686].
- [185] K. Greisen, *Phys. Rev. Lett.* **16** (1966) 748.
- [186] G. T. Zatsepin and V. A. Kuzmin, *JETP Lett.* **4**, 78 (1966) [*Pisma Zh. Eksp. Teor. Fiz.* **4**, 114 (1966)].
- [187] R. Aloisio and F. Tortorici, *Astropart. Phys.* **29** (2008) 307 [arXiv:0706.3196 [astro-ph]].
- [188] S. N. Bose, *Zeitschrift für Physik* **26** 178 (1924) (The German translation of Bose's paper on Planck's law)
- [189] A. Einstein, *Sitzungsberichte der Preussischen Akademie der Wissenschaften, Physikalisch-mathematische Klasse* (1924) p. 261; (1925) p. 3 (From [328], ref. 5, Chapter 1.)
- [190] A. Einstein, *Physika Zeitschrift*, **18** (1917) 121
- [191] J. Plateau, *Statique Expérimentale et Théorique des Liquides Soumis aux Seules Forces Moléculaires*, (Paris, Gauthier-Villars, 1873).
- [192] N. Bohr and J. A. Wheeler, *Phys. Rev.* **56** (1939) 426.
- [193] J. Anglin and W. Ketterle, *Nature*. **416** 211 (2002)

- [194] L. D. Landau and E. M. Lifshitz, “*Statistical Physics*” (Pergamon Press, Addison-Wesley Publishing Company, Inc., Reading, Mass., (1958))
- [195] V. L. Ginzburg and L. D. Landau, *Zh. Eksp. Teor. Fiz.* **20**, 1064 (1950)
- [196] J. Bardeen, L. N. Cooper and J. R. Schrieffer, *Phys. Rev.* **106** (1957) 162.
- [197] J. Bardeen, L. N. Cooper and J. R. Schrieffer, *Phys. Rev.* **108** (1957) 1175.
- [198] L. P. Gorkov, *Sov. Phys. JETP* **36** 1364 (1959)
- [199] P. W. Anderson, *Phys. Rev.* **130** (1963) 439.
- [200] F. Englert and R. Brout, *Phys. Rev. Lett.* **13** (1964) 321.
- [201] G. S. Guralnik, C. R. Hagen and T. W. B. Kibble, *Phys. Rev. Lett.* **13**, 585 (1964).
- [202] P. W. Higgs, *Phys. Lett.* **12**, 132 (1964).
- [203] P. W. Higgs, *Phys. Rev. Lett.* **13** (1964) 508.
- [204] <http://www.esf.org/index.php?id=2454> [accessed 3rd July 2009]
- [205] T. W. B. Kibble, *J. Phys. A* **9** (1976) 1387.
- [206] W. H. Zurek, *Nature* **317**, 505 (1985).
- [207] W. H. Zurek, *Acta Phys. Polon. B* **24**, 1301 (1993).
- [208] W. H. Zurek, *Phys. Rept.* **276**, 177 (1996) [arXiv:cond-mat/9607135].
- [209] T. W. B. Kibble, [arXiv:cond-mat/0111082.]
- [210] P. Laguna and W. H. Zurek, *Phys. Rev. Lett.* **78** (1997) 2519 [arXiv:gr-qc/9607041].
- [211] I. Chuang, R. Durrer, N. Turok and B. Yurke, “*Cosmology in the laboratory: Defect dynamics in liquid crystals*” Spires ref. PUPT-1208, Oct 1990. 28pp
- [212] M. J. Bowick, L. Chandar, E. A. Schiff and A. M. Srivastava, *Science* **263** (1994) 943 [arXiv:hep-ph/9208233].
- [213] C. Baeuerle, Yu. M. Bunkov, S. N. Fisher, H. Godfrin and G. R. Pickett, *Nature* **382**, 332 (1996).
- [214] V. M. H. Ruutu, V. B. Eltsov, A. J. Gill, T. W. B. Kibble, M. Krusius, Yu. G. Makhlin, B. Placasi, G. E. Volovik and Wen Xu, *Nature* **382**, 334 (1996).
- [215] P. C. Hendry, N. S. Lawson, R. A. M. Lee, P. V. E. McClintock and C. D. H. Williams, *Nature* **386**, 315 (1994)
- [216] M. E. Dodd, P. C. Hendry, N. S. Lawson, P. V. E. McClintock and C. D. H. Williams, *Phys. Rev. Lett.* **81** (1998) 3703

- [217] M. E. Dodd, P. C. Hendry, N. S. Lawson, P. V. E. McClintock and C. D. H. Williams, *J. Low. Temp. Phys.* **115** (1999) 89
- [218] N. T. Jones, H. Stoica and S. H. H. Tye, *Phys. Lett. B* **563**, 6 (2003) [arXiv:hep-th/0303269].
- [219] D. I. Bradley *et al.*, *Nature Phys.* **4** (2008) 46.
- [220] <http://onnes.ph.man.ac.uk/cmp/lt/mutualfriction.html> [accessed 4 July 2009]
- [221] T. D. C. Bevan, A. J. Manninen, J. B. Cook, J. R. Hook, H. E. Hall, T. Vachaspati and G. E. Volovik, *Nature* **386** (1997) 689. [arXiv.org:cond-mat/9611164]
- [222] T. Vachaspati, *Phil. Trans. Roy. Soc. Lond. A* **366**, 2915 (2008) [arXiv:0802.1533 [astro-ph]].
- [223] E. Noether, *Nachr. D. Knig. Gesellsch. D. Wiss. Zu Gttingen, Math-phys. Klasse* 1918: 235257. <http://arxiv.org/abs/physics/0503066v1> for translated English version which originally appeared in *Transport Theory and Statistical Physics*, **1** (3), 183207 (1971).
- [224] G. E. Volovik, “*The Universe in a helium droplet*,” *Int. Ser. Monogr. Phys.* **117**, 1 (2006).
- [225] H. F. Jones, “*Groups, Representations and Physics*” (Bristol, UK: Hilger (1990))
- [226] G. E. Volovik and T. Vachaspati, *Int. J. Mod. Phys. B* **10**, 471 (1996) [arXiv:cond-mat/9510065].
- [227] L. Crane, *J. Math. Phys.* **36** (1995) 6180 [arXiv:gr-qc/9504038].
- [228] G. 't Hooft, [arXiv:gr-qc/9310026.]
- [229] L. Susskind, *J. Math. Phys.* **36** (1995) 6377 [arXiv:hep-th/9409089].
- [230] J. M. Maldacena, *Adv. Theor. Math. Phys.* **2** (1998) 231 [*Int. J. Theor. Phys.* **38** (1999) 1113] [arXiv:hep-th/9711200].
- [231] V. L. Ginzburg, *Physica. Scripta. T.* **27** (1989) 76
- [232] J. R. Waldram, “*Superconductivity of Metals and Cuprates*”, (CRC Press, 1996)
- [233] S. Ness and G. Siopsis, *Phys. Lett. B* **536** (2002) 315 [arXiv:hep-th/0202096].
- [234] A. Guijosa, D. A. Lowe and J. Murugan, *Phys. Rev. D* **72** (2005) 046001 [arXiv:hep-th/0505145].
- [235] D. Podolski,  
<http://www.nonequilibrium.net/224-starting-dscft/>  
[.../234-continuing-dscft-hard-prove/](http://www.nonequilibrium.net/224-starting-dscft/)  
[.../254-continuing-dscft-correspondence/](http://www.nonequilibrium.net/224-starting-dscft/)  
[.../271-continuing-dscft-correspondence-part-2/](http://www.nonequilibrium.net/224-starting-dscft/)  
accessed 5th July, 2009

- [236] I. R. Klebanov and E. Witten, Nucl. Phys. B **556**, 89 (1999) [arXiv:hep-th/9905104].
- [237] S. A. Hartnoll and P. Kovtun, Phys. Rev. D **76** (2007) 066001 [arXiv:0704.1160 [hep-th]].
- [238] S. A. Hartnoll and C. P. Herzog, Phys. Rev. D **76**, 106012 (2007) [arXiv:0706.3228 [hep-th]].
- [239] S. A. Hartnoll, C. P. Herzog and G. T. Horowitz, [arXiv:0803.3295] [hep-th].
- [240] T. Albash and C. V. Johnson, [arXiv:0804.3466] [hep-th].
- [241] E. Nakano and W. Y. Wen, [arXiv:0804.3180 [hep-th]].
- [242] F. L. Lin and S. Y. Wu, [arXiv:0805.2933] [hep-th].
- [243] S. S. Gubser and S. S. Pufu, [arXiv:0805.2960] [hep-th].
- [244] J. L. Albacete, Y. V. Kovchegov and A. Taliotis, [arXiv:0805.2927] [hep-th].
- [245] S. S. Gubser, Class. Quant. Grav. **22**, 5121 (2005) [arXiv:hep-th/0505189].
- [246] S. S. Gubser, [arXiv:0801.2977] [hep-th].
- [247] S. S. Gubser, [arXiv:0803.3483] [hep-th].
- [248] W. H. Bennett, Phys. Rev. **45** 890 (1934)
- [249] F. L. Curzon, A. Folkierski, R. Latham and J. A. Nation, Proc. Roy. Soc. Lond. Serie. A. **257** (1960) 386
- [250] R. Gregory and R. Laflamme, Phys. Rev. Lett. **70** (1993) 2837 [arXiv:hep-th/9301052].
- [251] V. Cardoso and O. J. C. Dias, Phys. Rev. Lett. **96**, 181601 (2006) [arXiv:hep-th/0602017].
- [252] R. J. A. Hill and L. Eaves, Phys. Rev. Lett. **101** (2008) 234501
- [253] V. Cardoso and O. J. C. Dias, JHEP **0904** (2009) 125 [arXiv:0902.3560 [hep-th]].
- [254] S. W. Hawking, Nature **248** (1974) 30.
- [255] S. W. Hawking, Commun. Math. Phys. **43** (1975) 199 [Erratum-ibid. **46** (1976) 206].
- [256] J. M. Bardeen, B. Carter and S. W. Hawking, Commun. Math. Phys. **31** (1973) 161.
- [257] J. D. Bekenstein, Phys. Rev. D **7**, 2333 (1973).
- [258] W. G. Unruh, Phys. Rev. Lett. **46**, 1351 (1981).

- [259] R. Balbinot, A. Fabbri, S. Fagnocchi, A. Recati and I. Carusotto, [arXiv:0711.4520 [cond-mat.other]]
- [260] I. Carusotto, S. Fagnocchi, A. Recati, R. Balbinot and A. Fabbri, *New J. Phys.* **10** (2008) 103001 [arXiv:0803.0507 [cond-mat.other]].
- [261] H. Lange, B. Toomire and P. F. Zweifel, *Rep. Math. Phys.* **36** 331 (1995)
- [262] J. P. Ostriker and P. J. Steinhardt, *Science* **300**, 1909 (2003) [arXiv:astro-ph/0306402].
- [263] D. N. Spergel and P. J. Steinhardt, *Phys. Rev. Lett.* **84** (2000) 3760 [arXiv:astro-ph/9909386].
- [264] B. D. Wandelt, R. Dave, G. R. Farrar, P. C. McGuire, D. N. Spergel and P. J. Steinhardt, [arXiv:astro-ph/0006344.]
- [265] L. M. Widrow and N. Kaiser, *ApJ. Lett* **416** L71
- [266] C. J. Short and P. Coles, *JCAP* **0612** (2006) 016 [arXiv:astro-ph/0605013].
- [267] P. Coles, *Mon. Not. Roy. Astron. Soc.* **330** (2002) 421 [arXiv:astro-ph/0110615].
- [268] C. J. Short and P. Coles, *JCAP* **0612** (2006) 012 [arXiv:astro-ph/0605012].
- [269] P. Coles, [arXiv:astro-ph/0209576.]
- [270] P. Coles and K. Spencer, *Mon. Not. Roy. Astron. Soc.* **342** (2003) 176 [arXiv:astro-ph/0212433].
- [271] R. Johnston, A. N. Lasenby and M. P. Hobson, arXiv:0904.0611 [astro-ph.CO].
- [272] L. Hernquist and N. Katz, *Astrophys. J. Suppl.* **70** (1989) 419.
- [273] K. Husimi, *Proc. Phys. Math. Soc. Japan.* **22** (1940) 264
- [274] E. A. Spiegel, *Physica D: Nonlinear Phenomena*, **1**, Issue 2, 236-240 (1980)
- [275] W. Hu, R. Barkana and A. Gruzinov, *Phys. Rev. Lett.* **85** (2000) 1158 [arXiv:astro-ph/0003365].
- [276] C. G. Böhrer and T. Harko, *JCAP* **0706** (2007) 025 [arXiv:0705.4158 [astro-ph]].
- [277] S. Chandrasekhar, “*An Introduction to the Study of Stellar Structure*”, (Dover Publications, 1958)
- [278] K. R. W. Jones and D. Bernstein, *Class. Quant. Grav.* **18** (2001) 1513
- [279] M. P. Silverman and R. L. Mallett, *Gen. Rel. Grav.* **34** No.5 (2002) 633.
- [280] R. P. Yu and M. J. Morgan, *Class. Quant. Grav.* **19** (2002) L157.
- [281] M. J. Thatcher and M. J. Morgan, *Class. Quant. Grav.* **14** (1997) 3161.

- [282] J. C. Hwang, Phys. Lett. B **401** (1997) 241 [arXiv:astro-ph/9610042].
- [283] W. H. Press, B. S. Ryden and D. N. Spergel, Phys. Rev. Lett. **64**, 1084 (1990).
- [284] S. J. Sin, Phys. Rev. D **50** (1994) 3650 [arXiv:hep-ph/9205208].
- [285] J. W. Lee and I. G. Koh, Phys. Rev. D **53**, 2236 (1996) [arXiv:hep-ph/9507385].
- [286] F. E. Schunck, [arXiv:astro-ph/9802258.]
- [287] P. J. E. Peebles and A. Vilenkin, Phys. Rev. D **60**, 103506 (1999) [arXiv:astro-ph/9904396].
- [288] P. J. E. Peebles, Phys. Rev. D **62** (2000) 023502 [arXiv:astro-ph/9910350].
- [289] P. J. E. Peebles, [arXiv:astro-ph/0002495.] ApJ, **534**, L127
- [290] J. Goodman, [arXiv:astro-ph/0003018.]
- [291] T. Matos and F. S. Guzman, Class. Quant. Grav. **17**, L9 (2000) [arXiv:gr-qc/9810028].
- [292] F. S. Guzman, T. Matos and H. B. Villegas, Astron. Nachr. **320** (1999) 97.
- [293] T. Matos, Annalen Phys. **46** (1989) 462.
- [294] T. Matos, J. Math. Phys. **35** (1994) 1302 [arXiv:gr-qc/9401009].
- [295] T. Matos, [arXiv:hep-th/9405082.]
- [296] T. Matos and L. A. Ureña-López, Class. Quant. Grav. **17** (2000) L75 [arXiv:astro-ph/0004332].
- [297] T. Matos and L. A. Ureña-López, Phys. Rev. D **63**, 063506 (2001) [arXiv:astro-ph/0006024].
- [298] V. Sahni and L. M. Wang, Phys. Rev. D **62** (2000) 103517 [arXiv:astro-ph/9910097].
- [299] M. Alcubierre, F. S. Guzman, T. Matos, D. Nunez, L. A. Ureña-López and P. Wiederhold, Class. Quant. Grav. **19**, 5017 (2002) [arXiv:gr-qc/0110102].
- [300] T. Matos and F. S. Guzman, Class. Quant. Grav. **18** (2001) 5055 [arXiv:gr-qc/0108027].
- [301] L. A. Ureña-López, Class. Quant. Grav. **19**, 2617 (2002) [arXiv:gr-qc/0104093].
- [302] A. Arbey, J. Lesgourgues and P. Salati, Phys. Rev. D **68** (2003) 023511 [arXiv:astro-ph/0301533].
- [303] J. Lesgourgues, A. Arbey and P. Salati, New Astron. Rev. **46** (2002) 791.
- [304] A. Arbey, J. Lesgourgues and P. Salati, Phys. Rev. D **65** (2002) 083514 [arXiv:astro-ph/0112324].

- [305] A. Arbey, J. Lesgourgues and P. Salati, *Phys. Rev. D* **64** (2001) 123528 [arXiv:astro-ph/0105564].
- [306] B. Fuchs and E. W. Mielke, *Mon. Not. Roy. Astron. Soc.* **350** (2004) 707 [arXiv:astro-ph/0401575].
- [307] A. Bernal, T. Matos and D. Nunez, *RMxAA*, 2008, **44**, 149
- [308] T. Matos, J. A. Vazquez and J. Magana, [arXiv:0806.0683] [astro-ph].
- [309] J. W. Lee, [arXiv:0801.1442] [astro-ph].
- [310] J. W. Lee, [arXiv:0805.2877] [astro-ph].
- [311] J. W. Lee, S. Lim and D. Choi, [arXiv:0805.3827] [hep-ph].
- [312] D. O'Dell, S. Giovanazzi, G. Kurizki and V. M. Akulin, *Phys. Rev. Lett.* **84** 5687 (2000)
- [313] S. Giovanazzi, D. O'Dell and G. Kurizki, *Phys. Rev. A* **63** 031603(R) (2001)
- [314] J. Anglin, *Nature*. **406** 29 (2000)
- [315] D. Choi, *Phys. Rev. A* **66** 063609 (2002)
- [316] M. B. Altaie, *J. Phys. A* **11** (1978) 1603
- [317] J. Bernstein and S. Dodelson, *Phys. Rev. Lett.* **66** (1991) 683.
- [318] L. Parker and Y. Zhang, *Phys. Rev. D* **44** (1991) 2421.
- [319] A. R. Liddle and L. A. Ureña-López, *Phys. Rev. Lett.* **97**, 161301 (2006) [arXiv:astro-ph/0605205].
- [320] A. R. Liddle, C. Pahud and L. A. Ureña-López, *Phys. Rev. D* **77** (2008) 121301 [arXiv:0804.0869 [astro-ph]].
- [321] F. Ferrer and J. A. Grifols, *Phys. Rev. D* **63**, 025020 (2001) [arXiv:hep-ph/0001185].
- [322] F. Ferrer and J. A. Grifols, *JCAP* **0412** (2004) 012 [arXiv:astro-ph/0407532].
- [323] J. A. Grifols, *Astropart. Phys.* **25**, 98 (2006) [arXiv:astro-ph/0505602].
- [324] M. Morikawa, In *the Proceedings of 22nd Texas Symposium on Relativistic Astrophysics at Stanford University*, (Stanford, California, 13-17 Dec 2004, pp 1122).
- [325] M. Nishiyama, M. A. Morita and M. Morikawa, [arXiv:astro-ph/0403571.]
- [326] T. Fukuyama and M. Morikawa, *J. Phys. Conf. Ser.* **31**, 139 (2006).
- [327] T. Fukuyama, M. Morikawa and T. Tatekawa, [arXiv:0705.3091] [astro-ph].
- [328] C. J. Pethick and H. Smith, “*Bose-Einstein Condensation in Dilute Gases, Second Edition*” (Cambridge University Press, Cambridge) 2008

- [329] T. Fukuyama and M. Morikawa, [arXiv:0905.0173]
- [330] D. R. O. Morrison, *Nature* **366** (1993) 29
- [331] I. Dymnikova and M. Khlopov, *Mod. Phys. Lett. A* **15** (2000) 2305 [arXiv:astro-ph/0102094].
- [332] B. A. Bassett, M. Kunz, D. Parkinson and C. Ungarelli, *Phys. Rev. D* **68** (2003) 043504 [arXiv:astro-ph/0211303].
- [333] J. A. Wheeler, *Phys. Rev.* **97** (1955) 511.
- [334] D. J. Kaup, *Phys. Rev.* **172**, 1331 (1968).
- [335] D. A. Feinblum and W. A. McKinley, *Phys. Rev.* **168**, 1445 (1968)
- [336] S. Bonazzola and F. Pacini, *Phys. Rev.* **148** (1966) 1269.
- [337] R. Ruffini and S. Bonazzola, *Phys. Rev.* **187** (1969) 1767.
- [338] P. Jetzer, *Phys. Rept.* **220** (1992) 163.
- [339] F. S. Guzman and L. A. Ureña-López, *Phys. Rev. D* **68**, 024023 (2003) [arXiv:astro-ph/0303440].
- [340] F. S. Guzman and L. A. Ureña-López, *Phys. Rev. D* **69**, 124033 (2004) [arXiv:gr-qc/0404014].
- [341] T. D. Lee and Y. Pang, *Nucl. Phys. B* **315** (1989) 477.
- [342] E. W. Mielke and R. Scherzer, *Phys. Rev. D* **24** (1981) 2111.
- [343] M. Colpi, S. L. Shapiro and I. Wasserman, *Phys. Rev. Lett.* **57** (1986) 2485.
- [344] R. Ferrell and M. Gleiser, *Phys. Rev. D* **40**, 2524 (1989).
- [345] M. S. Madsen and A. R. Liddle, *Phys. Lett. B* **251** (1990) 507.
- [346] A. R. Liddle and M. S. Madsen, *Int. J. Mod. Phys. D* **1** (1992) 101.
- [347] E. Seidel and W. M. Suen, *Phys. Rev. Lett.* **72**, 2516 (1994) [arXiv:gr-qc/9309015].
- [348] J. Balakrishna, E. Seidel and W. M. Suen, *Phys. Rev. D* **58**, 104004 (1998) [arXiv:gr-qc/9712064].
- [349] E. Seidel and W. M. Suen, *Phys. Rev. D* **42**, 384 (1990).
- [350] D. F. Torres, S. Capozziello and G. Lambiase, *Phys. Rev. D* **62** (2000) 104012 [arXiv:astro-ph/0004064].
- [351] F. S. Guzman and L. A. Ureña-López, *Astrophys. J.* **645**, 814 (2006) [arXiv:astro-ph/0603613].
- [352] A. Bernal and F. S. Guzman, *Phys. Rev. D* **74**, 063504 (2006) [arXiv:astro-ph/0608523].

- [353] F. E. Schunck and E. W. Mielke, Phys. Lett. A **249**, 389 (1998).
- [354] M. J. Ablowitz, D. J. Kaup, A. C. Newell and H. Segur, Phys. Rev. Lett. **30** (1973) 1262.
- [355] E. Seidel and W. M. Suen, Phys. Rev. Lett. **66**, 1659 (1991).
- [356] L. A. Ureña-López, T. Matos and R. Becerril, Class. Quant. Grav. **19**, 6259 (2002).
- [357] J. A. Wheeler and W. H. Zurek, “*Quantum Theory And Measurement*,” (Princeton, Usa: Univ. Pr. (1983) 811 P. (Princeton Series In Physics))
- [358] D. Giulini, C. Kiefer, E. Joos, J. Kupsch, I. O. Stamatescu and H. D. Zeh, “*Decoherence And The Appearance Of A Classical World In Quantum Theory*,” (Berlin, Germany: Springer (2003) 496 p)
- [359] S. Weinberg, Phys. Today **58N11** (2005) 31.
- [360] R. Penrose, Gen. Rel. Grav. **28** (1996) 581.
- [361] R. Penrose, Phil. Trans. Roy. Soc. Lond. A **356** (1998) 1927.
- [362] I. M. Moroz, R. Penrose and P. Tod, Class. Quant. Grav. **15**, 2733 (1998).
- [363] R. Harrison, I. Moroz and K. P. Tod, [arXiv:math-ph/0208045]
- [364] R. Harrison, I. Moroz and K. P. Tod, [arXiv:math-ph/0208046]
- [365] R. Harrison, “*A Numerical Study of the Schrödinger-Newton Equation*”, Ph.D. Thesis, Oxford (2001)
- [366] O. Penrose, Phil. Mag. **42**, 1373 (1951)
- [367] O. Penrose and L. Onsager, Phys. Rev. **104**, 576 (1956)
- [368] C. N. Yang Rev. Mod. Phys. **34**, 694 (1962)]
- [369] N. Arkani-Hamed, H. C. Cheng, M. A. Luty and S. Mukohyama, JHEP **0405** (2004) 074 [arXiv:hep-th/0312099].
- [370] P. Sikivie and Q. Yang, [arXiv:0901.1106] [hep-ph].
- [371] L. Pitaevskii and S. Stringari, “*Bose Einstein Condensation*”, (Clarendon Press, Oxford) 2003
- [372] P. H. Roberts and N. G. Berloff, In “*Quantized Vortex Dynamics and Superfluid Turbulence*” edited by C. F. Barenghi, R. J. Donnelly and W. F. Vinen, Lecture Notes in Physics, **571**, Springer-Verlag (2001).  
[www.damtp.cam.ac.uk/user/ngb23/publications/review.pdf](http://www.damtp.cam.ac.uk/user/ngb23/publications/review.pdf)
- [373] B. H. Bransden and C. J. Joachain, “*Quantum Mechanics*” 2nd Ed. (Pearson, Harlow, UK)

- [374] L. D. Landau, *J. Phys. Moscow* **5** 71 (1941) Reprinted in I. M. Khalatnikov, “*Introduction to the Theory of Superfluidity*” pg. 185 (New York, W A Benjamin)
- [375] D. V. Osbourne, *Proc. Phys. Soc. A* **63** 909 (1950)
- [376] R. P. Feynman, “*Progress in Low Temperature Physics*” ed. C J Gorter Vol 1, Ch. 2 (Amsterdam, North Holland)
- [377] L. Onsager, *Nuovo Cimento* **6** suppl. **2** 249 (1949)
- [378] H. B. Nielsen and P. Olesen, *Nucl. Phys.* **B61** 4561 (1973)
- [379] A. A. Abrikosov, *Sov. Phys. JETP* **5**, 1174 (1957)
- [380] A. Vilenkin and E.P.S. Shellard, “*Cosmic Strings and Other Topological Defects*”, (Cambridge University Press, Cambridge)
- [381] R. E. Packard and T. M. Sanders Jr., *Phys. Rev. A* **6** 799 (1972)
- [382] N. Berloff, *J. Phys. A: Math. Gen.* **37** (2004) 11729 [arXiv:/cond-mat/0306596]
- [383] P. Coles and F. Lucchin, “*Cosmology: The Origin and evolution of cosmic structure*,” (Chichester, UK: Wiley (1995) 449 p)
- [384] W. F. Vinen, *J. Low. Temp. Phys.* **121**, 367 (2000)
- [385] G. R. Mamatsashvili and W. K. M. Rice, [arXiv:0901.1617] [astro-ph].
- [386] S. Carroll, Cosmic Variance <http://blogs.discovermagazine.com/cosmicvariance/2008/10/24/gravity-is-an-important-force/> [accessed 7/7/2009]
- [387] S. Carroll, Private Communication
- [388] J. R. Abo-Shaer, C. Raman, J. M. Vogels and W. Ketterle, *Science* **292** (2001) 476
- [389] I. Coddington, P. Engels, V. Schweikhard, and E. A. Cornell, *Phys. Rev. Lett.* **91**, 100402 (2003)
- [390] M. Sadd, G. V. Chester, L. Reatto, *Phys. Rev. Lett.* **79**, 2490 (1997)
- [391] J. M. Uson, S. P. Boughn and J. R. Kuhn, *Science* **250** 539 (1990)
- [392] Y. Nambu, *Phys. Rev.* **117** (1960) 648.
- [393] J. Goldstone, *Nuovo Cim.* **19** (1961) 154.
- [394] E. B. Bogomolny, *Sov. J. Nucl. Phys.* **24** (1976) 449 [*Yad. Fiz.* **24** (1976) 861].
- [395] E. Witten and D. I. Olive, *Phys. Lett. B* **78** (1978) 97.
- [396] D. Tong, arXiv:hep-th/0509216.
- [397] D. Tong, *Annals Phys.* **324**, 30 (2009) [arXiv:0809.5060 [hep-th]].

- [398] E. W. Kolb and M. S. Turner, “*The Early Universe*”, Front. Phys. **69**, 1 (1990), (Perseus books).
- [399] R. D. Pisarski, Phys. Rev. D **62**, 111501 (2000) [arXiv:hep-ph/0006205].
- [400] A. Hasenfratz, P. Hasenfratz, K. Jansen, J. Kuti and Y. Shen, Nucl. Phys. B **365** (1991) 79.
- [401] H. G. Dosch, Phys. Lett. B **190**, 177 (1987).
- [402] L. S. Celenza and C. M. Shakin, Phys. Rev. D **34**, 1591 (1986).
- [403] S. R. Coleman and E. J. Weinberg, Phys. Rev. D **7** (1973) 1888.
- [404] D. A. Kirzhnits, JETP Lett. **15** (1972) 529 [Pisma Zh. Eksp. Teor. Fiz. **15** (1972) 745].
- [405] D. A. Kirzhnits and A. D. Linde, Phys. Lett. B **42** (1972) 471.
- [406] N. N. Bogoliubov., J. Phys. USSR **11** (1947) 23, reprinted in D. Pines, Editor, “*The many-body problem*”, (Benjamin, New York (1961)).
- [407] C. W. Bernard, Phys. Rev. D **9**, 3312 (1974).
- [408] J. I. Kapusta, Phys. Rev. D **24**, 426 (1981).
- [409] H. E. Haber and H. A. Weldon, Phys. Rev. D **25** (1982) 502.
- [410] L. Dolan and R. Jackiw, Phys. Rev. D **9**, 3320 (1974).
- [411] S. Weinberg, Phys. Rev. D **9**, 3357 (1974).
- [412] H. E. Haber and H. A. Weldon, Phys. Rev. Lett. **46** (1981) 1497.
- [413] A. D. Linde, Rept. Prog. Phys. **42**, 389 (1979).
- [414] A. D. Linde, Phys. Lett. B **86** (1979) 39.
- [415] Physics World, Jan. 2004 <http://physicsworld.com/cws/article/news/18915> (accessed on 1st Sept. 2009)
- [416] C. A. Regal, M. Greiner and D. S. Jin, Phys. Rev. Lett. **92** (2004) 040403.
- [417] L. I. Schiff and M. V. Barnhill, Bull. Am. Phys. Soc. **11** 96 (1996)
- [418] L. I. Schiff and M. V. Barnhill, Phys. Rev. **151** 1067 (1966)
- [419] B. S. DeWitt, Phys. Rev. Lett. **16** (1966) 1092.
- [420] T. D. Lee and C. N. Yang, Phys. Rev. **104**, 254 (1956).
- [421] C. S. Wu, E. Ambler, R. W. Hayward, D. D. Hoppes and R. P. Hudson, Phys. Rev. **105** (1957) 1413.
- [422] J. H. Christenson, J. W. Cronin, V. L. Fitch and R. Turlay, Phys. Rev. Lett. **13** (1964) 138.

- [423] G. 't Hooft, Phys. Rev. Lett. **37** (1976) 8.
- [424] G. 't Hooft, Phys. Rev. D **14**, 3432 (1976) [Erratum-ibid. D **18**, 2199 (1978)].
- [425] R. D. Peccei and H. R. Quinn, Phys. Rev. Lett. **38** (1977) 1440.
- [426] R. D. Peccei and H. R. Quinn, Phys. Rev. D **16** (1977) 1791.
- [427] G. Carosi, K. van Bibber and M. Pivovarov Contemp. Phys. **49** (2008) 281
- [428] P. Sikivie, arXiv:astro-ph/0610440.
- [429] R. A. Battye and E. P. S. Shellard, arXiv:astro-ph/9706014.
- [430] E. W. Mielke and J. A. V. Perez, Phys. Lett. B **671** (2009) 174.
- [431] J. Mielczarek, T. Stachowiak and M. Szydlowski, arXiv:0705.3017 [astro-ph].
- [432] M. P. Silverman and R. L. Mallett, “*Gravity Research Foundation 2000 and 2001 essays*” (GRF, Wellesey Hills)
- [433] P. W. Hodge, “*Atlas of the Andromeda Galaxy*” (University of Washington Press, Seattle (1981))
- [434] Y. B. Zeldovich, I. Y. Kobzarev and L. B. Okun, Zh. Eksp. Teor. Fiz. **67**, 3 (1974) [Sov. Phys. JETP **40**, 1 (1974)].
- [435] H. Casini and S. Sarkar, Phys. Rev. D **65**, 025002 (2002) [arXiv:hep-ph/0106272].
- [436] S. E. Larsson, S. Sarkar and P. L. White, Phys. Rev. D **55**, 5129 (1997) [arXiv:hep-ph/9608319].
- [437] A. Vilenkin and A. E. Everett, Phys. Rev. Lett. **48** (1982) 1867.
- [438] B. S. Ryden, W. H. Press and D. N. Spergel, Ap. J. **357** (1989) 293
- [439] C. T. Hill, D. N. Schramm and J. N. Fry, Comments Nucl. Part. Phys. **19**, 25 (1989).
- [440] G. Lazarides and Q. Shafi, Phys. Lett. B **115**, 21 (1982).
- [441] E. P. S. Shellard, *In Cambridge 1989, Proceedings, The formation and evolution of cosmic strings 107-115. (see High Energy Physics Index 29 (1991) No. 7720)*
- [442] E. P. S. Shellard, *In Liege 1986, Proceedings, Origin and early history of the universe\* 173-180. (see Conference Index)*
- [443] C. Callender and N. Huggett, “*Physics meets philosophy at the Planck scale: Contemporary theories in quantum gravity*”, (Cambridge, UK: Univ. Pr. (2001) 365 p)
- [444] D. Tilley, J. Tilley, “*Superfluidity and Superconductivity*”, (IOP publishing, 1990)
- [445] N.G.Berloff, P.H.Roberts, J. Phys. A: Math. Gen. **32** (1999) 5611-5625

- [446] N.G.Berloff, Phys. Rev. Lett. **94** (2005) <http://arxiv.org/abs/cond-mat/0412099>
- [447] N.G.Berloff, P.H.Roberts, Lecture Notes in Physics, Vol. **571** (2001) (Springer, Berlin), [www.damtp.cam.ac.uk/user/ngb23/publications/qvd.pdf](http://www.damtp.cam.ac.uk/user/ngb23/publications/qvd.pdf) [accessed 23 Sept. 2009]
- [448] T. Skyrme, Nucl. Phys. **9** (1959) 615.
- [449] T. H. R. Skyrme, Nucl. Phys. **31**, 556 (1962).
- [450] J. Schechter and H. Weigel, arXiv:hep-ph/9907554.
- [451] S. M. H. Wong, arXiv:hep-ph/0202250.
- [452] R. A. Battye, N. R. Cooper and P. M. Sutcliffe, Phys. Rev. Lett. **88** (2002) 080401 [arXiv:cond-mat/0109448].
- [453] G. Chapline and P. O. Mazur, arXiv:gr-qc/0407033.
- [454] P. O. Mazur and E. Mottola, arXiv:gr-qc/0109035.
- [455] G. Chapline, E. Hohlfeld, R. B. Laughlin and D. I. Santiago, Int. J. Mod. Phys. A **18** (2003) 3587 [arXiv:gr-qc/0012094].
- [456] B. Najman, Annales de l'I.H.P. section C, tome 9, no. 1 (1992), pg. 3
- [457] P. Bechouche, N. Mauser, S. Selberg, arXiv:math.AP/0202201
- [458] B. Najman, Nonlinear Analysis: Theory, Methods and Applications, **15**, Iss. 3 (1990) 217 - 228
- [459] Masmoudi, Nakanishi, Int. Math. Res. Notices.2003; 2003: 697-734
- [460] J. Zinn-Justin, Int. Ser. Monogr. Phys. **113** (2002) 1.
- [461] R. M. Wald, "*General Relativity*", (Chicago, Usa: Univ. Pr. (1984))
- [462] C. W. Misner, K. S. Thorne and J. A. Wheeler, "*Gravitation*", (San Francisco, 1973)